Clinical and Laboratorial Research in Dentistry

Volume 20 • Número 3
Julho / Setembro • 2014

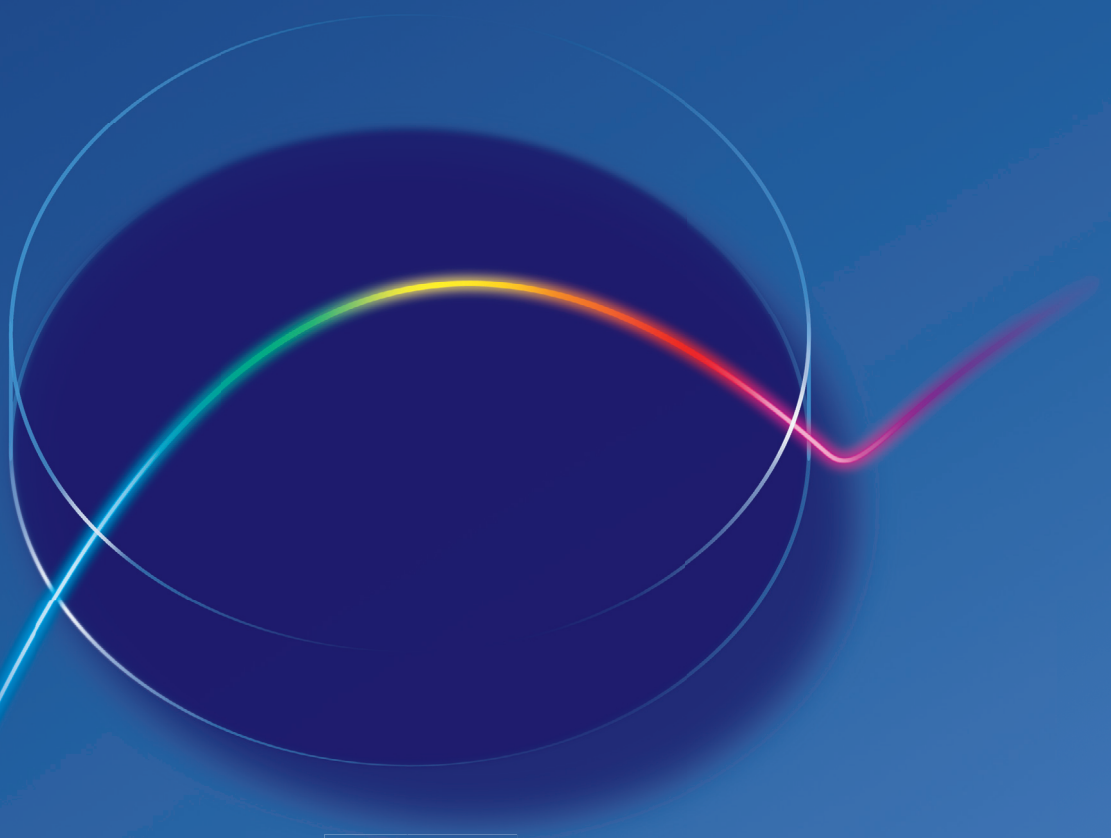

Publicação Oficial da Faculdade de Odontologia
da Universidade de São Paulo

CLRD in Clinical and Laboratorial Research in Dentistry

Volume 20 • Número 3
Julho / Setembro • 2014

Indexação
Clinical and Laboratorial Research in Dentistry é continuação da RPG - Revista da Pós Graduação da Faculdade de Odontologia da Universidade de São Paulo e está indexada em:
Base de Dados LILACS: 1987- ; Bibliografia Brasileira de Odontologia (BBO): 1987- ;

Endereço de Correspondência
Faculdade de Odontologia da Universidade de São Paulo
Av. Prof. Lineu Prestes, 2.227
Cidade Universitária "Armando Salles de Oliveira"
05508-000 - São Paulo, SP, Brasil
Fone: (55-11) 3091-7817
Fax: (55-11) 3091-8401

Catalogação na Publicação
Serviço de Documentação Odontológica - Faculdade de Odontologia da Universidade de São Paulo
CLRD - Clinical and Laboratorial Research in Dentistry - Vol. 20, n. 1 (Jan./Mar. 2014) - São Paulo : FOUSP : 2014 - Trimestral
Clinical and Laboratorial Research in Dentistry
1. Odontologia - Periódicos 2. Faculdade de Odontologia da Universidade de São Paulo


LRD in
Clinical and Laboratorial
Research in Dentistry

CLRD in Clinical and Laboratorial Research in Dentistry

Contents

Volume 20 • Número 3
Julho / Setembro • 2014

ORIGINAL RESEARCH

Influência do método de fotoativação na dureza de uma resina composta

• **Monique Mori** Department of Restorative Dentistry, School of Dentistry, University of São Paulo, São Paulo, SP, Brazil • **Carlos Alberto Kenji Shimokawa** Department of Restorative Dentistry, School of Dentistry, University of São Paulo, São Paulo, SP, Brazil • **Paula Mendes Acatauassú Carneiro** Department of Restorative Dentistry, School of Dentistry, University of São Paulo, São Paulo, SP, Brazil • **Tamile Rocha da Silva Lobo** Department of Restorative Dentistry, School of Dentistry, University of São Paulo, São Paulo, SP, Brazil • **Míriam Lacalle Turbino** Department of Restorative Dentistry, School of Dentistry, University of São Paulo, SP, Brazil

RESUMO | *Objetivo:* avaliar a dureza de uma resina composta fotoativada com dois métodos diferentes, contínuo e soft-start, por meio da variação da distância entre a ponta fotoativadora e a resina composta (7 mm e 0 mm). *Materiais e métodos*: Foram confeccionados 20 corpos-de-prova, nos quais a superfície irradiada e a oposta foram analisadas, totalizando 40 superfícies divididas em quatro grupos (n = 10): Grupo 1, método contínuo + superfície irradiada; Grupo 2, método contínuo + superfície oposta; Grupo 3, método soft-start + superfície irradiada; Grupo 4, método soft-start + superfície oposta. Os corpos-de-prova foram confeccionados com o auxílio de matrizes pretas de polipropileno, com 4 mm de diâmetro e 2 mm de espessura, utilizando a resina composta Z350 (3M ESPE) na cor AO3 e o fotoativador Elipar Freelight 2 (3M ESPE). Os corpos-de-prova foram submetidos ao teste de microdureza Vickers, no microdurômetro HMV-2000 (Shimadzu). Foram realizados cinco entalhes por superfície, com carga de 50 gf por 45 segundos. Para a análise estatística, foram realizados os testes de ANOVA e Tukey. *Resultados:* Não foi encontrada diferença estatisticamente significante entre os métodos avaliados nas superfícies irradiadas. Entretanto, nas superfícies opostas, houve diferença entre os protocolos, sendo que o soft-start obteve menores valores de dureza. Quando comparadas as diferentes profundidades, houve redução nos valores de dureza para ambos os métodos de fotoativação, de forma que a porcentagem de dureza máxima de 80% não foi atingida na superfície oposta à irradiada. *Relevância:* O cirurgião-dentista, em sua prática clínica, deve atentar para o método de fotoativação de suas restaurações, visto que este pode prejudicar a qualidade da polimerização de resinas compostas, especialmente na profundidade de 2 mm em resinas opacas.

DESCRITORES | Restauração Dentária Permanente; Polimerização; Dureza.

ABSTRACT | **Influence of the photoactivation method on the hardness of a composite resin** • *Objective:* to evaluate the hardness of a composite resin polymerized with two different methods, continuous and soft-start, by varying the distance between the activator tip and the composite resin (7 mm and 0 mm). *Materials and Methods:* Twenty test specimens were fabricated, in which the irradiated and the opposite surfaces were analyzed, totaling 40 surfaces divided into 4 groups (n = 10): Group 1, continuous method + irradiated surface; Group 2, continuous method + opposite surface; Group 3, soft-start method + irradiated surface; Group 4, soft-start method + opposite surface. The test specimens were prepared using black polypropylene matrices, with a diameter of 4 mm and thickness of 2 mm, Z350 composite resin (3M ESPE), shade AO3, and the Elipar Freelight 2 curing unit (3M ESPE). The test specimens were subjected to the Vickers hardness test in an HMV-2000 microhardness tester (Shimadzu). Five indentations were made per surface with a load of 50 gf for 45 seconds. The ANOVA and Tukey tests were used for the statistical analysis. *Results:* No statistically significant difference between the evaluated methods was found in the irradiated surfaces; however, in the opposite surfaces, there were differences between protocols, in that the soft-start protocol achieved the lowest hardness values. When comparing the different depths, there was a reduction in hardness values for both activation methods, so that the maximum hardness percentage of 80% was not achieved in the opposite surface. *Relevance:* The dentist should be knowledgeable of the photoactivation method applied to his/her restorations, since it may reduce the polymerization quality, especially in depths of 2 mm when using opaque resins.

DESCRIPTORS | Dental Restoration, Permanent; Polymerization; Hardness.

CORRESPONDING AUTHOR | • **Míriam Lacalle Turbino** Department of Restorative Dentistry, School of Dentistry, University of São Paulo • **Avenida Lineu Prestes, 2227** São Paulo, SP, Brazil • **05508-000** E-mail: miturbin@usp.br

• **Received:** Mar 27, 2014 • **Accepted:** May 09, 2014
• **DOI** http://dx.doi.org/10.11606/issn.2357-8041.clrd.2014.77662

INTRODUÇÃO

Compósitos poliméricos são rotineiramente utilizados como material restaurador na odontologia moderna, sendo que a exigência pela estética fez com que houvesse uma grande evolução desses materiais, tornando possível seu uso como material restaurador, inclusive em dentes posteriores.[1,2]

Apesar do grande avanço, as resinas compostas ainda apresentam deficiência, principalmente em relação à polimerização do material, sendo que as principais causas de falhas em restaurações de resina composta se devem à fratura do material restaurador ou à cárie secundária.[3-5]

Um dos fatores que colaboram para a fratura do material restaurador é a polimerização inadequada. Uma fotoativação insuficiente gera menores graus de conversão, ocasionando uma redução das propriedades mecânicas da restauração.[6]

A outra causa frequente de falhas, a cárie secundária, pode ser favorecida devido à tensão decorrente da contração de polimerização. Devido a essas tensões, podem surgir fendas entre dente e restauração, permitindo a infiltração de microrganismos que podem causar lesões cariosas ao redor das restaurações.[7,8]

Essa contração é um fenômeno inerente à reação de polimerização. Durante essa reação, ocorre uma conversão de monômeros em polímeros, fazendo com que o material ocupe um volume final menor do que o inicial. Isso causa uma tensão na interface entre dente e restauração, denominada de tensão de contração de polimerização. Quando essa tensão ocorre de forma exacerbada, pode-se ter, como consequência, o deslocamento da restauração das paredes da cavidade. Em alguns casos, é possível que essa tensão seja transmitida para o dente, ocasionando a fratura deste ou a deflexão de suas cúspides.[9,10]

Existem alguns métodos para minimizar as consequências da tensão de contração de polimerização, tais como a técnica de inserção do material e o controle da cinética de polimerização, por meio da variação do protocolo de fotoativação.[11,12]

Alguns autores vêm estudando protocolos que visam a uma polimerização mais lenta,[13-18] sendo que a redução da intensidade de luz causa uma diminuição na velocidade de conversão dos monômeros, aumentando a fase pré-gel da resina. O aumento dessa fase possibilita o escoamento da resina, reduzindo a magnitude das tensões geradas.[19,20]

Os equipamentos fotoativadores do tipo soft-start podem obter esse efeito, já que emitem uma menor intensidade de luz inicial, objetivando o aumento da fase pré-gel. Para complementar a polimerização, eles emitem uma intensidade de luz final alta, com o intuito de aumentar as propriedades mecânicas da restauração por meio do aumento do seu grau de conversão.[13,14,21,22]

A fotoativação soft-start também pode ser realizada por meio da variação da distância entre a restauração e a ponta fotoativadora, fazendo com que a intensidade de luz que incide na resina composta seja menor;[23-25] entretanto, deve-se atentar à qualidade de polimerização do material.

A avaliação da polimerização do material pode ser realizada por meio da análise do seu grau de conversão ou por meio de ensaios de microdureza. Estes representam uma forma indireta de avaliação daquela propriedade.

O objetivo deste estudo foi avaliar a dureza de uma resina composta fotoativada pelo método de variação de distância e compará-la à dureza obtida com o método contínuo, utilizando-se um equipamento fotoativador LED e analizando-se os resultados obtidos em diferentes profundidades.

MATERIAIS E MÉTODOS

Para este estudo, foi selecionada a resina composta Filtek Z350 (3M ESPE, Sumaré, SP, Brasil) na cor AO3. Para a fotoativação dessa resina, foi utilizado o aparelho de luz LED Elipar Freelight 2 (3M ESPE, St. Paul, MN, EUA).

A confecção dos corpos-de-prova foi realizada com o auxílio de matrizes de polipropileno pretas, com cavidade de 4 mm de diâmetro e espessura de 2 mm. As matrizes foram posicionadas sobre uma lâmina de vidro, possibilitando a obtenção de uma superfície plana e lisa. A inserção da resina foi realizada em porção única, utilizando-se uma espátula de inserção número 1.

Após a inserção da resina, uma película de polietileno foi posicionada sobre a matriz, e outra lâmina de vidro foi sobreposta, mantendo-se o paralelismo e a lisura da superfície. A lâmina de vidro foi retirada para a fotoativação do compósito.

Foram confeccionados 20 corpos-de-prova, divididos de acordo com a superfície analisada e com o tipo de fotoativação.

Para os grupos 1 e 2, foram confeccionados 10 corpos-de-prova a partir da técnica contínua de fotoativação, com a ponta do fotoativador em contato com a película de polietileno, por um tempo de 40 segundos. O grupo 1 representa a análise realizada na superfície irradiada desses corpos-de-prova, ao passo que, no grupo 2, a análise foi realizada na superfície oposta dos mesmos corpos-de-prova.

Para os grupos 3 e 4, foram confeccionados outros 10 corpos-de-prova utilizando-se o método de variação da distância da ponta do fotoativador, sendo a fotoativação inicial realizada com uma distância de 7 mm, padronizada por meio de uma matriz de polipropileno preta, por 20 segundos, seguida de uma fotoativação final, realizada com a ponta do fotoativador em contato com a película de polietileno, por mais 20 segundos (técnica soft-start). O grupo 3 representa a análise realizada na superfície irradiada e o 4, na superfície oposta.

A irradiância foi mensurada pelo radiômetro LED Radiometer (SDI; Bayswater, Victoria, Austrália), sendo registrados 995 mW/cm² quando a ponta do fotoativador estava em contato com o sensor do equipamento. Na distância de 7 mm, a irradiância era de 355 mW/cm².

Os corpos-de-prova foram armazenados por 24 h em estufa a 37°C previamente à realização dos ensaios de microdureza.

As medidas de microdureza Vickers foram obtidas com carga de 50 gf por 45 segundos no microdurômetro HMV-2000 (Shimadzu Co; Tokyo, Japão), com auxílio do software CAMS-WIN (Newage Testing Instruments; Feasterville, PA, EUA). Foram realizadas cinco entalhes em cada superfície (irradiada e oposta) dos corpos-de-prova, sendo uma realizada na porção mais central da superfície e as outras quatro a uma distância de 100 μm da primeira, nas quatro direções.

Foram obtidos 200 valores de dureza correspondentes às duas técnicas (contínua e soft-start), às duas superfícies (irradiada e oposta), a 10 repetições e a cinco medidas em cada superfície. Para a análise estatística, foram calculadas as médias dos cinco entalhes, resultando em 40 valores. Os resultados foram organizados em tabelas e estatisticamente analisados por meio dos testes de análise de variância e Tukey.

RESULTADOS

A análise de variância (Tabela 1) demonstrou haver diferenças estatisticamente significantes para os fatores técnica ($p < 0,05$) e superfície ($p < 0,001$), assim como para a interação dos mesmos ($p < 0,001$).

Para a comparação entre as médias dos quatro grupos, foi aplicado o teste de Tukey ao nível de 5% ($T = 9,52$). Pela comparação entre as médias, pôde-se notar que, na superfície irradiada, não houve diferença entre as técnicas de fotoativação, contínua ou soft-start. Porém, nas superfície opostas, houve redução da dureza em relação às superfícies irradiadas. Além disso, nas superfícies opostas, a resina fotoativada pela técnica soft-start apresentou menor dureza do que a resina fotoativada pela técnica contínua, conforme demonstrado na Tabela 2. Foi calculada a porcentagem de dureza máxima

Tabela 1 | Resultados da análise de variância: valores originais.

Fonte de variação	SQ	GL	QM	F	p
Entre técnicas	1150,4797	1	1150,4797	5,22	0,046%
Resíduo I	1982,2156	9	220,2462		
Entre superfícies	7944,4922	1	7944,4922	131,65	0,0000%
Interação	500,1578	1	500,1578	8,29	0,007640%
Resíduo II	1629,3267	27	60,3454		

SQ: soma dos quadrados; GL: Graus de liberdade; QM: Quadrado médio.

em relação à dureza na superfície irradiada com o método contínuo.

DISCUSSÃO

O aumento da distância entre a ponta fotoativadora e a resina composta causa uma diminuição da intensidade de luz que incide na restauração,[23,25] sendo que Price *et al.*[26] observaram uma redução de 66% quando essa distância é de 7 mm. Uma redução semelhante foi observada no presente estudo.

No entanto, no presente estudo não foi observada diferença estatisticamente significante entre os métodos de fotoativação estudados, quando avaliada a superfície irradiada. Isso pode ser explicado pelo fato de a resina dessas superfícies ter atingido uma dureza próxima à máxima possível, sendo que maiores densidades de energia não causariam alterações.

Na superfície oposta, houve uma acentuada redução dos valores de dureza, tanto no método contínuo, quanto no soft-start. Considerando-se que a resina composta na base do incremento deve alcançar, no mínimo, 80% da dureza encontrada na superfície irradiada para que uma polimerização seja considerada aceitável,[27] pode-se afirmar que a polimerização da resina composta na superfície oposta foi inadequada.

As resinas de coloração mais escuras e opacas, como a escolhida para este trabalho, possuem em sua composição maior concentração de óxidos pigmentantes, sendo que esses óxidos interferem na polimerização, tanto em sua velocidade, quanto em sua profundidade, devido ao fato de absorverem maior quantidade de luz. Autores afirmam que as resinas compostas de cor escura atingem menores graus de conversão do que as resinas mais claras.[28-30]

Tabela 2 | Médias e desvios-padrão de dureza. Os valores entre parênteses indicam a porcentagem da dureza máxima, representada pela condição fotoativação contínua / topo (letras iguais indicam médias estatisticamente semelhantes, p > 0,05).

		Técnica de fotoativação	
		Contínua	Soft-start
Superfície	Irradiada	68,4 ± 7,4^{a}	64,6 ± 6,3^{a} (95%)
	Oposta	47,3 ± 11,4^{b} (69%)	29,5 ± 7,3^{c} (43%)

No presente estudo, a dureza observada na superfície oposta, quando utilizado o método soft-start, foi estatisticamente menor do que a dureza obtida no grupo em que se utilizou o método contínuo. Como a dureza na superfície oposta ficou aquém da observada na irradiada (dureza máxima), a menor dose de energia recebida pelo grupo em que se utilizou o método soft-start foi capaz de influenciar a dureza. Os grupos de superfície oposta não atingiram o valor de 80% necessário para se obter a mínima polimerização aceitável.

Dessa forma, o cirurgião-dentista, em sua prática clínica, deve atentar para os fatores que podem influenciar a qualidade de polimerização de suas restaurações, tais como a fonte de luz, o método de fotoativação utilizado, a espessura do incremento e a cor da resina.

CONCLUSÃO

Com base no presente estudo, quando se utilizaram resinas opacas, o uso de incrementos de 2 mm produziu uma polimerização inadequada, tanto para o método contínuo, quanto para o método soft-start, dentro dos parâmetros aplicados. O método soft-start promoveu uma menor dureza apenas nas superfícies opostas.

REFERÊNCIAS

1. Van Nieuwenhuysen JP, D'Hoore W, Carvalho J, Qvist V. Long-term evaluation of extensive restorations in permanent teeth. J Dent. 2003 Aug;31(6):395-405. doi: 10.1016/S0300-5712(03)00084-8.
2. Cetin A, Unlu N, Cobanoglu N. A five-year clinical evaluation of direct nanofilled and indirect composite resin restorations in posterior teeth. Oper Dent. 2013 Mar-Apr;38(2):E1-E11. doi: 10.2341/12-160-C.
3. Mjor IA, Shen C, Eliasson ST, Richter S. Placement and replacement of restorations in general dental practice in Iceland. Oper Dent. 2002 Mar-Apr;27(2):117-23.
4. Opdam NJ, Bronkhorst EM, Roeters JM, Loomans BA. A retrospective clinical study on longevity of posterior composite and amalgam restorations. Dent Mater. 2007 Jan;23(1):2-8. doi: 10.1016/j.dental.2005.11.036.
5. Da Rosa Rodolpho PA, Donassollo TA, Cenci MS, Loguércio AD, Moraes RR, Bronkhorst EM, et al. 22-Year clinical evaluation of the performance of two posterior composites with different filler characteristics. Dent Mater. 2011 Oct;27(10):955-63. doi: 10.1016/j.dental.2011.06.001.
6. Ferracane JL. Resin-based composite performance: are there some things we can't predict? Dent Mater. 2013 Jan;29(1):51-8. doi: 10.1016/j.dental.2012.06.013.
7. Totiam P, Gonzáles-Cabezas C, Fontana MR, Zero DT. A new in vitro model to study the relationship of gap size and secondary caries. Caries Res. 2007;41(6):467-73. doi: 10.1159/000107934.
8. Nassar HM, González-Cabezas C. Effect of gap geometry on secondary caries wall lesion development. Caries Res. 2011 Sep;45(4):346-52. doi: 10.1159/000329384.
9. Anusavice KJ. Philips materiais dentários. Rio de Janeiro: Guanabara-Koogan; 2005.
10. Reis A, Loguercio AD. Materiais Dentários Restauradores Diretos: dos fundamentos à aplicação clínica. São Paulo: Editora Santos; 2007.
11. Ferracane JL. Buonocore Lecture. Placing dental composites--a stressful experience. Oper Dent. 2008 May-Jun;33(3):247-57. doi: 10.2341/07-BL2.
12. Malhotra N, Kundabala M, Shashirashmi A. Strategies to overcome polymerization shrinkage--materials and techniques. A review. Dent Update. 2010 Mar;37(2):115-8, 120-2, 124-5.
13. Cunha LG, Alonso RC, Pfeifer CS, Correr-Sobrinho L, Ferracane JL, Sinhoreti MA. Modulated photoactivation methods: Influence on contraction stress, degree of conversion and push-out bond strength of composite restoratives. J Dent. 2007 Apr;35(4):318-24. doi: 10.1016/j.jdent.2006.10.003.
14. El-Korashy DI. Post-gel shrinkage strain and degree of conversion of preheated resin composite cured using different regimens. Oper Dent. 2010 Mar-Apr;35(2):172-9. doi: 10.2341/09-072-L.
15. Knezevic A, Sariri K, Sovic I, Demoli N, Tarle Z. Shrinkage evaluation of composite polymerized with LED units using laser interferometry. Quintessence Int. 2010 May;41(5):417-25.
16. Leprince JG, Lamblin G, Devaux J, Dewaele M, Mestdagh M, Palin WM, et al. Irradiation modes' impact on radical entrapment in photoactive resins. J Dent Res. 2010 Dec;89(12):1494-8. doi: 10.1177/0022034510384624.
17. Sudheer V, Manjunath M. Contemporary curing profiles: Study of effectiveness of cure and polymerization shrinkage of composite resins: an in vitro study. J Conserv Dent. 2011 Oct;14(4):383-6. doi: 10.4103/0972-0707.87205.
18. Oliveira KM, Lancellotti AC, Ccahuana-Vásquez RA, Consani S. Shrinkage stress and degree of conversion of a dental composite submitted to different photoactivation protocols. Acta Odontol Latinoam. 2012;25(1):115-22.
19. Bouschlicher MR, Rueggeberg FA. Effect of ramped light intensity on polymerization force and conversion in a photoactivated composite. J Esthet Dent. 2000;12(6):328-39. doi: 10.1111/j.1708-8240.2000.tb00242.x.

20. Lim BS, Ferracane JL, Sakaguchi RL, Condon JR. Reduction of polymerization contraction stress for dental composites by two-step light-activation. Dent Mater. 2002 Sep;18(6):436-44. doi: 10.1016/S0109-5641(01)00066-5.
21. Mehl A, Hickel R, Kunzelmann KH. Physical properties and gap formation of light-cured composites with and without softstart-polymerization. J Dent. 1997 May-Jul;25(3-4):321-30. doi: 10.1016/S0300-5712(96)00044-9.
22. Braga RR, Ballester RY, Ferracane JL. Factors involved in the development of polymerization shrinkage stress in resin-composites: a systematic review. Dent Mater. 2005 Oct;21(10):962-70. doi: 10.1016/j.dental.2005.04.018.
23. Rode KM, Kawano Y, Turbino ML. Evaluation of curing light distance on resin composite microhardness and polymerization. Oper Dent. 2007 Nov-Dec;32(6):571-8. doi: 10.2341/06-163.
24. Thomé T, Steagall W Jr, Tachibana A, Braga SR, Turbino ML. Influence of the distance of the curing light source and composite shade on hardness of two composites. J Appl Oral Sci. 2007 Dec;15(6):486-91. doi: 10.1590/S1678-77572007000600006.
25. Fróes-Salgado NR, Francci C, Kawano Y. Influência do modo de fotoativação e da distância de irradiação no grau de conversão de um compósito. Perspect Oral Sci. 2009 maio-ago.;1(1):11-7.
26. Price R, Dérand T, Sedarous M, Andreou P, Loney RW. Effect of distance on the power density from two light guides. J Esthet Dent. 2000;12(6):320-7. doi: 10.1111/j.1708-8240.2000.tb00241.x.
27. Watts DC, Amer O, Combe EC. Characteristics of visible-light-activated composite systems. Br Dent J. 1984 Mar;156(6):209-15. doi: 10.1038/sj.bdj.4805312.
28. Swartz MI, Phillips RW, Rhodes B. Visible light-activated resins: depth of cure. J Am Dent Assoc. 1983 May;106(5):634-7.
29. Aguiar FHB, Lazzari CR, Lima DANL, Ambrosano GMB, Lovadino JR. Effect of light curing tip distance and resin shade on microhardness of a hybrid resin composite. Braz Oral Res. 2005 Oct-Dez;19(4):302-6. doi: 10.1590/S1806-83242005000400012.
30. Leloup G, Holvoet PE, Bebelman S, Devaux J. Raman scattering determination of the depth of cure of light-activated composites: influence of different clinically relevant parameters. J Oral Rehabil. 2002 Jun;29(6):510-5. doi: 10.1046/j.1365-2842.2002.00889.x.

Porosity, residual monomer and water sorption of conventional heat-cured, microwave-cured and cross-linked acrylic resins

• **Rodrigo Elias de Oliveira** Laboratory of Human Evolutionary Studies, Department of Genetics and Evolutionary Biology, Institute of Biosciences, University of São Paulo, São Paulo, SP, Brazil • **Fernando Neves Nogueira** Department of Biomaterials and Oral Biology, School of Dentistry, University of São Paulo, São Paulo, SP, Brazil • **Beatriz Silva Câmara Mattos** Department of Maxillofacial Surgery, Prothesis and Traumatology, School of Dentistry, University of São Paulo, São Paulo, SP, Brazil

ABSTRACT | This study compared the residual monomer release, water sorption and superficial porosity of different resins commonly employed in eye prostheses: heat-cured (HC); microwave-cured (MC) and self-curing cross-linked acrylic resins (SC). Four groups were established: G1, HC / water bath cycle; G2, MC / microwave cycle; G3, HC / microwave cycle; G4, SC. The amount of residual monomer was similar in G1 and G3, lower in G2 and higher in G4. Water sorption was similar in all groups. G2 showed more superficial porosity, and G1 and G3 were similar in this regard. Neither the conventional heat-curing cycle nor the microwave cycle affected the amount of residual monomer or porosity of the conventional heat-cured acrylic resin. Water sorption was not affected by the type of resin or polymerization cycle used. Residual monomer release and porosity were related to the type of resin employed rather than the polymerization cycle they were submitted to.

DESCRIPTORS | Acrylic Resins; Dental Materials; Chemical Properties; Ocular Prosthesis; Porosity.

RESUMO | **Porosidade, liberação de monômero residual e sorção de água de resinas termoativadas convencionais, resinas termoativadas para microondas e resinas quimicamente ativadas com ligações cruzadas** • Este estudo comparou a liberação de monômeros residuais, a sorção de água e a porosidade superficial de diferentes resinas acrílicas utilizadas na confecção de próteses oculares: ativadas por calor (HC); ativadas por micro-ondas (MC) e quimicamente polimerizáveis (SC). Quatro grupos foram estabelecidos: G1, HC / ciclo em banho aquecido; G2, MC / ciclo em micro-ondas; G3, HC / ciclo em micro-ondas; G4, SC. A quantidade de monômero residual foi similar nos grupos G1 e G3, menor no G2 e maior no G4. A sorção de água foi similar nos quatro grupos. O grupo G2 apresentou maior porosidade superficial, e os grupos G1 e G3 apresentaram porosidades similares. Os ciclos térmicos por banho aquecido e por micro-ondas não influenciaram a quantidade de monômero residual liberado ou a porosidade das resinas acrílicas polimerizadas por calor. A sorção de água não foi influenciada pelo tipo de resina ou pelo ciclo de polimerização utilizado. A liberação de monômero residual e a porosidade estão relacionadas ao tipo de resina utilizada e não ao ciclo de polimerização empregado.

DESCRITORES | Resinas Acrílicas; Materiais Dentários; Propriedades Químicas; Prótese Ocular; Porosidade.

CORRESPONDING AUTHOR | • **Rodrigo Elias de Oliveira** Laboratory of Human Evolutionary Studies, Department of Genetics and Evolutionary Biology, Institute of Biosciences, University of São Paulo • **Rua do Matão, trav. 14, n. 321,** São Paulo, SP, Brazil • **05508-090** E-mail: eliaso@usp.br

• **Received** Dec 12, 13 • **Accepted** May 16, 14
• **DOI** http://dx.doi.org/10.11606/issn.2357-8041.clrd.2014.68723

INTRODUCTION

Acrylic resins improved prosthetic treatment in cases of eye loss, which were originally treated with glass prostheses.[1] Ocular prostheses are essential to promote normal craniofacial development in children or to maintain facial symmetry in adults with eye loss.[2,3] Periodical changes of the ocular prosthesis are necessary in cases of eye loss during childhood or youth.[4,5] In addition, the loss of prosthetic fit and possible changes in the color of the prosthesis may increase the number of visits to maxillofacial clinics.

This study was conducted because of the constant search for new techniques for the construction of ocular prostheses that will efficiently meet the needs of patients with eye loss. The release of residual monomer in acrylic resins is an important factor, since it may lead to hypersensitivity to the resin and cause eczema in both the skin and mucosa.[6-8] Methyl-methacrylate ranks 8th among the methacrylates that may cause hypersensitivity, accounting for 7.4% of the cases of hypersensitivity to methacrylates.[9]

Water sorption is a feature of acrylic resins that significantly affects their mechanical and dimensional properties. The water pools among the polymers of the acrylic resin by diffusion, and pulls them apart, slightly expanding the resin. This small volume expansion, of approximately 1%, causes a linear expansion of 0.3%, which practically overrides the contraction caused by polymerization of the resin. The micropores that form in the resin, in turn, may lodge bacteria and fungi, favoring plaque formation and hindering proper cleaning of the prosthesis.[10-13]

Comparative analysis of acrylic resins, considering the release of residual acrylic monomer, superficial porosity and water sorption, processed with different polymerization cycles may contribute to the development of new techniques for the construction of ocular prostheses.

MATERIALS AND METHODS

Fifteen specimens 25 mm in diameter by 4 mm in height were manufactured for each of the following experimental groups:

- Group 1 (G1), conventional heat-cured acrylic resin (Clássico, Artigos Odontológicos Clássico Ltda., Brazil), polymerized in water bath;
- Group 2 (G2), microwave-cured acrylic resin (Onda Cryl, Artigos Odontológicos Clássico Ltda., Brazil), polymerized by microwave energy;
- Group 3 (G3), conventional heat-cured acrylic resin, polymerized by microwave energy; and
- Group 4 (G4), self-curing, cross-linked acrylic resin (Orto Clas, Artigos Odontológicos Clássico Ltda., Brazil), polymerized at room temperature.

The conventional heat-cured acrylic resin was prepared according to the manufacturer's instructions, using 14 mL of the monomer and 42 mL of the polymer. G1 specimens were processed raising the temperature of the water bath to 74°C, maintaining it at this temperature for 120 min. and then raising the water temperature to 100°C and maintaining it at this level for 60 additional min..[14] G2 specimens were prepared using the microwave-cured acrylic resin and plastic flasks, since the resin was polymerized in a microwave oven. The polymerization cycle was carried out using an 800 W microwave oven. Each flask was placed in the center of the oven and heated for 3 min. at 320 W. After resting for 4 min., they were reheated for 3 min. at 720 W. G3 specimens were prepared with conventional heat-cured resin, placed in plastic flasks and polymerized according to the processing cycle described for G2 specimens. G4 specimens were manufactured using self-curing acrylic resin, following the procedures described above. G4 was different from the others with regard to the proportion of monomer and polymer used. The powder/liquid

volume ratio was 2.5:1, according to the manufacturer's instructions.

The specimens were finished using a tungsten carbide bur and a white stone bur, and polished using a horizontal sander at 250 rpm with a sequence of sandpaper discs of different grit sizes—320, 400 and 600—under constant irrigation. They were then cleaned using an ultrasonic bath for 2 min.. From this stage on, all specimens were manipulated using tweezers to avoid contamination.

Residual monomer

The specimens were placed in amber-glass bottles filled with 10 mL of deionized water, sealed with plastic film, and kept in a sterilizer at 37°C. Different samples of the solutions in which the specimens were kept were collected every 24 hours and placed in 2 mL Eppendorf tubes for future analysis. After the samples were collected, the specimens were rinsed in distilled water for one second and the remaining solution was discarded. The specimens were then placed in the bottles again, and another 10 mL of deionized water was added. This procedure was repeated for 11 days.

The spectrophotometer used for our analysis was calibrated with a solution of known concentration of monomer. The wavelength used was 206 nm. A standard dilution curve was constructed to be compared with the values obtained by the spectrophotometer and to determine the correct concentrations of residual monomer in the samples collected. In order to do this, the stored solutions were transferred to crystal cuvettes which were then used in the spectrophotometer to measure residual monomer concentration.

Water sorption

The same specimens were used to assess water sorption. They were placed on a paper towel inside a desiccator containing silica gel for dehumidification. After dehydration in a sterilizer for 24 hours at 37°C, the specimens were weighed on a precision scale. The specimens were then immersed in beakers containing deionized water and kept in the sterilizer for seven days at 37°C. After this period, the specimens were retrieved, softly dried with a paper towel and weighed again on the precision scale.

Porosity

The specimens were immersed in beakers containing gentian violet (1% solution in water) and placed on a lab shaker, where they remained for 30 min.. The immersion in gentian violet aimed at staining the superficial micropores. After removal from the gentian violet solution, the specimens were rinsed in distilled running water for one second and dried with a paper towel. They were then analyzed under a stereoscopic microscope with magnification of 20×. The stained pores were clearly distinguished from the white-colored material of the acrylic resins commonly used in eye prostheses.

A built-in digital camera recorded images of five different areas of each specimen. The images were sent to a computer to be processed by ImageLab 2000® software (Softium Informática Ltda., São Paulo, SP, Brazil). The G4 specimens, constructed using self-curing, colorless, cross-linked acrylic resin, were not analyzed for porosity because the absence of contrast hindered image acquisition. Image processing using the software generated a percentage analysis of the darker areas per mm², which corresponded to the areas stained by gentian violet.

Statistical analysis of the properties assessed was made using split-plot one-way analysis of variance and Tukey's test. The significance level was set at $p \leq 0.05$.

RESULTS

Figure 1 shows that G1 specimens had a greater release of residual monomer in the first 24 hours.

Figure 1 | Residual monomer release.

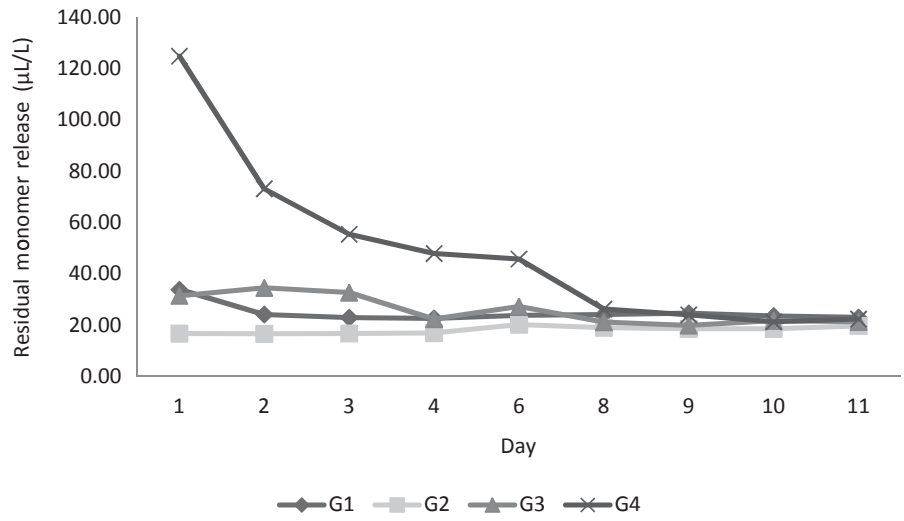

After this period of time, there was a drop of approximately 45% in the release of residual monomer, and this level was maintained until the end of the experiment. G2 specimens showed the lowest release of residual monomer in the first 24 hours, with a level below 20 µL/L throughout the experiment. G3 specimens showed lower release of residual monomer than G1 specimens in the first 24 hours. However, over the same period, this group showed a release of residual monomer twice as high as that showed by G2. G4 specimens showed a greater release of residual monomer in the first 24 hours, three times greater than that showed by G1 and G3, and seven times greater than that showed by G2 (Figure 1).

Statistical analysis of the release of residual monomer by ANOVA and Tukey's test yielded the following results:

- G1 specimens released the highest amount of residual monomer on day one ($p = 0.0001$);
- the amount of residual monomer released by G2 specimens was similar at all time intervals evaluated ($p = 1$);
- the amount of residual monomer released by G3 specimens was lower as of day eight ($p = 0.007$);
- the amount of residual monomer released by G4 specimens was similar on days three and four, and from day eight on ($p = 1$);
- a significant difference in the release of residual monomer was observed among the groups, except between G1 and G3 (Table 1).

The weights of the specimens (in grams), both dry and hydrated, are shown as mean values and standard deviations. There is no statistical difference among these groups when we analyze the water sorption through the weight of the specimens (Table 2).

The superficial porosity of five areas of each specimen was analyzed. For statistical analysis, however, only three areas were considered, disregarding the most discrepant values to avoid distortions. The results are shown as means and standard deviations, expressed in % of total area. Analysis of the data obtained showed that G2 specimens had higher superficial porosity than G1 and G3 specimens, and that G1 and G3 specimens had similar superficial porosity (Table 3).

DISCUSSION

The results obtained suggest that the process employed for polymerization of the heat-cured resin, either in conventional water bath or by microwave energy, does not affect the release of residual

Table 1 | Mean and standard deviation of residual monomer release (μL/L). Different letters (uppercase for groups and lowercase for days) show statistically significant difference ($p < 0.05$; n = 15).

Groups	Days									Total
	1	2	3	4	6	8	9	10	11	
G1	33.84 ± 8.31 Aa	24.16 ± 1.63 Ab	22.91 ± 1.52 Ab	22.58 ± 1.14 Ab	23.73 ± 2.02 ABb	24.12 ± 1.64 Ab	24.60 ± 1.67 Ab	23.54 ± 1.52 Ab	22.98 ± 1.31 Ab	222.45 ± 8.14 A
G2	16.73 ± 0.55 Ba	16.62 ± 0.20 Ba	16.76 ± 0.18 Aa	16.90 ± 0.22 Ba	20.15 ± 2.28 Ab	18.99 ± 1.40 Bb	18.56 ± 0.61 Bb	18.56 ± 0.61 Cb	19.68 3.06 Bb	162.94 4.95 B
G3	31.42 ± 7.75 Aa	34.55 ± 9.62 Ca	32.72 ± 10.86 Ba	22.38 ± 2.83 Ab	27.20 ± 9.77 Bb	21.17 ± 2.11 Cb	19.88 ± 0.70 Bb	21.72 2.84 ABb	21.28 2.30 ABb	244.19 22.13 A
G4	124.80 ± 2.73 Ca	73.13 ± 7.76 Db	55.43 ± 8.53 Cc	47.93 ± 6.29 Cc	45.77 ± 8.52 Cc	26.27 ± 2.05 Dd	24.01 ± 4.62 Ad	21.28 ± 2.15 Be	22.35 ± 2.39 Ae	440.97 ± 27.28 C

Table 2 | Mean and standard deviation of water sorption (grams). No statistically significant difference was observed (n = 15).

	G1	G2	G3	G4
Dried	2.021 ± 0.063	2.041 ± 0.074	2.144 ± 0.065	1.947 ± 0.078
Hydrated	2.037 ± 0.062	2.056 ± 0.075	2.155 ± 0.067	1.970 ± 0.086
Water sorption	0.016 ± 0.004	0.015 ± 0.005	0.011 ± 0.003	0.023 ± 0.037

monomer. Other studies have suggested that heat-cured acrylic resins polymerized by microwave energy release a greater amount of residual monomer than those polymerized by heat.[15,16] However, chemical tests have shown that a lower amount of residual monomer is released when the acrylic resin is polymerized by microwave energy,[17] suggesting that such differences might be due to variations in the composition of the different acrylic resins analyzed and the methodology employed in each study.

In the present study, Onda Cryl®—an acrylic resin for microwave ovens—polymerized by microwave energy released the least residual monomer. This may be due to the fact that the internal boiling of the acrylic monomer produces a smaller amount of residual monomer after final polymerization.[18] Another possible explanation is the higher powder/liquid ratio used with the Onda Cryl® resin, 3:1 in volume, since a high powder/liquid ratio provides a higher-quality resin.[19] The powder/liquid ratio of the Onda Cryl® resin is almost twice the ratio

Table 3 | Mean and standard deviation of porosity (% of the total area). Different letters represent statistically significant difference between groups ($p < 0.05$; n = 45).

G1	G2	G3
0.244 ± 0.079 A	0.456 ± 0.107 B	0.297 ± 0.087 A

of the Acron MC® resin, which was used most in the studies we reviewed. When both brands were compared, the Onda Cryl® resin showed better results.[20]

The amount of residual monomer released by the Orto Clas® resin—a self-curing, cross-linked acrylic resin—was at least three times higher than the amount released by the other groups in the first 24 hours.[21] This is in accordance with the fact that self-curing acrylic resins usually produce 3% to 5% of residual monomer, whereas heat-cured ones produce only 0.2% to 0.5%.[22]

The length of the observation period in this study took into consideration the 14 days which are necessary for the release of residual monomer

to become stable.[8,19] However, our results ran only through the 11th day, since the release of residual monomer became stable in all groups by that time. The results showed a tendency towards stabilization of the residual monomer release in all groups around the eighth day. The time it takes for the residual monomer to be released is an important factor because each different material and processing technique must receive specific treatment after polymerization in order to obtain an ideal prosthesis.[19] Both the acrylic resins and the polymerization cycles used in this study are considered acceptable for the construction of prostheses.[23]

Water sorption was assessed considering the weight of the specimens in grams, both dry and hydrated. The standard deviation for all specimens when dry was 0.01, indicating that the specimens were adequately manufactured. The four experimental groups yielded similar results regarding water sorption. The absence of a significant difference among the groups means that the three types of resin analyzed in this study showed similar water sorption, regardless of the polymerization cycle to which they were submitted.

The possibility of using microwave energy to polymerize conventional acrylic resins and obtain water sorption properties that comply with ADA (American Dental Association) specifications indicated that water sorption depends on the polymerization cycle used.[22,24,25] In the present study, the polymerization cycle in microwave oven to which the conventional acrylic resin was submitted did not affect water sorption. The lower water sorption of the cross-linked acrylic resin observed in another study[26] was not confirmed in this study.

Similarity in water sorption among the types of acrylic resin analyzed in this study was also found when the conventional acrylic resin was compared with hypoallergenic materials.[27] Although the time that we use to dry off and moisturize the samples could be shorter than necessary, making our results on the sorption of water among the four groups statistically similar, a study designed to analyze porosity in which the specimens were weighed both when dry and hydrated also found a similarity in weight among the different acrylic resins when hydrated.[28]

Polymerization of acrylic resins is an exothermic reaction, and the increase in temperature can cause the boiling of the reactive monomer, which leads to the formation of bubbles in the resin. When the acrylic portion of a prosthesis is thin, the heat can leave the resin and dissipate in the surrounding cast, preventing the appearance of superficial bubbles.[22] This has led to the study of adjustments made to microwave power and polymerization time, so that resins polymerized by microwave energy show porosity similar to that of conventional resins.[29-31] It has also been observed that the number of flasks and their placement in the microwave oven affect the amount of residual monomer and resin porosity.[32,33]

The method employed in this study considered the polymerization of each flask individually, placed in the center of the microwave oven. This was done to avoid interference caused by the number of flasks or their position during polymerization. The method employed by us to assess superficial porosity is quite accurate, since the computer analysis yields the sum of all the pores on the surface, presented as a percentage of the total area observed. The superficial porosity of the self-curing, colorless, cross-linked resin was not assessed because the lack of contrast made it impossible to acquire an image that could be processed by ImageLab 2000® software.

The absence of superficial porosity in heat-cured acrylic resins has already been described,[30] and in the present study this type of resin showed the lowest percentage of superficial porosity, corresponding to 0.24% of the resin surface. The microwave-cured resin showed a higher percentage of superficial porosity than the conventional resin regardless of the polymerization cycle employed,

which is in accordance with previous studies.[29,34] The conventional resin showed greater superficial porosity when polymerized by microwave energy than when polymerized in water bath. However, this difference in superficial porosity was not statistically significant, which is in disagreement with previous studies.[35]

CONCLUSIONS

The water-bath and microwave cycles did not affect the amount of residual monomer released by or the porosity of the conventional heat-cured acrylic resin. The amount of residual monomer produced varied according to the type of acrylic resin. Water sorption was not affected by the type of resin or polymerization cycle. Porosity was related to the type of acrylic resin employed rather than the polymerization cycle. The results of this comparative study regarding porosity, amount of residual monomer released and water sorption suggest that conventional heat-cured acrylic resins processed by microwave energy may be used to optimize treatment with an eye prosthesis. Nevertheless, other resin properties should be investigated before this can be recommended for clinical application.

ACKNOWLEDGMENT

We would like to thank Prof. Dr. Fausto Medeiros Mendes (University of São Paulo) for his support in the statistical analysis.

REFERENCES

1. Chalian V, Drane J, Standish S. Maxillofacial Prosthetics - multidisciplinary practice. Baltimore: The Williams & Wilkins; 1972.
2. Fountain TR, Goldberger S, Murphree AL. Orbital development after enucleation in early childhood. Ophthal Plast Reconstr Surg. 1999 Jan;15(1):32-6.
3. Gaia BF, Cheng CK, Perrone LJ, Rose MC, Mattos BS. Study of dimensional alterations of the orbit following loss of the eye. Int J Prosthodont. 2006 May-Jun;19(3):264-5.
4. Coas VR, Neves AC, Rode SM. Evaluation of the etiology of ocular globe atrophy or loss. Braz Dent J. 2005;16(3):243-6. doi: 10.1590/S0103-64402005000300013.
5. Mattos BSC, Montagna MC, Fernandes CS, Saboia AC. The pediatric patient at a maxillofacial service: Eye prosthesis. Braz Oral Res. 2006 Jul-Sep;20(3):247-51. doi: 10.1590/S1806-83242006000300012.
6. Bastiaan RJ. Denture estomatitis. In: Smith DC, Williams DF. Biocompatibility of dental materials. Boca Raton: CRC Press; 1982.
7. Manikantan NS, Ahila SC, Manojkumar AD. Cytotoxicity of acrylic denture base resins. KDJ (Kerala Dental Journal). 2011 Mar;34(1 Suppl):105-6.
8. Çelebi N, Yüzügüllü B, Canay S, Yücel U. Effect of polymerization methods on the residual monomer level of acrylic resin denture base polymers. Polym Adv Technol. 2008 Mar;19(3):201-6. doi: 10.1002/pat.996.
9. Kanerva L, Jolanki R, Estlander T. 10 years of patch testing with the (meth)acrylate series. Contact Dermatitis. 1997 Dec;37(6):255-8. doi: 10.1111/j.1600-0536.1997.tb02460.x.
10. Verran J, Maryan CJ. Retention of Candida albicans on acrylic resin and silicone of different surface topography. J Prosthet Dent. 1997 May;77(5):535-9. doi: 10.1016/S0022-3913(97)70148-3.
11. Radford DR, Sweet SP, Challacombe SJ, Walter JD. Adherence of Candida albicans to denture-base materials with different surface finishes. J Dent. 1998 Sep;26(7):577-83. doi: 10.1016/S0300-5712(97)00034-1.
12. Radford DR, Challacombe SJ, Walter JD. Denture plaque and adherence of Candida albicans to denture-base materials in vivo and in vitro. Crit Rev Oral Biol Med. 1999;10(1):99-116.
13. Salim N, Satterthwaite JD, Rautemaa R, Silikas N. Impregnation with antimicrobials challenge bonding properties and water sorption behaviour of an acrylic liner. J Dent. 2012 Aug;40(8):693-9. doi: 10.1016/j.jdent.2012.04.027.
14. Anusavice KJ. Phillips Materiais dentários. 10a ed. Rio de Janeiro: Guanabara Koogan; 1998.
15. Aldoori D, Huggett R, Bates JF, Brooks SC. A Comparison of Denture Base Acrylic Resins Polymerized by Microwave Irradiation and by Conventional Water Bath Curing Sys-

tems. Dent Mater. 1988 Feb;4(1):25-32. doi:10.1016/S0109-5641(88)80084-8.

16. Blagojevic V, Murphy VM. Microwave polymerization of denture base materials. A comparative study. J Oral Rehabil. 1999 Oct;26(10):804-8. doi: 10.1046/j.1365-2842.1999.00456.x
17. De Clerck JP. Microwave polymerization of acrylic resins used in dental prostheses. J Prosthet Dent. 1987 May;57(5):650-8. doi:10.1016/0022-3913(87)90353-2.
18. Reitz PV, Sanders JL, Levin B. The curing of denture acrylic resins by microwave energy. Physical properties. Quintessence Int. 1985 Aug;16(8):547-51.
19. Lamb DJ, Ellis B, Priestley D. Loss into water of residual monomer from autopolymerizing dental acrylic resin. Biomaterials. 1982 Jul;3(3):155-9. doi:10.1016/0142-9612(82)90005-9.
20. Del Bel Cury AA, Rached RN, Ganzarolli SM. Microwave-cured acrylic resins and silicone-gypsum moulding technique. J Oral Rehabil. 2001 May; 28(5):433-8. doi: 10.1046/j.1365-2842.2001.00684.x.
21. Tuna SH, Keyf F, Gumus HO, Uzun C. The Evaluation of Water Sorption/Solubility on Various Acrylic Resins. Eur J Dent. 2008 Jul;2(3):191-7.
22. Phoenix RD. Resinas para Base de Prótese Total. In: Anusavice KJ. Phillips Materiais dentários. 11a ed. Rio de Janeiro: Elsevier; 2005.
23. Paes-Junior TJA, Carvalho RF, Cavalcanti SCM, Saavedra GSFA, Borges ALS. Influence of plaster drying on the amount of residual monomer in heat-cured acrylic resins. Braz J Oral Sci. 2013 Abr-Jun;12(2):84-9.
24. Ilbay SG, Guvener S, Alkumru HN. Processing dentures using a microwave technique. J Oral Rehabil. 1994 Jan;21(1):103-9. doi:10.1111/j.1365-2842.1994.tb01129.x.
25. Revised American Dental Association specification no. 12 for denture base polymers. J Am Dent Assoc. 1975 Feb;90(2):451-8.
26. Arima T, Murata H, Hamada T. Properties of highly cross-linked autopolymerizing reline acrylic resins. J Prosthet Dent. 1995 Jan;73(1):55-9.
27. Pfeiffer P, Rosenbauer EU. Residual methyl methacrylate monomer, water sorption, and water solubility of hypoallergenic denture base materials. J Prosthet Dent. 2004 Jul;92(1):72-8. doi:10.1016/S0022391304002057.
28. Compagnoni MA, Barbosa DB, de Souza RF, Pero AC. The effect of polymerization cycles on porosity of microwave-processed denture base resin. J Prosthet Dent. 2004 Mar;91(3):281-5. doi:10.1016/S0022391304000083.
29. Levin B, Sanders JL, Reitz PV. The use of microwave energy for processing acrylic resins. J Prosthet Dent. 1989 Mar;61(3):381-3. doi:10.1016/0022-3913(89)90150-9.
30. Alkhatib MB, Goodacre CJ, Swartz ML, Munoz-Viveros CA, Andres CJ. Comparison of microwave-polymerized denture base resins. Int J Prosthodont. 1990 May-Jun;3(3):249-55.
31. Rizzatti-Barbosa CM, Ribeiro-Dasilva MC. Influence of Double Flask Investing and Microwave Heating on the Superficial Porosity, Surface Roughness, and Knoop Hardness of Acrylic Resin. J Prosthodont. 2009 Aug;18(6):503-6. doi: 10.1111/j.1532-849X.2009.00469.x.
32. Oliveira VM, Leon BL, Del Bel Cury AA, Consani S. Influence of number and position of flasks in the monomer release, Knoop hardness and porosity of a microwave-cured acrylic resin. J Oral Rehabil. 2003 Nov;30(11):1104-8. doi: 10.1046/j.1365-2842.2003.01195.x
33. Botega DM, de Souza Machado T, de Mello JA, Garcia RC, Del Bel Cury AA. Polymerization time for a microwave-cured acrylic resin with multiple flasks. Braz Oral Res. 2004 Jan-Mar;18(1):23-8.
34. Ganzarolli SM, Nunes de Mello JA, Shinkai RS, Del Bel Cury AA. Internal adaptation and some physical properties of methacrylate-based denture base resins polymerized by different techniques. J Biomed Mater Res B: Appl Biomater. 2007 Jul;82(1):169-73. doi: 10.1002/jbm.b.30718.
35. Yannikakis S, Zissis A, Polyzois G, Andreopoulos A. Evaluation of porosity in microwave-processed acrylic resin using a photographic method. J Prosthet Dent. 2002 Jun;87(6):13-9. doi: 10.1067/mpr.2002.124490.

Clinical and Laboratorial Research in Dentistry

Cytotoxicity of substances leached from a root canal sealer based on mineral trioxide aggregate

• **Roberta Souza D'Almeida Couto** Department of Restorative Dentistry, School of Dentistry, University of São Paulo, São Paulo, SP, Brazil • **Sueli Patricia Harumi Miyagi** Departament of Endodontics, School of Dentistry, Braz Cubas University, Mogi das Cruzes, SP, Brazil • **Maria Stella Moreira** Department of Restorative Dentistry, School of Dentistry, University of São Paulo, São Paulo, SP, Brazil • **José Ricardo Archilla** Department of Restorative Dentistry, School of Dentistry, University of São Paulo, São Paulo, SP, Brazil • **Márcia Martins Marques** Department of Restorative Dentistry, School of Dentistry, University of São Paulo, São Paulo, SP, Brazil

ABSTRACT | *Aim:* Based on its biological and physicochemical characteristics, mineral trioxide aggregate (MTA) could be considered the most appropriate material for root canal obturation; nevertheless, handling of MTA is not easy. The MTA Fillapex (MTA-F) was created in an attempt to combine the physicochemical properties of a root canal sealer with the biological properties of MTA. However, the studies on the biological characteristics of MTA-F are still controversial. Thus, this study aimed to analyze the cytotoxicity of MTA-F. *Materials and Methods:* Cultured human gingival fibroblasts were grown in Dulbecco's modified Eagle Medium (DMEM) and submitted to a cell culture medium conditioned by MTA or MTA-F. The conditioned medium contained substances leached from the root canal sealers. Cells grown on a fresh medium served as a positive control. Cell viability was assessed by MTT assay at 1, 3, 5 and 7 days. Data was compared by ANOVA followed by Tukey's test ($p < 0.05$). *Results:* Cells submitted to media conditioned by MTA presented a cell growth curve similar to that of the control cells. For the MTA-F group, cell growth was not observed and cell viability was significantly lower than for the other groups during the entire experiment. *Conclusion:* Substances leached from MTA-F did not allow cell growth, indicating that this MTA-based root sealer is highly cytotoxic. The biocompatibility characteristic of MTA can be lost with MTA-F, and may compromise the endodontic treatment outcome.

DESCRIPTORS | Endodontics; Cell Culture Techniques; Biocompatible Materials.

RESUMO | **Citotoxicidade de substâncias liberadas por um cimento endodôntico à base do agregado de trióxido mineral** • *Objetivo:* Com base nas características biológicas e físico-químicas do agregado de trióxido mineral (MTA), este seria o material mais adequado para a obturação do canal radicular. No entanto, esse material apresenta baixo escoamento e, consequentemente, difícil manipulação. O MTA Fillapex (MTA-F) foi criado na tentativa de combinar as propriedades físico-químicas do cimento endodôntico com as propriedades biológicas do MTA. No entanto, os estudos sobre as características biológicas do MTA-F ainda são controversos. Dessa forma, este estudo teve como objetivo analisar *in vitro* a citotoxicidade do MTA-F. *Materiais e Métodos:* fibroblastos gengivais foram cultivados em *Dulbecco's modified Eagle Medium* (DMEM) e submetidos ao meio de cultura condicionado pelo MTA ou MTA-F. Esse meio condicionado continha substâncias liberadas pelos cimentos endodônticos. Células cultivadas em meio fresco serviram como controle positivo. A viabilidade celular foi avaliada por ensaio do MTT após 1, 3, 5 e 7 dias. Os dados obtidos foram comparados por análise de variância (ANOVA) seguida pelo teste de Tukey ($p < 0,05$). *Resultados:* As células submetidas ao meio condicionado pelo MTA apresentaram curva de crescimento celular semelhante à das células do grupo controle. Para o grupo MTA-F, não houve crescimento celular e foi observado um número de células viáveis significativamente menor do que o dos demais grupos durante todo o experimento. *Conclusão:* Substâncias liberadas a partir de MTA-F não permitiram o crescimento celular, mostrando que esse cimento endodôntico à base de MTA é altamente citotóxico. A característica de biocompatibilidade do MTA pode ser perdida com o MTA-F e comprometer o sucesso do tratamento endodôntico.

DESCRIPTORS | Endodontia; Técnicas de Cultura de Células; Materiais Biocompatíveis.

CORRESPONDING AUTHOR | • **Márcia Martins Marques** Department of Restorative Dentistry, School of Dentistry, University of São Paulo • **Av. Prof. Lineu Prestes, 2227** São Paulo, SP, Brazil • **005508-000** E-mail: mmmarques@usp.br

• **Received** Mar 11, 2013 • **Accepted** Mar 24, 2014
• **DOI** http://dx.doi.org/10.11606/issn.2357-8041.clrd.2014.63160

INTRODUCTION

Mineral trioxide aggregate (MTA®, Loma Linda University, Loma Linda, CA, USA) has been reported to be a biocompatible material. Moreover, MTA presents osteogenic, inductive and conductive activities on hard tissue formation. MTA is also able to improve the secretion of interleukin (IL-1β) by neutrophils *in vitro*,[1] a cytokine secreted *in vivo* during the inflammatory process which is important for tissue repair.[2] This material has been used in several dental procedures and presents an advantage over other endodontic filling materials due to its physicochemical, bioactive and sealing ability properties.[3-10] However, despite these favorable characteristics, MTA does not exhibit the physical properties needed to be used as a sealer, owing to its long setting time and difficult handling in the insertion of material into the canal.[6-11]

To circumvent the handling difficulty of MTA, the industry has searched for compositions of MTA-based root canal sealers which combine the desirable physicochemical properties of endodontic sealers and the biological properties of MTA.[12] MTA Fillapex® (Angelus®, Londrina, PR, Brazil) is an MTA-based root canal sealer introduced to the market with this proposal. However, there are few studies on the biological characteristics of this material and they are controversial.

The biological aspects of MTA Fillapex® (MTA-F) have been tested *in vivo*[13,14] using an animal model, applying the sealer in rat subcutaneous tissue and *in vitro* using cells in culture.[15-21] Initial studies were carried out in rat subcutaneous tissue. MTA-F evoked a tissue response similar to that of Angelus MTA®, leading to the conclusion that both materials are biocompatible, bioactive and stimulate mineralization.[13] On the other hand, Zmener *et al.*[14] concluded that the material remained toxic until 90 days after implantation in rat subcutaneous tissue. Reports on the *in vitro* cytotoxicity of MTA-F have shown effects regardless of testing time.[15,18] Moreover, it causes cell death and micronucleus formation in cultured cells.[16] On the other hand, another *in vitro* study observed that, once set, the material cytotoxicity decreases, resulting in suitable bioactivity.[17] In these studies the MTA-based sealer was applied to the cultures at different times after handling. Knowing that the substances leached from root canal sealers during setting are important in determining the initial periapical tissue response, the present study aimed to analyze the cytotoxicity of substances leached from an MTA-based canal sealer during its setting on human cultured fibroblasts and discuss current knowledge about the biological properties of MTA-F.

MATERIALS AND METHODS

Cell culture

This study was approved by the Human Research Ethics Committee of the School of Dentistry, University of São Paulo (CAAE 0116.0.017.000-11). Human gingival fibroblasts (FMM1 cells) grown between the fifth and the tenth passages were used. These cells were retrieved from the files of the cell bank, Department of Restorative Dentistry, School of Dentistry, University of São Paulo. The cells were cultured in high glucose Dulbecco's modified Eagle Medium (DMEM, LGC Biotecnologia, Cotia, SP, Brazil) supplemented with 10% fetal bovine serum (FBS, Cultilab, Campinas, SP, Brazil) and a 1% antibiotic-antimicotic solution (Penicilin-Streptomicin, LGC Biotecnologia, Cotia, SP, Brazil). The cell growth was monitored daily using phase contrast microscopy, the medium was changed every other day, and the cells were maintained in an incubator at 37°C in a humid atmosphere containing 5% CO_2 and 95% air.

Conditioned medium

The mineral trioxide aggregate endodontic sealer (MTA®, Loma Linda University, Loma Linda, CA, USA), White MTA (MTA) and MTA Fillapex (MTA-F) were prepared according to the manu-

facturers' instructions and immediately applied to the bottom of 50 mL centrifuge tubes. The material was weighed and fresh medium was added to the tubes to produce a proportion of 0.02 g of MTA-F for each mL of medium.

Experiments

Prior to the experiments, cells were plated (2×10^3 cells/well) in 24-well culture plates and maintained in an incubator for 24 h. Then, the culture medium of each well was replaced by the experimental medium (i.e. fresh medium for the control group and conditioned media for the test groups). The conditioned media remained in contact with the cells for 1, 3, 5 and 7 days. Every other day, half of the medium of each well was replaced by fresh medium, in order to simulate the solubility of canal sealers in periapical tissues. All the experimental groups were tested in triplicates.

Cytotoxicity analysis

After exposure of the cultured cells to the conditioned media, the cell viability of all groups was measured. This analysis was based on a measurement of cell mitochondrial activity using the MTT-based (Invitrogen, Eugene, OR, USA) cytotoxicity assay. This assay involves the conversion of water-soluble MTT [3-(4,5-dimethylthiazol-2-yl)-2,5-diphenyltetrazolium bromide] to insoluble formazan. This salt is then solubilized in order to measure its concentration by optical density (570 nm, Biotrak II, Biochrom Ltd., Eugendorf, Austria). According to Freshney,[18] this assay indirectly determines cell viability. Thus, the percentage of cell viability was calculated by using the mean absorbance data of the control group as 100%. Viabilities smaller than 70% are considered cytotoxic according to ISO 10993-5:2009.[22]

Experimental groups

The experimental groups were as follows:

- Control Group (CG): Cells grown in fresh medium;
- MTA-F: Cells grown in medium conditioned by MTA Fillapex root canal sealer;
- MTA: Cells grown in medium conditioned by White MTA cement.

Statistical analysis

The data was presented as optical density mean ± standard error of the mean (SEM) or cell viability percentages. Data was compared by analysis of variance (ANOVA) complemented by Tukey's test. The significance level was 5% ($p \leq 0.05$).

RESULTS

Figure 1 graphically illustrates the cell growth curves of all the experimental groups. The control group showed continuous growth. The amount of viable cells was significantly higher at the end of the experiment than at the beginning ($p < 0.01$). A similar result was observed for the MTA group ($p < 0.01$). The cells in the MTA-F group did not show cell growth. The number of viable cells in this group was significantly smaller than that of the other groups during the entire experiment ($p < 0.01$).

Figure 2 shows the percentage of cell viability of all the experimental groups during the entire experiment. Only the MTA-F group showed cell viabilities smaller than 20%.

DISCUSSION

The characteristics of mineral trioxide aggregate (MTA) such as biocompatibility, bioactivity, and osteoconductivity[6,23,24] are the most desirable biological properties of an endodontic sealer. However, handling of MTA is not easy. So, in an attempt to combine the physicochemical properties of a resinous root canal sealer with the biological properties of White MTA (MTA), MTA Fillapex (MTA-F) was created. The biological properties of this material have been studied with controversial results.

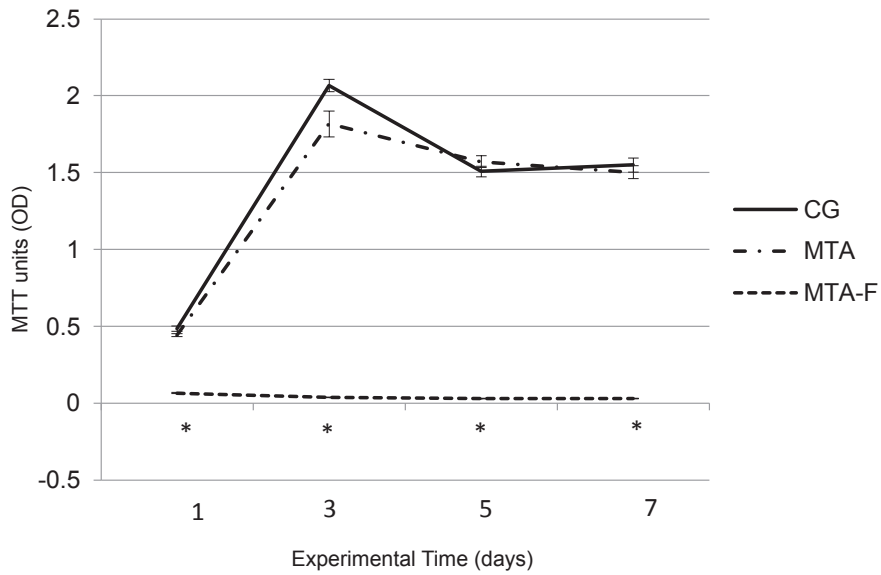

Figure 1 | Graphic representation of mean (± standard error of the mean, SEM) cell viability (MTT units in optical densities, OD) as a function of experimental time (hours). **CG:** Control Group; **MTA:** White MTA cement; **MTA-F:** MTA Fillapex canal sealer.

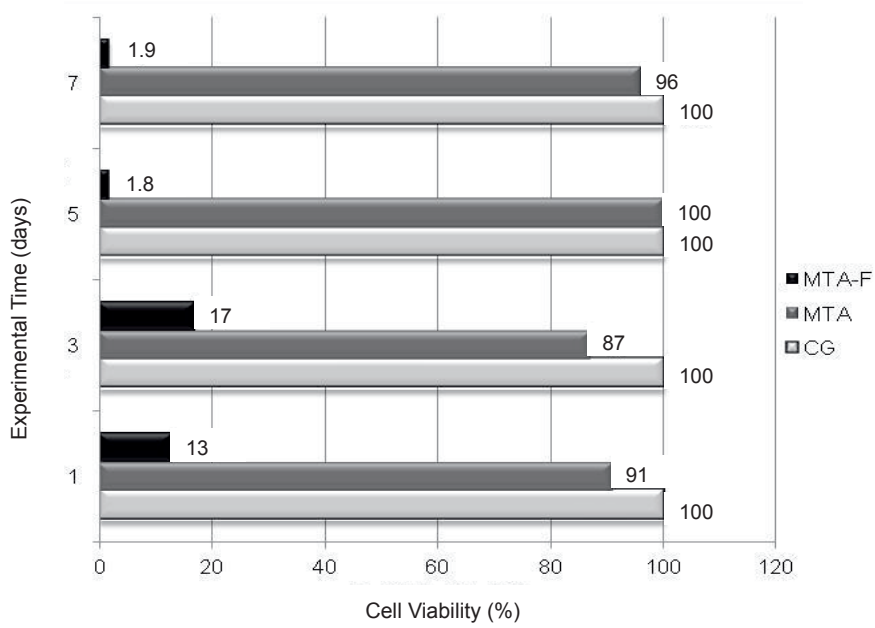

Figure 2 | Graphic representation of cell viability (in percentage) as a function of experimental time (hours). **CG:** Control Group; **MTA:** White MTA cement; **MTA-F:** MTA Fillapex canal sealer. Note that only MTA-F showed viabilities lower than 20% during the entire experimental time.

For this reason, this study compared the MTA-F and MTA root canal sealers by analyzing the effects of substances leached from these materials on cell viability. The method chosen was the analysis of mitochondrial activity, the MTT assay, against cultured media conditioned by the endodontic sealers.

The MTA group presented viability and cell growth similar to that of the control group. This would explain the favorable response of the periapical tissues to MTA.[15,22] This material has been confirmed over the years as a promising endodontic material for root canal filling, perforation repair, vital pulp therapy, apical barrier formation for teeth with necrotic pulps and open apexes, and internal and external root resorptions.[4,25-27] Nevertheless, MTA presents disadvantages such as handling difficulty and long setting time.[3,6,11]

The present study showed that MTA-F is highly

cytotoxic, because it prevented cellular growth during the entire experimental time. This finding corroborates previous *in vitro*[15,16,18,19,21] and *in vivo*[14] studies suggesting that this material is cytotoxic, even a long time after exposure. A possible explanation for the high level of MTA-F cytotoxicity could be related to the presence of toxic products from resin and/or unpolymerized resin monomers of the paste-paste MTA-F system. Concurring with this hypothesis, Zmener *et al.*[14] reported a severe inflammatory reaction *in vivo* that persisted until the end of the experiment (90 days) with MTA-F in rat subcutaneous tissue.

The cytotoxic effect of MTA-F persisted even 7 days after exposure. On the other hand, a study by Salles *et al.*[17] showed that this cytotoxicity effect occurred only up to day 7 in culture, after which cell viability recovered. The differences in methodology of these two studies could explain this disagreement. In fact, these authors placed polymerized MTA-F in direct contact with osteoblasts, whereas, in the present study, the contact was indirect, using cultured medium that was conditioned by MTA-F during the polymerization process. Thus, this conditioned medium would contain MTA-F byproducts (e.g. unpolymerized resin monomers or other byproducts) that leached from the MTA-F during the polymerization process. Another *in vivo* study also showed that the cytotoxicity of MTA-F was only observed in the early periods of analysis, and that, after 2 weeks, the MTA-F and the MTA produced similar tissue reactions.[13] Thus, further research must be conducted to better understand the tissue response to MTA-F before polymerization, by mimicking the clinical situation in which unpolymerized material remains in contact with periapical tissues until complete polymerization occurs.

Clinically, an adequate apical seal is considered an important factor for improving endodontic success.[28,29] Moreover, the material must not impair periapical tissue repair.[3] Although MTA does not impair periapical tissue repair,[24,30] when resin is incorporated, as in MTA-F, this biocompatible characteristic of MTA is lost, thus jeopardizing the endodontic treatment.

The present study confirmed the cytotoxicity of MTA-F. Only a few authors have studied this material and some of them showed similar results;[15,16,18,19,21] however, confirmation of these results is important to support this piece of evidence. An interesting finding of this study is that there was a higher cytotoxic effect of MTA-F at 5 and 7 days despite the continuing dilution of the conditioned media. This data may suggest that, besides affecting cell viability, MTA-F may affect important biological aspects of the surviving cells that impaired their continued growth. Taken together, the available data allow us to suggest that the hypothesis that MTA-F would combine the physicochemical properties of a resin root canal sealer with the biological properties of MTA was wrong. Thus, future studies are warranted to understand the degree of cellular changes caused by the soluble components of MTA-F to living cells. Additionally, *in vivo* studies must be conducted using MTA-F in the dental root canal system in order to observe the response of periapical tissues when tissue conditions are quite different from those of the *in vitro* studies and even *in vivo* studies conducted in rat subcutaneous tissue.

ACKNOWLEDGEMENTS

The authors wish to thank the "Angelus® Science and Technology" company for donating the endodontic sealers used in this study.

REFERENCES

1. Cavalcanti BN, Rode S de M, França CM, Marques MM. Pulp capping materials exert an effect on the secretion of IL-1β and IL-8 by migrating human neutrophils. Braz Oral Res. 2011Jan-Feb;25(1):13-8.
2. Barkhordar RA, Ghani QP, Russell TR, Hussain MZ. Interleukin-1beta activity and collagen synthesis in human dental pulp fibroblasts. J Endod. 2002 Mar;28(3):157-9.
3. Parirokh M, Torabinejad M. Mineral trioxide aggregate: a comprehensive literature review-part III: Clinical applications, drawbacks, and mechanism of action. J Endod. 2010 Mar;36(3):400-13. doi: 10.1016/j.joen.2009.09.009.
4. Mente J, Hage N, Pfefferle T, Koch MJ, Geletneky B, Dreyhaupt J, et al. Treatment outcome of mineral trioxide aggregate: repair of root perforations. J Endod. 2010 Feb;36(2):208-13. doi: 10.1016/j.joen.2009.10.012. Epub 2009 Dec 16.
5. Damle SG, Bhattal H, Loomba A. Apexification of anterior teeth: a comparative evaluation of mineral trioxide aggregate and calcium hydroxide paste. J Clin Pediatr Dent. 2012 Spring;36(3):263-8.
6. Torabinejad M, Hong CU, McDonald F, Pitt Ford TR. Physical and chemical properties of a new root-end filling material. J Endod. 1995 Jul;21(7):349-53.
7. Fridland M, Rosado R. Mineral trioxide aggregate (MTA) solubility and porosity with different water-to-powder ratios. J Endod. 2003 Dec;29(12):814-7.
8. Camilleri J, Montesin FE, Brady K, Sweeney R, Curtis RV, Ford TR. The constitution of mineral trioxide aggregate. Dent Mater. 2005 Apr;21(4):297-303. Epub 2007 Jul 19.
9. Gomes-Filho JE, Moreira JV, Watanabe S, Lodi CS, Cintra LT, Dezan Junior E, et al. Sealability of MTA and calcium hydroxide containing sealers. J Appl Oral Sci. 2012 May-Jun;20(3):347-51.
10. Mozayeni MA, Milani AS, Marvasti LA, Asgary S. Cytotoxicity of calcium enriched mixture cement compared with mineral trioxide aggregate and intermediate restorative material. Aust Endod J. 2012;38:70-75. doi: 10.1111/j.1747-4477.2010.00269.x. Epub 2010 Oct 24.
11. Parirokh M, Torabinejad M. Mineral Trioxide Aggregate: a comprehensive literature review-part I: chemical, physical, and antibacterial properties. J Endod. 2010 Jan;36(1):16-27. doi: 10.1016/j.joen.2009.09.006.
12. Al-Hiyasat AS, Tayyar M, Darmani H. Cytotoxicity evaluation of various resin based root canal sealers. Int Endod J. 2010 Feb;43(2):148-53. doi: 10.1111/j.1365-2591.2009.01669.x.
13. Gomes-Filho JE, Watanabe S, Lodi CS, Cintra LT, Nery MJ, Filho JA, et al. Rat tissue reaction to MTA FILLAPEX(®). Dent Traumatol. 2012 Dec;28(6):452-6. doi: 10.1111/j.1600-9657.2011.01096.x. Epub 2011 Dec 8.
14. Zmener O, Martinez Lalis R, Pameijer CH, Chaves C, Kokubu G, Grana D. Reaction of rat subcutaneous connective tissue to a mineral trioxide aggregate–based and a zinc oxide and eugenol sealer. J Endod. 2012 Sep;38(9):1233-8. doi: 10.1016/j.joen.2012.05.010. Epub 2012 Jul 6.
15. Scelza MZ, Linhares AB, da Silva LE, Granjeiro JM, Alves GG. A multiparametric assay to compare the cytotoxicity of endodontic sealers with primary human osteoblasts. Int Endod J. 2011 Jan;45(1):12-8. doi: 10.1111/j.1365-2591.2011.01941.x. Epub 2011 Sep 8.
16. Bin CV, Valera MC, Camargo SE, Rabelo SB, Silva GO, Balducci I, et al. Cytotoxicity and genotoxicity of root canal sealers based on mineral trioxide aggregate. J Endod. 2012 Apr;38(4):495-500. doi: 10.1016/j.joen.2011.11.003. Epub 2011 Dec 23.
17. Salles LP, Gomes-Cornélio AL, Guimarães FC, Herrera BS, Bao SN, Rossa-Junior C, et al. Mineral trioxide aggregate-based endodontic sealer stimulates hydroxyapatite nucleation in human osteoblast-like cell culture. J Endod. 2012 Jul;38(7):971-6. doi: 10.1016/j.joen.2012.02.018. Epub 2012 Apr 6.
18. Silva EJNL, Rosa TP, Herrera DR, Jacinto RC, Gomes BPFA, Zaia AA. Evaluation of Cytotoxicity and physicochemical properties of calcium silicate-based endodontic sealer MTA Fillapex. J Endod. 2013 Feb;39(2):274-7. doi: 10.1016/j.joen.2012.06.030. Epub 2012 Aug 9.
19. Yoshino P, Nishiyama CK, Modena KC, Santos CF, Sipert CR. In vitro cytotoxicity of white MTA, MTA Fillapex® and Portland cement on human periodontal ligament fibroblasts. Braz Dent J. 2013;24(2):111-6. doi: 10.1590/0103-6440201302115.
20. Silva EJ, Santos CC, Zaia AA. Long-term cytotoxic effects of contemporary root canal sealers. J Appl Oral Sci. 2013 Jan-Feb;21(1):43-7.
21. Güven EP, Yalvaç ME, Kayahan MB, Sunay H, Şahın F, Bayirli G. Human tooth germ stem cell response to calcium-silicate based endodontic cements. J Appl Oral Sci. 2013 Jul-Aug;21(4):351-7. doi: 10.1590/1678-775720130047.
22. International Organization for Standardization ISO10993-5: biological evaluation of medical devices - Part 5: tests for in vitro cytotoxicity. [place unknown]: ISO; 2009.

23. Torabinejad M, Parirokh M. Mineral trioxide aggregate: a comprehensive literature review-part II: leakage and biocompatibility investigations. J Endod. 2010 Feb;36(2):190-202. doi: 10.1016/j.joen.2009.09.010.
24. Viola NV, Guerreiro-Tanomaru JM, da Silva GF, Sasso-Cerri E, Tanomaru-Filho M, Cerri PS. Biocompatibility of an experimental MTA sealer implanted in the rat subcutaneous: quantitative and immunohistochemical evaluation. J Biomed Mater Res B Appl Biomater. 2012 Oct;100B(7):1773-81. doi: 10.1002/jbm.b.32744. Epub 2012 Jul 23.
25. Cintra LT, Ribeiro TA, Gomes-Filho JE, Bernabé PF, Watanabe S, Facundo AC, et al. Biocompatibility and biomineralization assessment of a new root canal sealer and root-end filling material. Dent Traumatol. 2013 Apr;29(2):145-50. doi: 10.1111/j.1600-9657.2012.01142.x. Epub 2012 Apr 18.
26. Annamalai S, Mungara J. Efficacy of mineral trioxide aggregate as an apical plug in non-vital young permanent teeth: preliminary results. J Clin Pediatr Dent. 2010 Winter;35(2):149-55.
27. Kqiku L, Ebeleseder KA, Glockner K. Treatment of invasive cervical resorption with sandwich technique using mineral trioxide aggregate: a case report. Oper Dent. 2012 Jan-Feb;37(1):98-106. doi: 10.2341/11-143-S. Epub 2011 Sep 27.
28. Torabinejad M, Pitt Ford TR. Root end filling materials: a review. Endod Dent Traumatol. 1996 Aug;12(4):161-78.
29. Sritharan A. Discuss that the coronal seal is more important than the apical seal for endodontic success. Aust Endod J. 2002 Dec;28(3):112-5.
30. Song M, Kim E. A prospective randomized controlled study of mineral trioxide aggregate and super ethoxy-benzoic acid as root-end filling materials in endodontic microsurgery. J Endod. 2012 Jul;38(7):875-9. doi: 10.1016/j.joen.2012.04.008. Epub 2012 May 16.

CLRD in Clinical and Laboratorial Research in Dentistry | Laser Therapy

Efeito da laserterapia sobre IGF-1 nas glândulas submandibulares e parótidas de animais diabéticos induzidos por estreptozotocina

• **Danielle Lima Corrêa de Carvalho** Department of Biomaterials and Oral Biology, School of Dentistry, University of São Paulo, São Paulo, SP, Brazil • **José Nicolau** Department of Biomaterials and Oral Biology, School of Dentistry, University of São Paulo, São Paulo, SP, Brazil • **Alyne Simões** Department of Biomaterials and Oral Biology, School of Dentistry, University of São Paulo, São Paulo, SP, Brazil

RESUMO | O Diabetes mellitus é um distúrbio metabólico de etiologia múltipla, caracterizado por hiperglicemia, podendo ocasionar disfunções e falências de órgãos e tecidos, incluindo as glândulas salivares. Estudos demonstraram uma diminuição da glicemia de ratas diabéticas com o uso de laser de baixa potência (LBP) em glândulas salivares; no entanto, o mecanismo de ação do laser sobre o metabolismo dos carboidratos ainda é desconhecido. Assim, o objetivo do presente estudo foi analisar o efeito da irradiação com LBP na concentração de IGF-1 nas glândulas parótidas e submandibulares de ratas diabéticas induzidas por estreptozotocina. Trinta e oito ratas da raça Wistar receberam uma injeção intraperitoneal de estreptozotocina ou de tampão conforme o grupo ao qual pertenciam, C (controle) ou D (diabetes). Posteriormente, as ratas foram divididas em 4 subgrupos (C0, D0, C5 e D5), de acordo com a dose de irradiação recebida (0 ou 5 J/cm²). Após 29 dias da indução, os animais foram submetidos à simulação ou à irradiação. Após vinte e quatro horas, os animais foram sacrificados e as glândulas salivares, coletadas para a análise da concentração de IGF-1. No dia do sacrifício, a glicemia dos animais diabéticos que receberam irradiação estava diminuída quando comparada com a glicemia de diagnóstico ($p \leq 0,05$). A concentração de IGF-1, entretanto, não sofreu influência da irradiação. Com base nesses resultados, podemos concluir que o LBP pode alterar a glicemia dos animais diabéticos; no entanto, esse efeito parece não estar relacionado com a concentração de IGF-1.

DESCRITORES | Diabetes Mellitus; Glicemia; Fator de Crescimento Insulin-Like I; Terapia a Laser; Glândulas Salivares.

ABSTRACT | **Effect of laser therapy on IGF-1 in the parotid and submandibular glands of streptozotocin-induced diabetic rats** • Diabetes mellitus is a metabolic disease of multiple etiologies that leads to hyperglycemia and can cause numerous dysfunctions and failure of organs and tissues, including the salivary glands. Some studies using diabetic rats have shown a decrease in glucose blood concentration when low-power laser (LPL) was used on salivary glands; however, the mechanism of action of lasers on carbohydrate metabolism is yet unknown. Thus, the aim of this study was to assess whether LPL irradiation on salivary glands can change the IGF-1 concentration of diabetic rats. Thirty-eight female rats were divided into 4 groups: D0 and D5 (diabetic animals) and C0 and C5 (control animals), respectively irradiated with 0 and 5 J/cm². Diabetes was induced by administration of streptozotocin and confirmed later by the glycaemia results. Twenty-nine days after induction, the parotid and submandibular glands of groups D5 and C5 were irradiated with a diode laser. Twenty-four hours after irradiation, the animals were sacrificed and their salivary glands were collected to assess IGF-1 concentration. Diabetic animals that received irradiation showed lower glucose concentration on the day of sacrifice in comparison with the day they had been diagnosed ($p \leq 0.05$); however, IGF-1 concentration was unchanged by irradiation. Based on the results of this study, it was concluded that LPL irradiation can decrease blood glucose concentration of diabetic animals; however, this effect appears to be unrelated to the concentration of IGF-1.

DESCRIPTORS | Diabetes Mellitus; Blood Glucose; Insulin-Like Growth Factor I; Laser Therapy; Salivary Glands.

CORRESPONDING AUTHOR | • **Alyne Simões** Department of Biomaterials and Oral Biology, School of Dentistry University of São Paulo • **Avenida Professor Lineu Prestes, 2227** São Paulo, SP, Brazil • **05508-000** E-mail: lysimoes@usp.br

• **Received** Sep 16, 2013 • **Accepted** Apr 7, 2014
• **DOI** http://dx.doi.org/10.11606/issn.2357-8041.clrd.2014.59344

INTRODUÇÃO

O diabetes mellitus é um distúrbio metabólico de etiologia múltipla caracterizada pela falta parcial ou total de insulina, por meio da produção insuficiente de insulina pelo pâncreas ou pela incapacidade do organismo em utilizar efetivamente a insulina produzida, causando uma hiperglicemia crônica, um dos principais fatores relacionados com as complicações do diabetes.[1]

Com o passar do tempo, a hiperglicemia ocasiona algumas complicações no paciente diabético, como, por exemplo, disfunções e falências em alguns órgãos como rins, olhos e coração, além de alterações nos sistemas vascular e nervoso.[2] Na cavidade oral, as complicações relacionadas à hiperglicemia são gengivite, periodontite, cárie dental, candidíase oral, perda de osso alveolar e xerostomia.[3-5]

Alguns estudos com modelos animais verificaram que a hiperglicemia altera bioquimicamente as glândulas salivares parótidas e submandibulares de ratos diabéticos induzidos quimicamente por estreptozotocina.[6-12]

Trabalhos anteriores do nosso grupo de pesquisa analisaram o efeito de algumas terapias sobre as alterações que o diabetes pode causar nas glândulas salivares e na glicemia, como o tungstato de sódio e a terapia com laser de baixa potência (Laser Phototherapy, LPT).[9,11,13] Simões *et al.*[11] e Ibuki *et al.*[13] observaram que a LPT atua revertendo algumas alterações bioquímicas encontradas em glândulas salivares de animais diabéticos, principalmente relacionadas com estresse oxidativo, e atua também diminuindo a glicemia dos animais irradiados.[11,13] No entanto, o mecanismo de ação da LPT sobre o metabolismo dos carboidratos não é conhecido.

Uma vez que o *insulin-like growth factor 1* (IGF-1) é sintetizado e secretado pelas glândulas salivares e que possui uma estrutura tridimensional semelhante à insulina — sugerindo que o IGF-1 possa mimetizar algumas das atividades metabólicas da insulina como, por exemplo, auxiliar no controle glicêmico —,[14-18] o objetivo deste estudo foi analisar se a irradiação com laser de baixa potência é capaz de atuar na concentração de IGF-1 das glândulas parótidas (GPs) e submandibulares (GSMs) de ratas diabéticas induzidas por estreptozotocina, o que poderia justificar a diminuição na glicemia observada nos trabalhos anteriores realizados em animais diabéticos irradiados.

MATERIAIS E MÉTODOS

O presente trabalho foi aprovado pela Comissão de Ética no Uso de Animais (CEUA) do Instituto de Ciências Biomédicas da Universidade de São Paulo.

Trinta e oito ratas adultas da raça Wistar do Biotério do Laboratório de Biologia Oral da Faculdade de Odontologia da Universidade de São Paulo (FOUSP), com peso corporal de aproximadamente 200 g, foram utilizadas, as quais foram mantidas em gaiolas individuais durante todo o período experimental. Os animais foram divididos em dois grupos, Controle (C) e Diabetes (D), e aleatoriamente subdivididos em quatro grupos de acordo com a dose de irradiação laser recebida, sendo C0 e D0 as denominações dos animais controle e diabéticos, respectivamente, que receberam somente uma simulação de irradiação (0 J/cm²), e C5 e D5 as denominações dos animais controle e diabéticos, respectivamente, que receberam 5 J/cm² de irradiação.

O diabetes mellitus foi induzido após um período de 15 horas de jejum, com uma injeção intraperitoneal de estreptozotocina (60 mg/kg de peso corporal) dissolvida em tampão de citrato de sódio 0,1 M, pH 4,5 (Grupo D). Os animais do Grupo C receberam somente uma injeção do veículo. A glicemia de diagnóstico foi aferida 72 horas após a indução do diabetes, e os animais com glicemia igual ou superior a 250 mg de glicose/dL de sangue foram considerados diabéticos.

Após 29 dias da confirmação do estado diabéti-

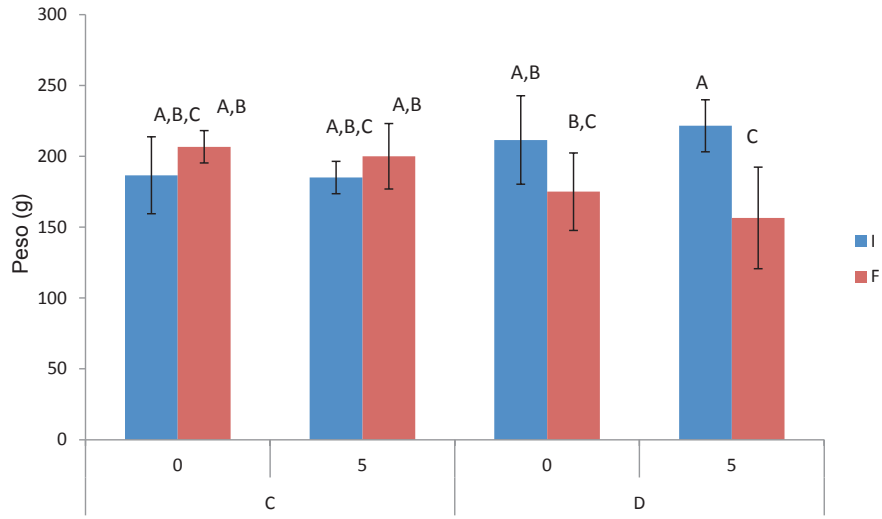

Figura 1 | Peso inicial e final (g) para os diferentes grupos. As colunas representam os valores médios e as barras, o desvio padrão. As letras diferentes indicam diferença estatística ($p < 0,05$) entre os grupos (C0, C5, D0 e D5) e tempos experimentais (inicial e final; C0, n = 10; C5, n = 8; D0, n = 10; D5, n = 10).

co, os animais foram anestesiados com ketamina e xilasina, tricotomizados e irradiados na região das GSMs e GPs e sacrificados 24 horas após a irradiação. Nos animais dos Grupos C0 e D0, foi feita somente uma simulação da irradiação.

Um laser de diodo InGaAlP (Photon Lase III; DMC Equipamentos Ltda., São Carlos, SP, Brasil), com comprimento de onda de 660 nm e área do *spot* de 0,028 cm², do Laboratório de Biologia Oral da FOUSP, foi utilizado para o estudo, com potência fixa em 70 mW e com tempo de irradiação de 2 s por ponto para os Grupos C5 e D5, sendo a energia por ponto de 0,14 J e a densidade de energia de 5 J/cm². Os animais foram irradiados uma única vez, de maneira pontual e em contato, no total de 40 pontos (5,6 J de energia total por área) na região de cada GP e nas duas GSMs de uma vez (sendo 3 áreas de irradiação). Cada área foi demarcada com um círculo de aproximadamente 1,13 cm².

Os animais foram eutanasiados 24 horas após a irradiação por destroncamento medular após anestesia com ketamina/xilasina. Para a análise da concentração de IGF-1, as glândulas foram removidas imediatamente, limpas de tecidos aderentes, prensadas entre placas de alumínio e mantidas em gelo seco até serem armazenadas em freezer a –80°C, onde permaneceram até o momento de sua utilização.

As análises da glicemia (de diagnóstico e de sacrifício) foram realizadas com um glicosímetro comercial (Accu-Check Advantage; Roche Brasil, São Paulo, SP, Brasil). Para a determinação da concentração de IGF-1 nas GSMs e GPs, foi utilizado um kit para ELISA (enzyme-linked immune-sorbent assay; AbFrontier's rat IGF-1 ELISA Kit; Young In Frontier Co., Ltd., Seoul, Coreia), adaptado para glândulas salivares.

Os resultados foram analisados pelo teste estatístico de análise de variância (ANOVA) e teste de contraste de Tukey. Adotou-se uma significância de 5%.

RESULTADOS

Ao final dos 30 dias do experimento, os animais diabéticos tiveram uma tendência de perda de peso, sendo esta significativa somente no grupo diabético irradiado ($p < 0,05$; Figura 1). A ingestão de ração e o consumo de água apresentaram um aumento significativo para os grupos D0 e D5 quando comparados, respectivamente, com os grupos C0 e C5 ($p < 0,05$; Tabela 1).

Os animais dos grupos D0 e D5 apresentaram uma média de glicemia de diagnóstico de 502,10 mg e 570,60 mg de glicose por dL de sangue, respectivamente, e os animais dos grupos C0 e C5, de 92,2 mg e 111,25 mg de glicose por dL

Tabela 1 | Médias e desvio padrão da ingestão de ração (g/semana) e do consumo de água (mL/semana) para os diferentes grupos. Letras diferentes representam diferença estatisticamente significante dentro das linhas (p < 0,05).

	Controle		Diabetes	
	0 J/cm²	5 J/cm²	0 J/cm²	5 J/cm²
Água (mL/semana)	82,25 ± 8,40 B (n = 10)	86,56 ± 8,84 B (n = 8)	528,5 ± 63,45 A (n = 10)	516,5 ± 32,97 A (n = 10)
Comida (g/semana)	66,37 ± 11,73 B (n = 10)	63,75 ± 9,93 B (n = 8)	99,62 ± 17,95 A (n = 10)	108,50 ± 6,68 A (n = 10)

Figura 2 | Glicemia inicial (diagnóstico) e final (sacrifício; em jejum) para os diferentes grupos. As colunas representam os valores médios e as barras o desvio padrão. As letras diferentes indicam diferença estatística (p < 0,05) entre os diferentes grupos (C0, C5, D0 e D5) e tempos experimentais (inicial e final; C0, n = 10; C5, n = 8; D0, n = 10; D5, n = 10).

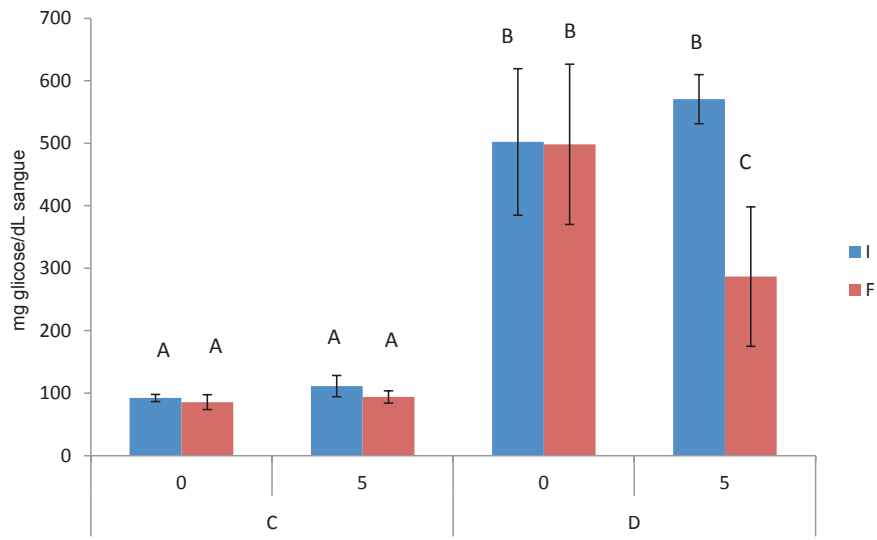

de sangue, respectivamente. A glicemia aferida no dia de sacrifício, entretanto, foi de 498,30 mg e 286,54 mg de glicose por dL de sangue para os grupos D0 e D5, respectivamente, e de 85,60 mg e 93,87 mg de glicose por dL de sangue para os grupos C0 e C5, respectivamente. No grupo D5, houve uma diminuição significativa na glicemia final quando comparada com sua respectiva glicemia inicial (p < 0,05; Figura 2).

Em relação à concentração de IGF-1, observamos que, em glândulas salivares parótidas e submandibulares, não foram vistas diferenças estatisticamente significantes entre os animais dos grupos controle e diabetes (dados não mostrados), independentemente do grupo de irradiação ao qual pertenciam. Porém, ao se comparar a concentração de IGF-1 nas glândulas parótidas e submandibulares na mesma condição sistêmica (controle ou diabetes), foi observado um aumento na concentração de IGF-1 para as glândulas parótidas em comparação com as glândulas submandibulares (p < 0,05; Figura 3a e 3b, respectivamente para animais controles e diabéticos).

DISCUSSÃO

Como a LPT tem demonstrado efeito sobre a glicemia dos animais diabéticos[11,13] e sobre a concentração do IGF-1 em alguns tecidos, além de este estar relacionado com a homeostase da concentração de glicose, o presente estudo teve como objetivo analisar a concentração de IGF-1 nas glândulas parótidas e submandibulares de animais controles e diabéticos que receberam ou não a laserterapia.

A perda de peso observada nos animais diabéticos, além do aumento na ingestão de ração e água, condiz com a literatura que afirma que perda de peso, fraqueza, polifagia, polidipsia e poliúria são alguns dos sinais e sintomas que caracterizam o

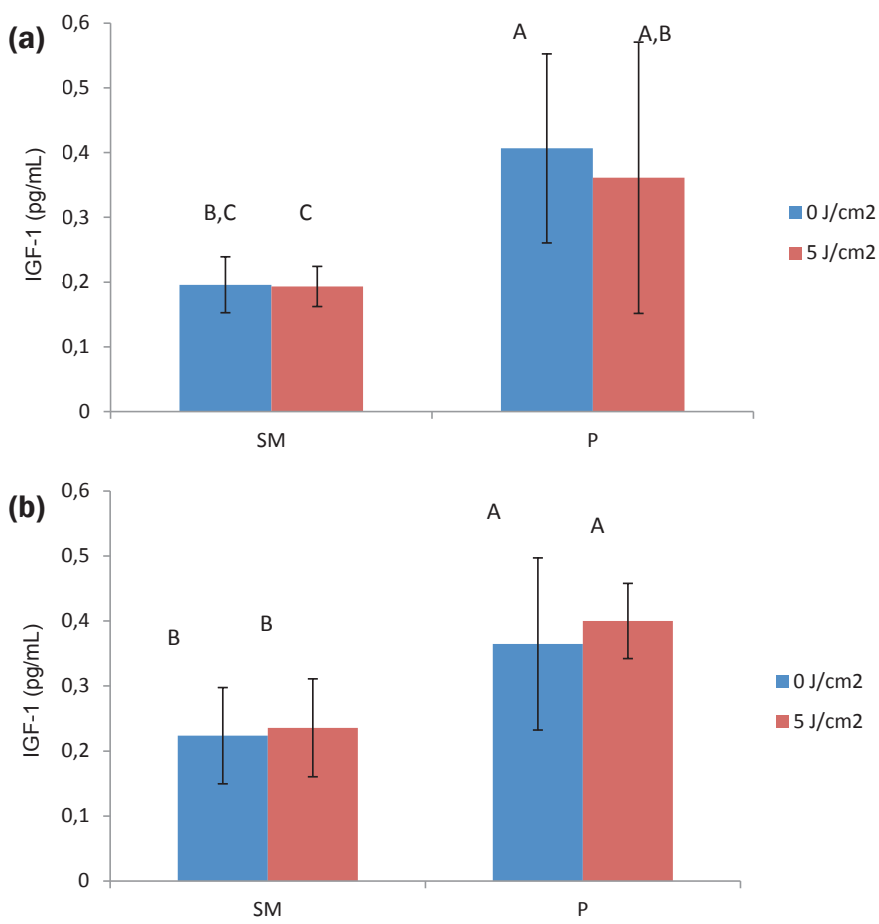

Figura 3 | Concentração de IGF-1 (pg/mL) das glândulas submandibulares (SM) e parótidas (P) para os animais controles **(a)** e diabéticos **(b)**. As colunas representam os valores médios e as barras, o desvio padrão. As letras diferentes indicam diferença estatística ($p < 0,05$) entre as glândulas SM e P que receberam determinada irradiação (0 ou 5 J/cm²; C0, n = 8; C5, n = 10; D0, n = 10; D5, n = 10).

diabetes mellitus, sendo este também caracterizado pela hiperglicemia, dado este também encontrado neste trabalho.[6,19-21]

O diabetes experimental induzido quimicamente por estreptozotocina afeta as glândulas salivares, além de outros tecidos, sendo que esta droga age pela destruição das células beta do pâncreas, levando a alterações no metabolismo de carboidratos, proteínas e lipídeos.[22,23]

As glândulas salivares sofrem inúmeras alterações devido ao diabetes mellitus induzido quimicamente, como, por exemplo, alterações nas atividades do glicogênio, o qual é a principal forma de armazenamento de glicose nos tecidos de mamíferos. Em um estudo de Nicolau *et al.*,[24] foi demonstrado que o diabetes causa um acúmulo de glicogênio nas glândulas parótidas e submandibulares por meio de um aumento da atividade da glicogênio sintase e uma diminuição da atividade da glicogênio fosforilase. Outro estudo demonstrou que a atividade especifica da hexoquinase estava aumentada em animais diabéticos, interferindo no metabolismo de carboidratos.[7] Além disso, já foram descritas alterações nas enzimas do sistema antioxidante, e já é de conhecimento que o aumento da glicemia e os excessos de espécies reativas de oxigênio estão associados com as complicações do diabetes.[12,25]

Além dessas alterações descritas anteriormente, já foi observado que o diabetes causa diminuição na atividade da amilase, aumento da peroxidase e catalase, aumento na concentração de malondialdeido, ácido siálico livre e total e redução na concentração de proteína total das glândulas salivares

de animais diabéticos. Além disso, foi observada também a presença de vacúolos lipídicos nas glândulas salivares desses animais, sendo que essas alterações bioquímicas e estruturais podem estar relacionadas à hipofunção das glândulas salivares relacionada ao diabetes.[6-8,10-12,24,25]

Alguns estudos prévios do nosso laboratório objetivaram minimizar os efeitos deletérios do diabetes sobre as glândulas salivares, como o estudo de Leite e Nicolau,[9] que utilizaram o tungstato de sódio, o qual possui propriedades antidiabetôgenicas. Nesse estudo, os animais diabéticos receberam um tratamento com tungstato de sódio durante dois tempos experimentais de 2 e 6 semanas, e a glândula parótida foi analisada. Foi observado pelos autores que a glicemia final, do dia da eutanásia, estava diminuída quando comparada com a glicemia inicial (diagnóstico) dos animais que foram tratados por 2 semanas. Observaram-se também uma diminuição da concentração de proteínas totais e um aumento da atividade das enzimas amilase e peroxidase, além de um aumento da concentração de ácido siálico livre e total quando comparadas com as dos animais não diabéticos, sugerindo uma mudança de composição na glândula parótida.[9]

Além do tungstato de sódio, nosso grupo de pesquisa vem estudando o efeito da laserterapia (LPT) sobre as glândulas salivares de animais diabéticos induzidos por estreptozotocina, assim como o efeito da LPT sobre a concentração da glicemia desses animais. Foi observada uma diminuição da glicemia final, quando comparada com a glicemia inicial, nos animais que receberam irradiação. Além disso, Simões *et al.*[11] observaram uma diminuição dos vacúolos lipídicos nas glândulas salivares parótidas, sugerindo uma possível alternativa para auxiliar no tratamento da hipofunção das glândulas salivares causadas pelo diabetes.[11]

Uma vez que em glândulas salivares foi observada a presença de IGF-1, que é sintetizado nas células acinares, especialmente na região dos ductos secretores, em humanos e roedores,[26-28] e que em outros tecidos já foi observado que a LPT pode estimular a produção de IGF-1,[29-31] este trabalho foi o primeiro a analisar se a irradiação com laser de baixa potência é capaz de alterar a concentração de IGF-1 nas glândulas salivares, o que poderia estar relacionado com a diminuição da glicemia observada nos animais irradiados.

Nossos dados claramente mostram a presença de IGF-1 nas glândulas salivares de animais diabéticos e não diabéticos, tanto nas submandibulares quanto nas parótidas; porém, os animais irradiados não apresentaram alteração na concentração de IGF-1, muito embora a glicemia de sacrifício tenha diminuído em relação à glicemia de diagnóstico, após a irradiação, como também observado por Simões *et al.*[11] e Ibuki *et al.*[13]

Sabe-se que os parâmetros de irradiação influenciam os resultados apresentados; dessa forma, outros estudos com LPT, IGF-1, glicemia e outros fatores relacionados com a hiperglicemia são importantes para que possamos entender como a laserterapia age na concentração da glicemia, e para gerar um consenso sobre os parâmetros adequados para a utilização da laserterapia como auxiliar no tratamento das complicações do diabetes.

Com base nos dados obtidos, podemos concluir que a alteração da glicemia dos animais diabéticos irradiados com laser de baixa potência parece não ter relação com a concentração de IGF-1 nas glândulas salivares parótidas e submandibulares, dentro do protocolo utilizado neste estudo.

AGRADECIMENTOS

Os autores gostariam de agradecer à FAPESP (Fundação de Amparo à Pesquisa do Estado de São Paulo, processo 2011/14013-1) e a CAPES (Coordenação de Aperfeiçoamento de Pessoal de Nível Superior).

REFERÊNCIAS

1. Expert Committee on the Diagnosis and Classification of Diabetes Mellitus. Report of the expert committee on the diagnosis and classification of diabetes mellitus. Diabetes Care. 2003 Jan;26 Suppl 1:S5-20.
2. Centers for Diasease Control and Federation. IDF Diabetes atlas. 6th ed. Brussels: International Diabetes Federation; 2013 [cited 2013 Mar. 14]. Avaliable from: http://www.idf.org/diabetesatlas.
3. Moore PA, Guggenheimer J, Etzel KR, Weyant RJ, Orchard T. Type 1 diabetes mellitus, xerostomia, and salivary flow rates. Oral Surg Oral Med Oral Pathol Oral Radiol Endod. 2001 Sep;92(3):281-91.
4. Greenspa FS, Gardner DG, editors. Basic and clinical endocrinology. 7th ed. New York: McGraw-Hill; 2007.
5. Negrato CA, Tarzia O. Buccal alterations in diabetes mellitus. Diabetol Metab Syndr. 2010 Jan 15;2:3. doi: 10.1186/1758-5996-2-3.
6. Nogueira FN, Carvalho AM, Yamaguti PM, Nicolau J. Antioxidant parameters and lipid peroxidation in salivary glands of streptozotocin-induced diabetic rats. Clin Chim Acta. 2005 Mar;353(1-2):133-9.
7. Nogueira FN, Santos MF, Nicolau J. Influence of streptozotocin-induced diabetes on hexokinase activity of rat salivary glands. J Physiol Biochem. 2005 Sep;61(3):421-7.
8. Nicolau J, Souza DN, Nogueira FN. Activity, distribution and regulation of phosphofructokinase in salivary gland of rats with streptozotocin-induced diabetes. Braz Oral Res. 2006 Apr-Jun;20(2):108-13.
9. Leite MF, Nicolau J. Sodium tungstate on some biochemical parameters of the parotid salivary gland of streptozotocin-induced diabetic rats: a short-term study. Biol Trace Elem Res. 2009 Feb;127(2):154-63. doi: 10.1007/s12011-008-8233-5. Epub 2008 Sep 20.
10. Nicolau J, De Souza DN, Simões A. Alteration of Ca(2+)-ATPase activity in the homogenate, plasma membrane and microsomes of the salivary glands of streptozotocin-induced diabetic rats. Cell Biochem Funct. 2009 Apr;27(3):128-34. doi: 10.1002/cbf.1544.
11. Simões A, de Oliveira E, Campos L, Nicolau J. Ionic and histological studies of salivary glands in rats with diabetes and their glycemic state after laser irradiation. Photomed Laser Surg. 2009 Dec;27(6):877-83. doi: 10.1089/pho.2008.2452.
12. Ibuki FK, Simões A, Nogueira FN. Antioxidant enzymatic defense in salivary glands of streptozotocin-induced diabetic rats: a temporal study. Cell Biochem Funct. 2010 Aug;28(6):503-8. doi: 10.1002/cbf.1683.
13. Ibuki FK, Simões A, Nicolau J, Nogueira FN. Laser irradiation affects enzymatic antioxidant system of streptozotocin-induced diabetic rats. Lasers Med Sci. 2013 May;28(3):911-8. doi: 10.1007/s10103-012-1173-5. Epub 2012 Aug 7.
14. Joshi S, Ogawa H, Burke GT, Tseng LY, Rechler MM, Katsoyannis PG. Structural features involved in the biological activity of insulin and the insulin-like growth factors: A27 insulin/BIGF-I. Biochem Biophys Res Commun. 1985 Dec 17;133(2):423-9.
15. Kerr M, Lee A, Wang PL, Purushotham KR, Chegini N, Yamamoto H, et al. Detection of insulin and insulin-like growth factors I and II in saliva and potential synthesis in the salivary glands of mice. Effects of type 1 diabetes mellitus. Biochem Pharmacol. 1995 May 17;49(10):1521-31.
16. Rocha EM, de M Lima MH, Carvalho CR, Saad MJ, Velloso LA. Characterization of the insulin-signaling pathway in lacrimal and salivary glands of rats. Curr Eye Res. 2000 Nov;21(5):833-42.
17. Amano O, Iseki S. Expression and localization of cell growth factors in the salivary gland: a review. Kaibogaku Zasshi. 2001 Apr;76(2):201-12. Japanese.
18. Okada T, Liew CW, Hu J, Hinault C, Michael MD, Krtzfeldt J, et al. Insulin receptors in beta-cells are critical for islet compensatory growth response to insulin resistance. Proc Natl Acad Sci U S A. 2007 May 22;104(21):8977-82. Epub 2007 Apr 6.
19. Anderson LC. Parotid gland function in streptozotocin-diabetic rats. J Dent Res. 1987 Feb;66(2):425-9.
20. Kim SK, Cuzzort LM, McKean RK, Allen ED. Effects of diabetes and insulin on alpha-amylase messenger RNA levels in rat parotid glands. J Dent Res. 1990 Aug;69(8):1500-4.
21. Anderson LC, Bevan CA. Effects of streptozotocin diabetes on amylase release and cAMP accumulation in rat parotid acinar cells. Arch Oral Biol. 1992;37(5):331-6.
22. Ashcroft FM, Rorsman P. Diabetes mellitus and the β cell: the last ten years. Cell. 2012 Mar 16;148(6):1160-71. doi: 10.1016/j.cell.2012.02.010. Review.
23. King AJ. The use of animal models in diabetes research. Br J Pharmacol. 2012 Jun;166(3):877-94. doi: 10.1111/j.1476-5381.2012.01911.x.
24. Nicolau J, de Matos JA, de Souza DN, Neves LB, Lopes AC. Altered glycogen metabolism in the submandibular and parotid

salivary glands of rats with streptozotocin-induced diabetes. J Oral Sci. 2005 Jun;47(2):111-6.

25. Simões A, Ganzerla E, Yamaguti PM, de Paula Eduardo C, Nicolau J. Effect of diode laser on enzymatic activity of parotid glands of diabetic rats. Lasers Med Sci. 2009 Jul;24(4):591-6. doi: 10.1007/s10103-008-0619-2. Epub 2008 Nov 4.
26. Shubnikova EA, Volkova EF, Printseva OYa. Submandibular glands as organs of synthesis and accumulation of insulin-like protein. Acta Histochem. 1984;74(2):157-71.
27. Patel DG, Begum N, Smith PH. Insulin-like material in parotid and submaxillary salivary glands of normal and diabetic adult male mice. Diabetes. 1986 Jul;35(7):753-8.
28. Murakami K, Taniguchi H, Baba S. Presence of insulin-like immunoreactivity and its biosynthesis in rat and human parotid gland. Diabetologia. 1982 May;22(5):358-61.
29. Luo L, Sun Z, Zhang L, Li X, Dong Y, Liu TC. Effects of low-level laser therapy on ROS homeostasis and expression of IGF-1 and TGF-β1 in skeletal muscle during the repair process. Lasers Med Sci. 2013 May;28(3):725-34. doi: 10.1007/s10103-012-1133-0. Epub 2012 Jun 20.
30. Shimizu N, Mayahara K, Kiyosaki T, Yamaguchi A, Ozawa Y, Abiko Y. Low-intensity laser irradiation stimulates bone nodule formation via insulin-like growth factor-I expression in rat calvarial cells. Lasers Surg Med. 2007 Jul;39(6):551-9.
31. Fujimoto K, Kiyosaki T, Mitsui N, Mayahara K, Omasa S, Suzuki N, et al. Low-intensity laser irradiation stimulates mineralization via increased BMPs in MC3T3-E1 cells. Lasers Surg Med. 2010 Aug;42(6):519-26. doi: 10.1002/lsm.20880.

CLRD in Clinical and Laboratorial Research in Dentistry | Oral Radiology

Effectiveness of ultrasonography in detecting intraosseous vascularization: an *in-vitro* study

• **Marina Gazzano Baladi** Discipline of Radiology, Department of Stomatology, School of Dentistry, University of São Paulo, São Paulo, SP, Brazil • **Maria José Albuquerque Pereira de Souza e Tucunduva** Discipline of Radiology, Department of Stomatology, School of Dentistry, University of São Paulo, São Paulo, SP, Brazil • **Renato Tucunduva Neto** Discipline of Radiology, Department of Stomatology, School of Dentistry, University of São Paulo, São Paulo, SP, Brazil • **Arthur Rodriguez Gonzalez Cortes** Discipline of Radiology, Department of Stomatology, School of Dentistry, University of São Paulo, São Paulo, SP, Brazil • **Eduardo Massaharu Aoki** Discipline of Radiology, Department of Stomatology, School of Dentistry, University of São Paulo, São Paulo, SP, Brazil • **Emiko Saito Arita** Discipline of Radiology, Department of Stomatology, School of Dentistry, University of São Paulo, São Paulo, SP, Brazil • **Claudio Fróes de Freitas** Discipline of Radiology, Department of Stomatology, School of Dentistry, University of São Paulo, São Paulo, SP, Brazil

ABSTRACT | Ultrasonography is useful to diagnose lesions, insofar as it detects the type of injury, and to assess the degree of vascularization of tumors. However, intraosseous lesions may represent a challenge, since the surrounding bone thickness could prevent ultrasound signal capture. The aim of this study was to evaluate the influence of surrounding bone thickness on the ability of ultrasonography in capturing the echo signal of blood vessels. Macerated porcine hemimandibles (n = 20) with different buccal bone thicknesses were prepared and adapted to receive CFlex-type rubber tubes connected to a glass capillary through which pump-driven water was conducted to simulate blood vasculature. Doppler ultrasonography was used to assess the blood flow in the region of the mandibular canal at the level of the molar teeth. Student's t-test was used to assess differences between the bone thicknesses of hemimandibles with a negative and with a positive ultrasound signal. The presence of the echo signal in the simulated vasculature was assessed by ultrasonography. Reproducibility and reliability were confirmed for the analyses. The simulated flow signal was captured in cortical bones with a thickness in the 0.2–1.0 mm range (0.59 ± 0.42 mm), but was not captured in those with a thickness greater than 1.0 mm (1.39 ± 0.59 mm). In conclusion, ultrasonography can be used to investigate intraosseous vascularization in mandibular areas with a buccal bone thickness up to 1.0 mm.

DESCRIPTORS | Ultrasonography; Ultrasonography, Doppler; Diagnostic Imaging; Bone and Bones / blood supply.

RESUMO | **Eficácia da ultrassonografia na detecção de vascularização intraóssea: um estudo *in vitro*** • A ultrassonografia é um recurso de imagem para a finalidade de diagnosticar lesões e para avaliar o grau de vascularização intraóssea de tumores. No entanto, lesões intraósseas podem representar um desafio devido à espessura de osso circundante que poderá impedir a captura do sinal de ultrassom. O objetivo deste estudo foi avaliar a influência da espessura óssea na captura do sinal de eco dos vasos utilizando a ultrassonografia. Hemimandíbulas maceradas suínas (n = 20) com espessuras ósseas diferentes foram adaptadas para receber tubos de borracha tipo CFlex ligados a um capilar de vidro, por onde água foi conduzida por meio de uma bomba para simular a vascularização sanguínea. A ultrassonografia Doppler foi usada para avaliar o fluxo de sangue na região do canal mandibular ao nível dos dentes molares. O teste t de Student foi utilizado para avaliar as diferenças entre as espessuras de osso das hemimandíbulas por meio de sinal negativo e sinal positivo do ultrassom. A reprodutibilidade e a confiabilidade foram confirmadas para as análises. O sinal de fluxo simulado foi capturado em ossos corticais com espessura na faixa de 0,2 a 1,0 mm (0.59 ± 0.42 mm), mas não foi capturado a uma espessura superior a 1,0 mm (1.39 ± 0.59 mm). Concluindo, a ultrassonografia pode ser usada para investigar a vascularização intraóssea em áreas mandibulares com uma espessura óssea vestibular de até 1,0 mm.

DESCRITORES | Ultrassonografia; Ultrassonografia Doppler; Diagnóstico por Imagem; Osso e Ossos / irrigação sanguínea.

CORRESPONDING AUTHOR: | • **Marina Gazzano Baladi** Discipline of Radiology, Department of Stomatology, School of Dentistry, University of São Paulo • **Av. Professor Lineu Prestes, 2227** São Paulo, SP, Brazil • **05508-000** E-mail: marina.baladi@usp.br

• **Received** May 14, 14 • **Accepted** Sep 01, 14
• **DOI** http://dx.doi.org/10.11606/issn.2357-8041.clrd.2014.80783

INTRODUCTION

Ultrasonography is an imaging examination using sound waves with a frequency above the human audible threshold.[1] The image of anatomical structures is formed by real-time emission and capture of ultrasound wave echoes.[2] This method allows assessment of subcutaneous body structures, and has been used in the oral cavity to identify alterations of soft and hard tissues,[3] blood flow and vascularization.[4,5]

The capability of ultrasonography to detect blood vessels has validated it as a useful tool in the diagnosis of neoplasms. Accordingly, the differentiation of malignant lesions can be made on the basis of the vascularization pattern of the lesion.[6,7] In addition, ultrasonography is a non-invasive method, which causes little discomfort to the patient, and is affordable and relatively easy to use.[8]

According to the literature, it is possible to employ ultrasonography to detect signals of simulated blood flow, using macerated porcine jaws and rubber vessels with flexibility and stiffness comparable to those of a real artery.[9,10]

An ultrasonic signal is not detected in healthy mandibular bone tissues, since dense cortex acts as a shield that blocks sound waves.[9] However, if the bone tissue has suffered thinning due to any type of injury, trauma resorption, or an intraosseous lesion, the ultrasound device can capture the signal from this tissue.[5] This property enables the clinician to detect the intraosseous content and extent of a mandibular lesion, thus allowing for a precise surgical plan. However, little is known regarding the limit of bone thickness allowing ultrasound signal capture, and subsequent diagnosis of the degree of vascularization using ultrasonography.[10] Thus, the purpose of this study was to evaluate capture of ultrasonography signals in porcine hemimandibles of different thicknesses to determine the thickness limit in which this imaging method can be used.

MATERIALS AND METHODS

The procedures of the study involving porcine jaws were submitted to and approved by the Research Ethics Committee (Subcommittee for Animal Bioethics) of the School of Dentistry, University of São Paulo (Protocol no. 147).

Macerated porcine mandibles (n = 10) were used, insofar as their bone structure is similar to that of humans in the region of molar teeth.[10] Each mandible was sectioned in the region of incisor teeth and numbered, generating 20 hemimandibles, which composed the study material.

The hemimandibles were randomly eroded with a common electric plaster cutter in the region of third molars and assessed with a Terason t3000 ultrasound system (Terason Division, Teratech Corporation, New York, NY), set at Doppler mode, and using an adapted vascular simulator. The vascular simulator was installed in the anatomical region of the mandibular canal. It consisted of a glass capillary tube, connected on both ends to CFlex-type rubber tubes supported by nylon clamps, according to previously described methodology.[11-13] Thus, blood plasma was simulated using water, whereas erythrocytes were simulated using graphite powder. In all cases, blood flow simulation was run using the same regular aquarium pump connected to the capillary tube, in order to simulate blood flow under the same pressure conditions (170 mmHg; Figure 1).

The mandibles were sectioned twice, at the respective region of both mental foramina. Only the parts posterior to the mental foramina were considered. The bone thickness of all hemimandibles was measured at the buccal aspect of the mandibular canal, in millimeters, using a caliper, 5 mm distally to the mental foramen (Figure 2). The 0.5 mm corresponding to the glass capillary was subtracted from the total to obtain a value considered as the bone thickness measurement.

Digital images for the negative (Figure 3A) and

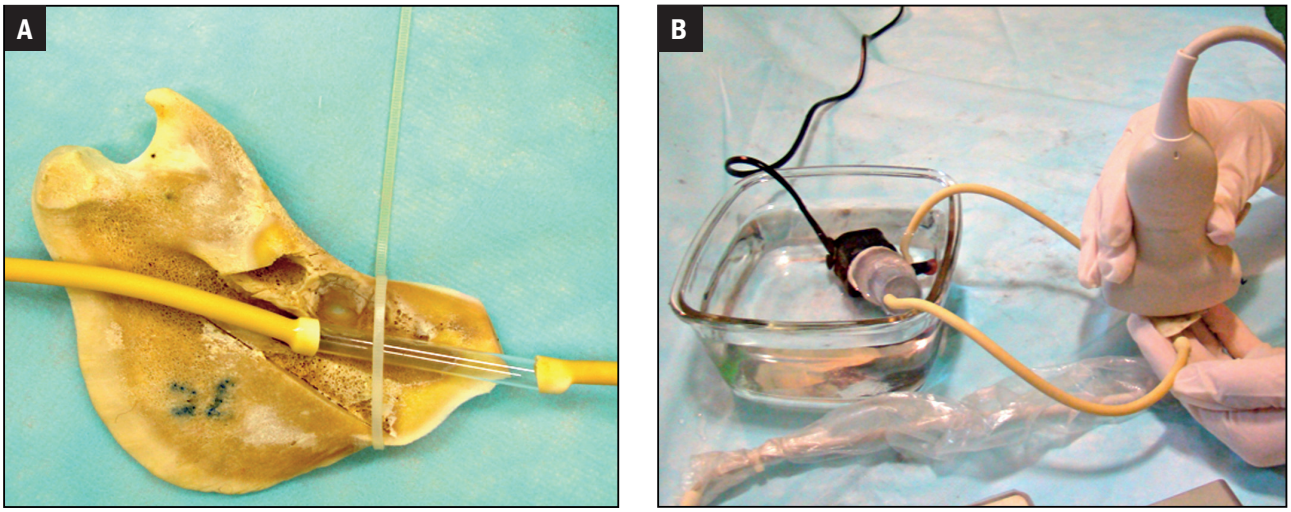

Figure 1 | Methodology used in the present study; **A:** ultrasound vascular simulator; **B:** capture of the ultrasonic signal.

positive signals (Figure 3B) were displayed in the monitor of the ultrasound system. Positivity of the ultrasonic signal was recorded for all hemimandibles in random order by two trained observers (i.e. dentists with expertise in oral radiology). Intraobserver reliability was assessed between measurements performed 2 weeks apart to eliminate memory bias. Intra- and interobserver agreement was assessed using the kappa test. Student's t-test was used to assess differences between bone thicknesses of hemimandibles with negative and positive ultrasound signals.

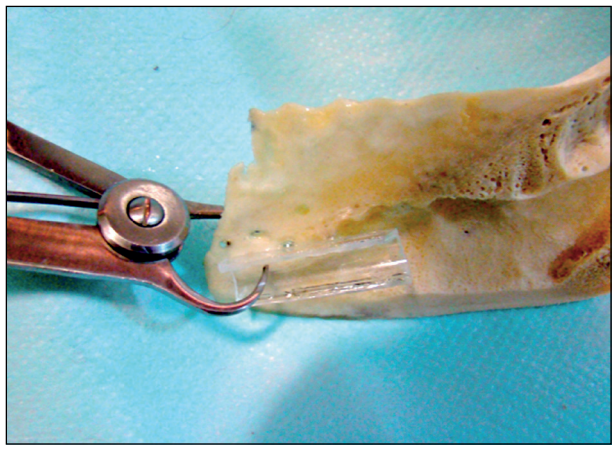

Figure 2 | Measurement using the thickness gauge (caliper).

RESULTS

The echo signals of the simulated flow in porcine hemimandibles were captured in the cortical bones with a thickness in the 0.2–1.0 mm range (0.59 ± 0.42 mm). However, signals in jaws with a thickness greater than 1.0 mm (1.3 ± 1.2 mm) could not be captured (Figure 4). No false positive results were recorded, leading to a sensitivity of 100% for Doppler ultrasonography as a diagnostic method.

Intraobserver reproducibility and interobserver reliability were confirmed for the ultrasound analysis, according to the kappa index result (0.93, $p = 0.001$ and 0.88, $p = 0.001$, respectively). The results for Student's t-test showed statistically significant differences between mean values for buccal bone thickness in cases with positive and negative signals (Table 1).

DISCUSSION

As supported by the present results, Doppler ultrasonography has been regarded as a useful method to assess the degree of vascularization of a lesion in real time. This attribute is considered the

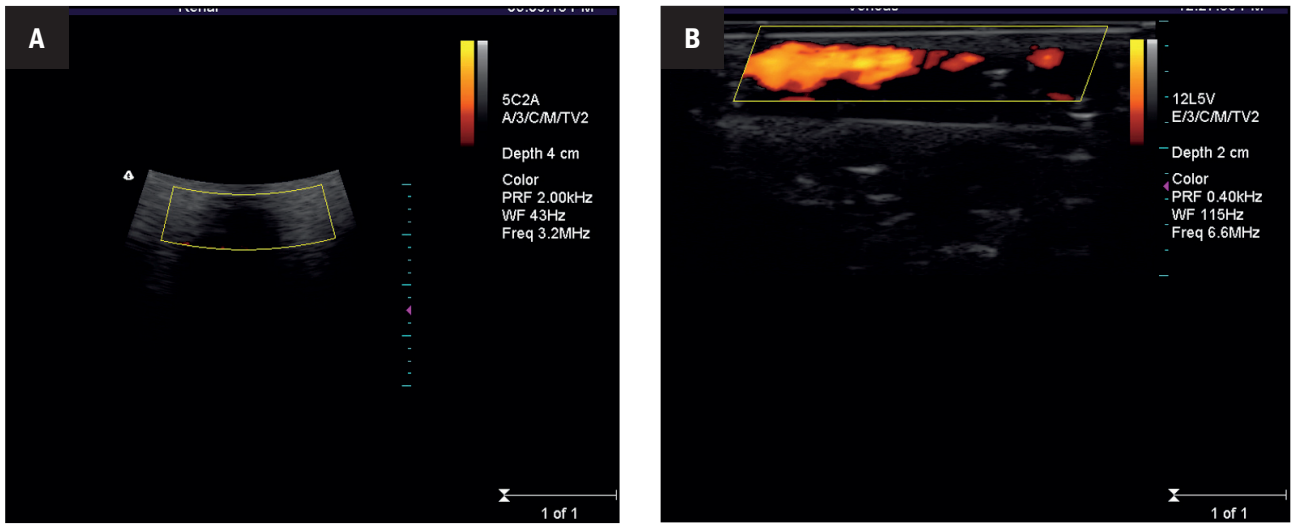

Figure 3 | Digital images of ultrasonography; **A:** example of an image with a negative signal; **B:** ultrasound images showing the positive signal for blood vasculature, captured during examination of hemimandibles.

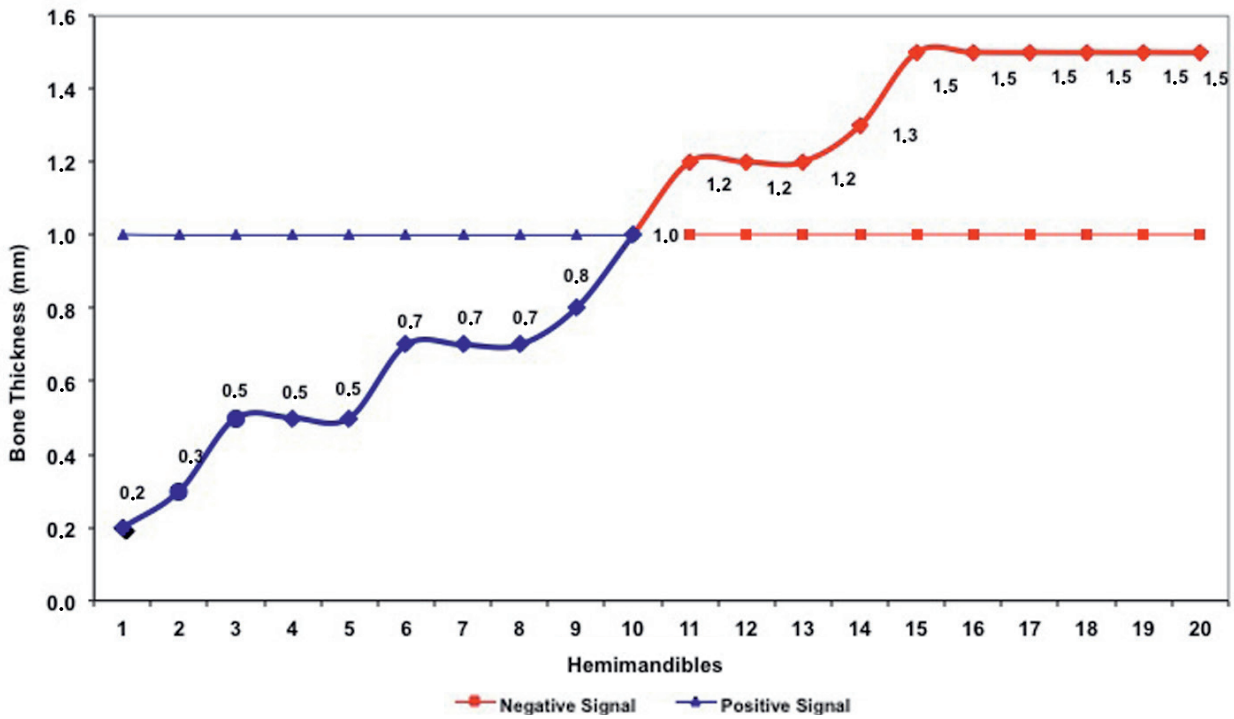

Figure 4 | Relationship between thickness of hemimandibles and capture of the signal obtained.

distinct feature of this method, because it enables a detailed evaluation of the activity and aggressiveness of the change.[7,10,14] To our knowledge, this is the first study assessing reliability and reproducibility for ultrasonography as a method to detect intraosseous blood flow in the oral cavity. Ultrasonography does not use radiation or contrast dyes. Furthermore, compared to computed tomography

Table 1 | Descriptive measurements of bone thickness in relation to capture of signal.

Capture of total signal	Bone thickness (mm)					Student's T test
	Minimum values	Maximum values	Mean values	Standard deviation	Variance	P value
Negative	1.20	1.50	1.39	0.14	0.02	0.001
Positive	0.20	1.00	0.59	0.45	0.20	

and magnetic resonance imaging, ultrasonography offers advantages such as lower cost, shorter scan acquisition time and wider availability, although it produces less detailed images.[15]

The ultrasound technique has important characteristics not only for assessing bone tissues but also for detecting blood flow alterations in soft tissues, thus helping to diagnose oral lesions and tumors, and plan related surgical treatments.[3-5,9] Some authors have sought to understand bone resistance to sound waves, and have found that it is possible to assess the degree of vascularization and blood flow of lesions surrounded by cortical bone, provided this bone has anatomical alterations (i.e., irregularity or discontinuity).[3,7-9] Thus, Doppler-mode ultrasonography can be used to provide information on the intraosseous content of osteolytic lesions before surgical procedures are performed.[6,7,9] Our results support the aforementioned statement, insofar as there was a statistically significant difference between the groups with positive and negative capture of echo signals from mandibles with different bone thicknesses. Furthermore, two other studies on oral pathologies confirmed the usefulness of ultrasonography to detect bone healing after surgical removal of intraosseous lesions,[16,17] confirming the clinical relevance of the present study.

Studies in the literature on computational models have validated ultrasonography simulation in evaluating pathological processes, emphasizing that this method can be useful in assessing the conditions of complex outflow and the regions where the shear stress of pulsatile flow occurs, thus providing accurate diagnosis.[5,8,10-13] In the present study, blood flow was observed in a mandible with a thickness in the 0.2–1.0 mm range. This imaging diagnosis result is of fundamental clinical interest for the analysis of certain mandibular intraosseous injuries, such as median dermoid cyst and aneurysmal bone cyst, in order to detect the degree of vascularization using Doppler ultrasound examination.[6,9,10]

In conclusion, ultrasonography can be applied in studying the intraosseous vascularization of lesions surrounded by cortical bone with a thickness in the 0.2–1.0 mm range, using the Doppler mode. However, this was an *in-vitro* study. Further clinical assessments are required to confirm the validity of this method in diagnosing osteolytic lesions.

ACKNOWLEDGEMENTS

A scholarship (DS type) was granted to Marina G. Baladi from the Coordination for the Improvement of Higher Education Personnel (CAPES, Brazil). A PhD scholarship was granted to Arthur R. G. Cortes from the National Council for Scientific and Technological Development (CNPq, Brazil, 2011/3). We also wish to thank Dr. Marlene Fenyo Soeiro de Matos Pereira for her encouragement and kind support.

REFERENCES

1. Reinfeldt S, Stenfelt S, Good T, Hakansson B. Examination of bone conducted transmission from sound field excitation measured by thresholds, ear-canal sound pressure, and skull vibrations. J Acoust Soc Am. 2007 Mar;121(3):1576-87. http://dx.doi.org/10.1121/1.2434762.

2. Kuo J, Bredthauer GR, Castellucci JB, Von Ramm OT. Interactive volume rendering of real-time three-dimensional ultrasound images. IEEE Trans Ultrason Ferroelectr Freq Control. 2007 Feb;54(2):313-8. doi: 10.1109/TUFFC.2007.245.
3. Gateano J, Miloro M, Hendler BH, Horrow M. The use of ultrasound to determine the position of the mandibular condyle. J Oral Maxillofac Surg. 1993 Oct;51(10):1081-6. doi: 10.1016/S0278-2391(10)80444-6.
4. Ng SY, Songra AK, Ali N, Carter JLB. Ultrasound features of osteosarcoma of the mandible – a first report. Oral Surg Oral Med Oral Pathol Oral Radiol Endod. 2001 Nov;92(5):582-6. doi: 10.1067/moe.2001.116821.
5. Sumer AP, Danaci M, Ozen Sandikçi E, Sumer M, Celenk P. Ultrasonography and Doppler ultrasonography in the evaluation of intraosseous lesions of the jaws. Dentomaxillofac Radiol. 2009 Jan;38(1):139-43. doi: 10.1259/dmfr/20664232.
6. Dangore SB, Degwekar SS, Bhowate RR. Evaluation of the efficacy of colour Doppler ultrasound in diagnosis of cervical lymphadenopathy. Dentomaxillofac Radiol. 2008 May;37(2):205-12. doi: 10.1259/dmfr/57023901.
7. Lu L, Yang J, Liu JB, Yu Q. Ultrasonographic evaluation of mandibular ameloblastoma: a preliminary observation. Oral Surg Oral Med Oral Pathol Oral Radiol Endod. 2009 Aug;108(2):e32-8. doi: 10.1016/j.tripleo.2009.03.046.
8. Jones JK, Frost DE. Ultrasound as a diagnostic aid in maxillofacial surgery. Oral Surg Oral Med Oral Pathol Oral Radiol Endod. 1984 Jun;57(6):589-94. doi: http://dx.doi.org/10.1016/0030-4220(84)90277-9.
9. Thurmuller P, Troulis M, O"Neill MJ, Kaban LB. Use of Ultrasound to assess healing of a mandibular distraction wound. J Oral Maxillofac Surg. 2002 Sept;60(9):1038-44. doi: 10.1053/joms.2002.34417.
10. Cotti E, Simbola V, Dettori C, Campisi G. Echographic evaluation of bone lesions of endodontic origin: report of two cases in the same patient. J Endod. 2006 Sept;32(9):901-5. doi: 10.1016/j.joen.2006.01.013.
11. Ryan LK, Foster FS. Tissue equivalent vessel phantoms for intravascular ultrasound. Ultrasound Med Biol. 1997;23(2):261-73. doi: 10.1016/S0301-5629(96)00206-2.
12. Rickey DW, Picot PA, Christopher DA, Fenster A. A wall-less vessel phantom for Doppler ultrasound studies. Ultrasound Med Biol. 1995;21(9):1163-76. doi: 10.1016/0301-5629(95)00044-5.
13. Steel R, Fish PJ. Lumen pressure within obliquely insonated absorbent solid cylindrical shells with application to Doppler flow phantoms. IEEE Transac Ultrason Ferroelec Freq Control. 2002 Feb;49(2):271-80. doi: 10.1109/58.985711.
14. Astl J, Jablonický P, Lastuvka P, Taudy M, Dubová J, Betka J. Ultrasonography (B scan) in the head and neck region. Int Congr Ser. 2003 Oct;1240:1423-7. doi: 10.1016/S0531-5131(03)00791-X.
15. Sham ME, Nishat S. Imaging modalities in head-and-neck cancer patients. Indian J Dent Res. 2012 Nov-Dec;23(6):819-21. doi: 10.4103/0970-9290.111270.
16. Rajendran N, Sundaresan B. Efficacy of ultrasound and color power Doppler as a monitoring tool in the healing of endodontic periapical lesions. J Endod. 2007 Feb;33(2):181-6. doi: 10.1016/j.joen.2006.07.020.
17. Dib LL, Curi MM, Chammas MC, Pinto DS, Torloni H. Ultrasonography evaluation of bone lesions of the jaw. Oral Surg Oral Med Oral Pathol Oral Radiol Endod. 1996 Sep;82(3):351-7. doi: 10.1016/S1079-2104(96)80365-9.

CLRD in Clinical and Laboratorial Research in Dentistry | Oral Radiology

Evaluation of basilar expansion and internal septa of human sphenoidal sinus using cone beam computed tomography

• **Marcio Yara Buscatti** Discipline of Radiology, Department of Stomatology, School of Dentistry, University of São Paulo, São Paulo, SP, Brazil • **Karina Cecília Panelli Santos** Discipline of Radiology, Department of Stomatology, School of Dentistry, University of São Paulo, São Paulo, SP, Brazil • **Emiko Saito Arita** Discipline of Radiology, Department of Stomatology, School of Dentistry, University of São Paulo, São Paulo, SP, Brazil • **Junichi Asaumi** Oral and Maxillofacial Radiology, Okayama University Graduate School of Medicine, Dentistry and Pharmaceutical Sciences, Okayama, Japan • **Plauto Christopher Aranha Watanabe** Discipline of Radiology, Department of Stomatology, School of Dentistry, University of São Paulo, Ribeirão Preto, SP, Brazil • **Jefferson Xavier Oliveira** Discipline of Radiology, Department of Stomatology, School of Dentistry, University of São Paulo, São Paulo, SP, Brazil

ABSTRACT | The objective of this study was to assess the types and frequencies of basilar expansion of the sphenoidal sinus and internal septa by using cone beam computed tomography. Archived images from 300 adult subjects of both genders were retrieved. A descriptive analysis relating age and gender to basilar expansion of the sphenoidal sinus and internal septa types and frequencies was performed. The associations between basilar expansion of the sphenoidal sinus, internal septa and gender for each age group were assessed using the chi-square test or Fisher's exact test. Among all the images evaluated, 69% showed basilar expansion of the sphenoidal sinus, of which 81% were considered critical. Internal septa were observed in 60% of the images. There was no relationship between the presence of basilar expansion of the sphenoidal sinus and gender and age. Internal septa were independent of gender; however, of the subjects older than age 40, 36% had only a main septum, 6% had accessory septa, and 18% had both types of septa. Cone beam computed tomography is an accurate method that should be considered for the evaluation of this anatomic segment in order to avoid unnecessary exposure to radiation.

DESCRIPTORS | Paranasal Sinuses; Sphenoid Sinus; Anatomy; Cone Beam Computed Tomography.

RESUMO | **Avaliação de expansão basilar e septos internos do seio esfenoidal humano por meio de tomografia computadorizada de feixe cônico** • O objetivo deste estudo foi avaliar os tipos e as frequências de expansão basilar do seio esfenoidal e septos internos utilizando tomografia computadorizada de feixe cônico. Imagens arquivadas de 300 indivíduos adultos de ambos os gêneros foram recuperadas. Foi realizada uma análise descritiva relacionando idade e gênero à expansão basilar do seio esfenoidal e a tipos de septos internos e frequências. As associações entre expansão basilar do seio esfenoidal, septos internos e gênero para cada grupo de idade foram avaliadas por meio do teste do qui-quadrado ou teste exato de Fisher. Entre todas as imagens avaliadas, 69% apresentaram expansão basilar do seio esfenoidal, das quais 81% foram consideradas críticas. Septos internos foram observados em 60% das imagens. Não houve relação entre presença de expansão basilar do seio esfenoidal, gênero e idade. Septos internos apresentaram-se independentes do gênero; no entanto, dentre os indivíduos com mais de 40 anos de idade, 36% tinham apenas um septo principal, 6% tinham septos acessórios, e 18% tinham ambos os tipos de septos. A tomografia computadorizada é um método preciso que deve ser considerado para a avaliação desse segmento anatômico a fim de evitar a exposição desnecessária à radiação.

DESCRITORES | Seios Paranasais; Seio Esfenoidal; Anatomia; Tomografia Computadorizada de Feixe Cônico.

CORRESPONDING AUTHOR | • **Karina Cecília Panelli Santos** •Discipline of Radiology, Department of Stomatology, School of Dentistry, University of São Paulo • **Avenida Professor Lineu Prestes, 2227** São Paulo, SP, Brazil • **05508-000** E-mail: kapanelli@usp.com

• **Received** Nov 27, 2013 • **Accepted** Apr 14, 2014
• **DOI** http://dx.doi.org/10.11606/issn.2357-8041.clrd.2014.68234

INTRODUCTION

The sphenoidal sinus (SS) and its variation between individuals and between sides of the same skull were described by Zuckerkandl in 1893.[1] This variability underlies the reason for the few papers published in the literature defining the standard sinonasal configuration and the significance of its internal septa (IS) and limits. Considering the range of imaging resources currently available, it seems important to explore this anatomic structure with the object of contributing to the study of human anatomy.

The basilar expansion of the sphenoidal sinus (BESS) is a posterior expansion located anteriorly and inferiorly to the clivus. It was studied to better understand its relevance in performing endoscopic or microscopic endonasal surgical interventions, including access to the SS itself, and in using transsphenoidal pituitary approaches. Inappropriate surgical planning, or even an inaccurate approach during surgery, may cause significant damage, such as clival perforation or internal carotid artery injury.[2-5]

The use of cone beam computed tomography (CBCT) has been growing. This technique combines high-quality images, owing to its isotropic voxels, with low-radiation doses, as compared to helical computed tomography (HCT).[6-7] Revision of tissue-weighting factors in the 2007 International Commission on Radiological Protection (ICRP) recommendations considered the cancer incidence data that was not available when the 1990 guidelines were drawn up. Weighted tissues and organs and revised weights in the 2007 recommendations are justified because of accumulated epidemiologic information on the tumorigenic effects of radiation that is now sufficient for estimating cancer risks. Because of cumulative X-ray risks, defining strategies for dose reduction is imperative, including the choice of radiographic unit. However, to date, patients are mostly submitted to HCT examinations and to their high-radiation doses for SS evaluation or surgical planning.[7-9]

The aim of this study was thus to investigate the presence and type of BESS and IS in human SS by using CBCT, and correlate the data with gender and age. Validating this imaging method for SS evaluation is also one of the study objectives.

METHODS

Archived images from 300 adult subjects of both genders were retrieved from the files of a private radiology clinic located in the city of Campinas, SP, Brazil. The images had been obtained using a CBCT device (i-Cat 3D Dental Imaging System; Imaging Sciences International, Hatfield, PA, USA), set at the following parameters:

- scan time, 40 s;
- field of view, 13 cm;
- 120 kVp;
- 36 mA; and
- pixel size, 0.25 mm.

All images selected for this analysis were of high quality, therefore allowing accurate SS evaluation and interpretation. Only patients with no history of neurological or paranasal sinus surgery were considered for this study. Any type of intervention in this area could cause IS changes or other anatomical damage, potentially invalidating the results of this study.

The analysis was conducted using Xoran software (Imaging Sciences International, Hatfield, PA, USA) provided by the CBCT device, which allows evaluation of axial and sagittal views, and identification of the BESS and the IS. The image selected for evaluation was that which presented the foramen lacerum in the most posterior part of the SS in the axial view. This central image was the image of choice for SS evaluation.

Following the Haetinger[1] protocol, the presence or absence of BESS was evaluated considering

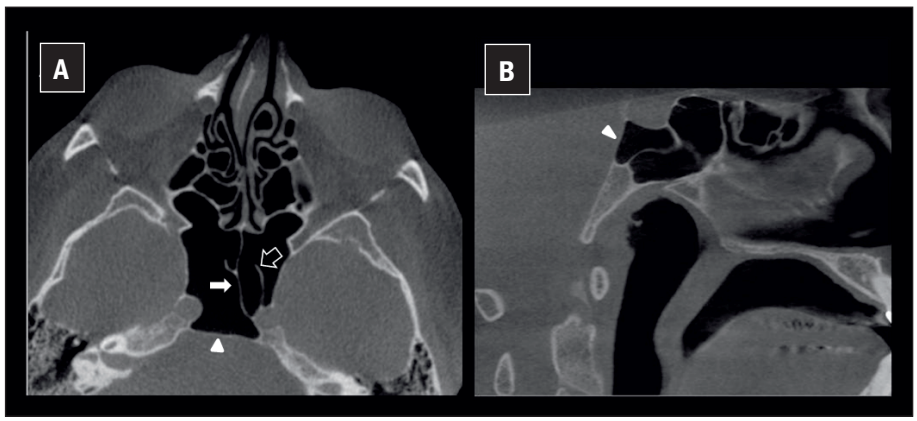

Figure 1 | **A:** Axial view; **B:** sagittal view. Presence of a critical basilar expansion of the sphenoidal sinus (white arrow head), main septum (white arrow), and accessory septum (black arrow).

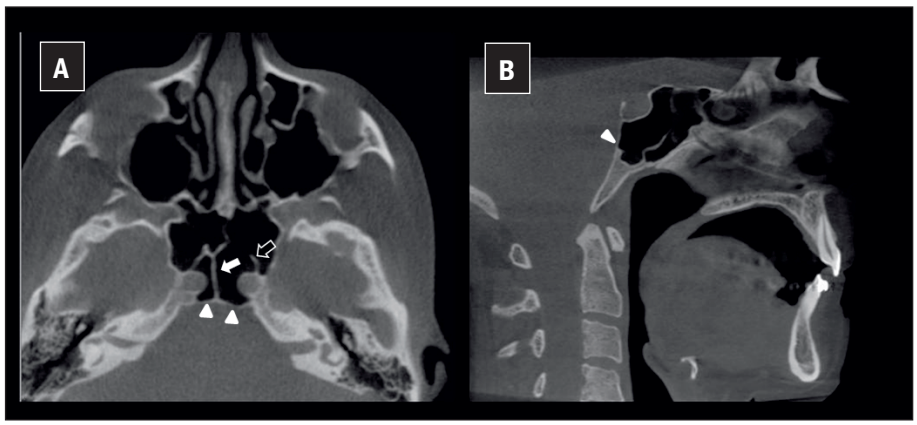

Figure 2 | **A:** Axial view; **B:** sagittal view. Presence of bilateral critical basilar expansion of the sphenoidal sinus (white arrow head), main septum (white arrow), and accessory septum (black arrow).

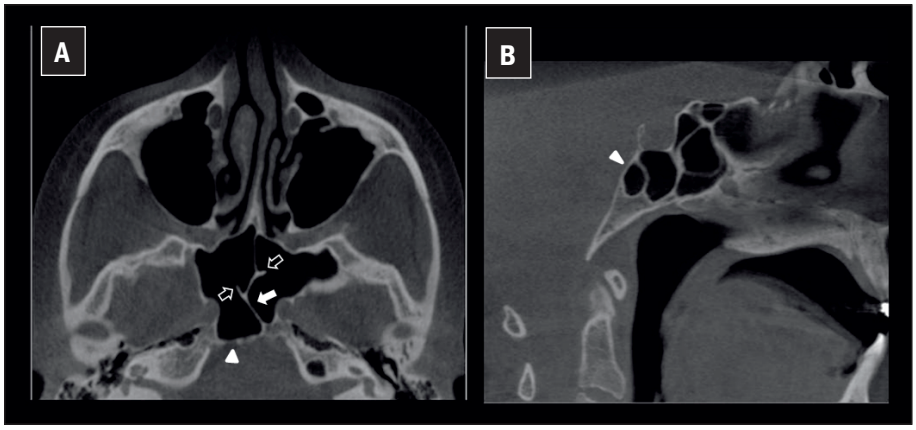

Figure 3 | **A:** Axial view; **B:** sagittal view. Presence of a unilateral, critical basilar expansion of the sphenoidal sinus (white arrow head), main septum (white arrow), and accessory septa (black arrow).

the anterior portion of the foramen lacerum as its limit. When expansions were found, they were classified as unilateral or bilateral and, based on posterior SS wall thickness, as critical or noncritical. The wall thickness was measured using a software tool; when the wall thickness was less than 2 mm, the SS was classified as critical. The presence of IS and its types, i.e., main septum or accessory septa, was also evaluated (Figures 1 through 3)

A descriptive analysis relating gender and age to

BESS and IS types and frequencies was performed. The associations between BESS, IS, gender, and age were evaluated using the chi-square test and Fisher's exact test. The chi-square test evaluates the association between categorical variables in a contingency table with R rows and C columns. When the expected frequency is less than 5, it is appropriate to use Fisher's exact test instead.

For all the tests, a p-value corresponding to 5% was considered significant. All the analyses were performed using SAS software for Windows, v.9.3.1 (SAS Institute, Cary, NC, USA).

The percentages of subjects with IS (main, accessory, and both) were obtained among the total subjects. These percentages were compared using the proportion difference test. This test is based on the chi-square test and determines whether the proportions are equal (homogeneity proportion test). This test was performed on the total sample and was also stratified according to gender.

This study was conducted ethically and was approved by the Research Ethics Committee, School of Dentistry, University of São Paulo (Brazil).

RESULTS

Among all the 300 images evaluated, 69% showed BESS, of which 81% were considered critical. IS was observed in 60% of the images.

Table 1 presents the association of the presence or absence of BESS with gender and age. These results, as assessed using Fisher's exact test, show no association between BESS and gender at various ages.

Table 2 presents the relationship between critical and noncritical expansions, age, and gender. These results show no association between unilateral and bilateral BESS, critical and noncritical BESS, and gender at various ages.

Table 3 shows the relationship between septa and gender at various ages. According to Table 3, there is no correlation between IS and gender.

Table 1 | Association between BESS and gender at various ages.

Age	Gender	Without basilar expansion	With basilar expansion	Total
20–29	Male	5	12	17
	Female	3	8	11
	Total	8	20	28
		P = 1.0000*		
30–39	Male	8	16	24
	Female	12	24	36
	Total	20	40	60
		P = 1.0000*		
40–49	Male	9	25	34
	Female	5	26	31
	Total	14	51	65
		P = 0.3749*		
50–59	Male	10	29	29
	Female	12	19	31
	Total	22	48	60
		P = 0.3033*		
60–69	Male	14	15	29
	Female	9	15	24
	Total	23	30	53
		P = 0.5787		
70–79	Male	4	10	14
	Female	2	8	10
	Total	6	18	24
		P = 1.0000*		

*Fisher's exact test.

However, there is a relevant correlation between septa and gender for the following age groups:

- 30–39,
- 40–49,
- 60–69, and
- 70–79.

Table 4 presents the logistic regression model, with BESS as a response variable, and gender and age as explanatory variables. According to this table, age and gender have no effect on the occurrence of BESS; in other words, the occurrence of BESS is independent of age and gender, as deter-

Table 2 | Association between critical and noncritical basilar expansion, gender, and age.

Age	Gender	Basilar expansion					
		Critical			Noncritical		
		Unilateral	Bilateral	Total	Unilateral	Bilateral	Total
20–29	Male	0	10	2	0	2	2
	Female	0	7	7	0	1	1
	Total	0	17	17	0	3	3
		P = **			P = **		
30–39	Male	0	14	14	0	2	2
	Female	2	15	17	2	5	7
	Total	2	29	31	2	7	9
		P = 0.4882*			P = 1.0000*		
40–49	Male	2	18	20	0	5	5
	Female	2	20	22	0	4	4
	Total	4	38	42	0	9	9
		P = 1.0000*			P = **		
50–59	Male	4	21	25	0	4	4
	Female	2	11	13	0	6	6
	Total	6	32	38	0	10	10
		P = 1.0000*			P = **		
60–69	Male	0	11	11	0	4	4
	Female	0	13	13	0	2	2
	Total	0	34	34	0	6	6
		P = **			P = **		
70–79	Male	2	6	8	0	2	2
	Female	0	8	8	0	0	0
	Total	2	14	16	0	2	2
		P = 0.4667*			P = **		

*Fisher's exact test; **No test was performed because of an excessive frequency of zero.

mined using the chi-square test (Table 1). A greater standard error than that expected would give an odds-ratio confidence-interval value of 1, indicating that the presence or absence of basilar expansion is independent of gender and age.

DISCUSSION

The SS is highly variable in regard to size and format, and expansions are often observed. Its thin walls can render its relationship with neighboring structures critical, thus requiring a more careful surgical approach.[1] In this study, basilar expansion was observed in 69% of the cases.

The presence of septa and projections is more frequent in the SS than in other paranasal sinuses[10] due to the fusion lines between bone components of the SS and its development process.[11] SS development starts at 3 or 4 months of fetal life as a cartilaginous capsule. Ossification starts in the fifth month of fetal life, but fusion to the sphenoid bone occurs only by the fourth year after birth. Areas of bone resistance to pneumatization may occur at the junction points, resulting in IS formation.[12]

The presence of BESS promotes contact be-

Table 3 | Association between septa and gender at various ages.

Septa					
Age	Gender	Main	Accessory	Both	Total
20–29	Male	1	0	4	5
	Female	2	2	0	4
	Total	3	2	4	9
		P = 0.0476*			
30–39	Male	8	2	3	13
	Female	15	2	7	24
	Total	23	4	10	37
		P = 0.7743*			
40–49	Male	14	0	9	23
	Female	11	4	4	19
	Total	25	4	13	42
		P = 0.0485*			
50–59	Male	20	4	7	31
	Female	11	6	4	21
	Total	31	10	11	52
		P = 0.4205*			
60–69	Male	6	0	9	15
	Female	11	0	0	11
	Total	17	0	9	26
		P = 0.0024**			
70–79	Male	2	0	7	9
	Female	7	0	0	7
	Total	9	0	7	16
		P = 0.0032**			

*Fisher's exact test; **Fisher's exact test excluding the zeros.

tween the foramen lacerum and IS.[1] BESS may also be close to other important adjacent structures, or even promote the attachment of IS from ossification center junctions to these adjacent structures.[2] These aspects explain the importance of studying SS and identifying BESS and IS, in order to avoid errors during surgical interventions.[3]

The surgical importance of these anatomical variations (BESS and IS),[13,14] in conjunction with the precise anatomical knowledge of the SS and its variations, is crucial when a surgical approach is necessary.[1] These are all confirmed by HCT, an imaging method that contributes to better understanding craniofacial complexity.[15] A great variety of SS formats and sizes is frequently investigated,[16] and HCT provides accurate linear and volumetric data for anatomic evaluation of the SS, as well as for that of neighboring structures.[1, 17-20]

In 1998, a different technique of computed tomography based on a cone beam was presented.[21] This technique (CBCT) is also highly accurate for maxillofacial diagnosis, including linear, angular, and volumetric measurements, and provides improved image quality for dental structures and nearby structures.[6,22,23] On the other hand, multislice HCT has proved only slightly more accurate than CBCT for making linear and volumetric measurements.

In fact, the most important advantage of CBCT is its low-radiation dose as compared to that required by HCT.[7-9,24] Loubele *et al.*[9] compared the effective dose levels of CBCT with HCT for maxillofacial applications, according to 2007 ICRP guidelines. Effective dose values ranged from 13 to 82 μSv for CBCT and from 474 to 1160 μSv for HCT. The authors concluded that CBCT dose levels are lower than those used in HCT protocols. This reduced dose, combined with ease of use and economic accessibility, highlights the importance of using CBCT technique for BESS and IS evaluation.

Our results show that the BESS can be visualized with CBCT, since the BESS frequency found in this study (Tables 1 and 2) is in agreement with that reported in the related literature.[5,25-28] This means that changing the imaging method from HCT to CBCT did not affect or jeopardize the proposed SS analysis. The same occurs with the IS evaluation, insofar as the IS frequency was 60% in our study (Table 3), whereas the related literature reports an endoscopically determined IS frequency of 68.8%.[4]

The related literature also describes the presence or absence of BESS as independent of patient

Table 4 | Logistic regression model with and without BESS variables.

Without basilar expansion					
Variable	Estimated	Standard error	P value	OR	CI 95%
Gender					
Male	–0.0482	0.1278	0.7060	0.908	0.550–1.499
Female	1	-	-	-	-
Age					
20–29	–0.0820	0.3697	0.8244	1197	0.348–4.119
30–39	0.1612	0.2663	0.5450	1527	0.522–4.465
40–49	–0.4506	0.2835	0.1119	0.828	0.276–2.482
50–59	0.0590	0.2527	0.8155	1379	0.481–3.952
60–69	0.5747	0.2662	0.0309	2309	0.790–6.747
70–79	1	-	-	-	-

OR, odds ratio; CI 95%, confidence interval of 95%.

gender or age,[29,30] an observation confirmed by the results obtained in our study (Tables 1, 2 and 4). Additionally, in accordance with the study by Haetinger *et al.*,[1] 81% of all BESS cases were classified as critical, highlighting the importance of this evaluation for surgical planning.[1-3,13-15,26] In contrast, there was a strong correlation between IS frequency and patient age, starting at age 30, regardless of gender (Table 3).

In conclusion, CBCT proved a valuable tool for the evaluation of both BESS and IS. It provides high-quality images using low-radiation doses, and should therefore be considered for the evaluation of this anatomic segment. Neither BESS nor IS was found to be gender-dependent, and their high frequencies indicate that they should be taken into consideration when planning a surgical intervention.

REFERENCES

1. Haetinger RG, Navarro JA, Liberti EA. Basilar expansion of the human sphenoidal sinus: an integrated anatomical and computerized tomography study. Eur Radiol. 2006 Sep;16(9):2092-9.
2. Peele JC. Unusual anatomical variations of the sphenoid sinuses. Laryngoscope. 1957 Mar;67(3):208-37.
3. Hammer G, Radberg C. The sphenoidal sinus. An anatomical and roentgenologic study with reference to transsphenoid hypophysectomy. Acta radiol. 1961 Dec;56:401-22.
4. Elwany S, Yacolt YM, Talaat M, El-Nahassm, Gonied A. Surgical anatomy of the sphenoid sinus. J Laryngol Otol. 1983 Mar;97(3):227-41.
5. Elwany S, Elsaeid I, Thabet H. Endoscopic anatomy of the sphenoid sinus. *J* Laryngol Otol. 1999 Feb;113(2):122-6.
6. Farman AG, Scarfe WC. Development of imaging selection criteria and procedures should precede cephalometric assessment with cone-beam computed tomography. Am J Orthod Dentofacial Orthop. 2006 Aug;130(2):257-65.
7. Ludlow JB, Ivanovic M. Comparative dosimetry of dental CBCT devices and 64-slice CT for oral and maxillofacial radiology. Oral Surg Oral Med Oral Pathol Oral Radiol Endod. 2008 Jul;106(1):106-14.
8. Roberts JA, Drage NA, Davies J, Thomas DW. Effective dose from cone beam CT examinations in dentistry. Br J Radiol. 2009 Jan;82(973):35-40.
9. Loubele M, Bogaerts R, Van Dijck E, Pauwels R, Vanheusden S, Suetens P, Marchal G, Sanderink G, Jacobs R. Comparison between effective radiation dose of CBCT and MSCT scanners for dentomaxillofacial applications. Eur J Radiol. 2009 Sep;71(3):461-8.

10. Congdon ED. The distribution and mode of origin of septa and walls of the sphenoidal sinus. Anat Rec. 1920 Mar;18(2):97-123.
11. Cope VZ. The internal structure of the sphenoidal sinus. J Anat. 1917 Jan;51(Pt 2):127-36.
12. Fujioka M, Young LW. The sphenoidal sinuses: radiographic patterns of normal development and abnormal findings in infants and children. Radiology. 1978 Oct;129(1):133.
13. Navarro JA. Surgical Anatomy of the Nose, Paranasal Sinuses, and Pterygopalatine Fossa. In: Stamm AC, Draf W, editors. Micro-endoscopic Surgery of the Paranasal Sinuses and the Skull Base. Berlim: Springer; 2000. p. 17-34.
14. Navarro JA. The Nasal Cavity and Paranasal Sinuses: Surgical Anatomy. 1st ed. Berlin: Springer; 2001.
15. Mutlu C, Unlu HH, Goktan C, Tarhan S, Egrilnez M. Radiologic anatomy of the sphenoid sinus for intranasal surgery. Rhinology. 2001 Sept;39(3):128-32.
16. Cheung DK, Martin GF, Rees J. Surgical Approaches to the sphenoid sinus. J Otolaryngol. 1992 Feb;21(1):1-8.
17. Yonetsu K, Watanabe M, Nakamura T. Age related expansion and reduction in aeration of the sphenoid sinus: volume assessment by helical CT scanning. Am J Neuro Radiol. 2000 (1);21:179-82.
18. Perella A, Rocha SS, Cavalcanti MG. Quantitative analysis of maxillary sinus using computed tomography. J Appl Oral Sci. 2003 Sep;11(3):229-33.
19. Santos DT, Miyazaki O, Cavalcanti MG. Clinical, embryological and radiological correlations of oculo-auriculo-vertebral spectrum using 3D-CT. Dentomaxillofac Radiol. 2003 Jan;.;32(1):8-14.
20. Enatsu K, Takasaki K, Kase K, Jinnouchi S, Kumagami H, Nakamura T, Takahashi H. Surgical anatomy of the sphenoid sinus on the CT using multiplanar reconstruction technique. Otolaryngol Head Neck Surg. 2008 Feb;138(2):182-6. doi: 10.1016/j.otohns.2007.10.010.
21. Mozzo P, Procacci C, Tacconi A, Martini PT, Andreis IA. A new volumetric CT machine for dental imaging based on the cone-beam technique: preliminary results. Eur Radiol. 1998;8(9):1558-64.
22. Mischkowski RA, Scherer P, Ritter L, Neugebauer J, Keeve E, Zöller JE. Diagnostic quality of multiplanar reformations obtained with a newly developed cone beam. Dentomaxillofac Radiol. 2008 Jan;37(1):1-9. doi: 10.1259/dmfr/25381129.
23. Yamashina A, Tanimoto K, Sutthiprapaporn P, Hayakawa Y. The reliability of computed tomography (CT) values and dimensional measurements of the oropharyngeal region using cone beam CT: comparison with multidetector CT. Dentomaxillofac Radiol. 2008 Jul;37(5):245-51. doi: 10.1259/dmfr/45926904.
24. Suomalainen A, Vehmas T, Kortesniemi M, Peltola J. Accuracy of linear measurements using dental cone beam and conventional multislice computed tomography. Dentomaxillofac Radiol. 2008 Jan;37(1):10-7. doi: 10.1259/dmfr/14140281.
25. Kinnman J. Surgical aspects of the anatomy of the sphenoidal sinuses and the sella turcica. J Anat. 1977 Dec;124(Pt 3):541-53.
26. Rothon AL, Hardy DG, Chambers SM. Microsurgical anatomy and dissection of the sphenoid bone, cavernous sinus and sellar region. Surg Neurol. 1979 Jul;12(1):63-104.
27. Banna M, Olutola PS. Patterns of pneumatization and septation of the sphenoidal sinus. J Can Assoc Radiol. 1983 Dec;34(4):291-3.
28. Zecchi S, Orlandini GE, Gulisano M. Statistical study of the anatomo-radiologic characteristics of the sphenoid sinus and sella turcica. Boll Soc Ital Biol Sper. 1983 Apr; 59(4):413-7.
29. Vidic B. The postnatal development of the sphenoid sinus and its spread into the dorsun sallae and posterior clinoid processes. HYPERLINK "http://www.ncbi.nlm.nih.gov/pubmed/?term=The+postnatal+development+of+the+sphenoid+sinus+and+its+spread+into+the+dorsun+sallae+and+posterior+clinoid+processes" \o "The American journal of roentgenology, radium therapy, and nuclear medicine." Am J Roentgenol Radium Ther Nucl Med. 1968 Sep;104(1):177-83.
30. Yune HY, Holden RW, Smith JA. Normal variations and lesions of the sphenoid sinus. Am J Roentgenol Radium Ther Nucl Med. 1975 May;124(1):129-38.

eLRD in Clinical and Laboratorial Research in Dentistry | Prosthodontics

Comparative spectrophotometric study of the color stability of three dental porcelains after repeated firings

• **Marcelo Weber** Graduate Program in Oral Diagnosis, Department of Stomatology, School of Dentistry, University of São Paulo, São Paulo, SP, Brazil • **Denise Sabbag Haddad** Graduate Program in Oral Diagnosis, Department of Stomatology, School of Dentistry, University of São Paulo, São Paulo, SP, Brazil • **Marina Gazzano Baladi** Graduate Program in Oral Diagnosis, Department of Stomatology, School of Dentistry, University of São Paulo, São Paulo, SP, Brazil • **Emiko Saito Arita** Discipline of Oral Radiology, Department of Stomatology, School of Dentistry, University of São Paulo, São Paulo, SP, Brazil

ABSTRACT | The purpose of this investigation was to quantify the color differences in CIE ΔE units produced by multiple firings of three all-ceramic systems used in the fabrication of prosthodontic teeth. Thirty samples of the following brands were fabricated: AllCeram, Noritake Cerabien CZR and Vita VM7. A spectrophotometer was used for reflectance measurement of color after 1 firing, 3 firings, 5 firings and 10 firings. The results were converted into CIELAB units. Color differences (ΔE) were calculated in the CIE color space. The color differences resulting from multiple firings proved to be dependent on the number of firings and on the porcelain brand tested.

DESCRIPTORS | Tooth, Artificial; Dental Porcelain; Dental Prosthesis; Spectrophotometry; Color.

RESUMO | **Estudo espectrofotométrico comparativo da estabilidade de cor de três porcelanas dentais após queimas consecutivas** • O objetivo deste estudo foi avaliar a estabilidade de cor de três marcas comerciais de porcelanas dentais aluminizadas durante seu processo de queima. Essas porcelanas são utilizadas para a confecção de dentes de prótese fixa. Para o experimento foram confeccionados 30 corpos-de-prova em forma de disco com 2 mm de espessura e 10 mm de circunferência, sendo 10 da marca AllCeram, 10 da marca Noritake Cerabien CZR e 10 da marca Vita VM7. As amostras foram queimadas 10 vezes. As leituras de cor foram feitas em espectrofotômetro de reflexão nos seguintes intervalos: após a 1ª queima, após a 3ª queima, após a 5ª queima e após a 10ª queima. As curvas de reflexão foram convertidas em valores LAB e a diferença de cor foi medida por meio do método CIELAB (ΔE). Os resultados obtidos demonstraram que existe variação de cor e que essa variação depende do número de queimas realizadas e da marca comercial utilizada.

DESCRITORES | Dente Artificial; Porcelana Dentária; Prótese Dentária; Espectrofotometria; Cor.

CORRESPONDING AUTHOR | • **Marcelo Weber** Department of Stomatology, School of Dentistry, University of São Paulo • **Av. Prof. Lineu Prestes, 2227** São Paulo, SP, Brazil • **05508-900** E-mail: mweber@usp.br

• **Received** Jun 19, 2013 • **Accepted** Apr 25, 2014
• **DOI** http://dx.doi.org/10.11606/issn.2357-8041.clrd.2014.56875

INTRODUCTION

Dental porcelains have been described as the preferred material for the substitution or repair of dental tissue owing to their color and esthetic stability.

Dental porcelains, although esthetic, are susceptible to fracture, which means they require a strong metal or porcelain framework to resist masticatory forces.[1]

Although color stability during the firing of porcelain onto metal has been studied, few studies have focused on the influence of the firing process on the color and translucency of aluminized porcelains owing to their recent development and use.[1]

There are currently many commercial brands of dental porcelains for use over alumina copings in the market. These porcelains are applied in layers, through a technique called stratification. Stratification allows the application of layers with different colors and translucencies, just like natural teeth, requiring repeated firings, for characterization and for size and color corrections. However, dentists and prosthesis technicians have empirically observed that these repeated firings somehow change the color of porcelains.

Spectrophotometric analysis is 45% more accurate than visual analysis for color measurement and for the manufacturing of porcelain-fused-to-metal crowns.[2]

This study evaluated the color stability of three commercial brands of aluminized porcelains applied onto alumina copings, by means of a spectrophotometric analysis after repeated firings, as is the case in stratification and correction firings.

MATERIALS AND METHODS

The following commercial brands were selected for this experiment:

- Noritake Cerabien CZR (Noritake Kizai Co, Nishi-Ku, Nagoya, Japan), dentin A2, lot OE903
- VITAVM7 (VITA Zahnfabrik, Bad Säckingen, Germany), dentin 2M2, lot 7633
- AllCeram (DeguDent GmbH, Hanau, Wolfgang, Germany), dentin A2, lot 25796

Different lots of the same commercial brand may have different colors;[3] therefore, all the samples of each brand were produced with powder from the same lot.

Two procedures were performed in a Ney Centurion VPC oven (Dentsply, Burlington, NJ, USA) prior to porcelain firings:

- one to decontaminate it and
- another to determinate its real temperature.

Pure silver was used to determinate the temperature, as recommended by the manufacturer. A silver lamina was burnt at a temperature of 940°, and the process was observed through the oven window. It was observed that the silver started to fuse at 920°, not at 940°, so all the porcelain firings were performed discounting 20°, as recommended by the oven manufacturer.

A firing at program no. 0 was performed to promote oven decontamination, in order to eliminate any oxides present.

Ten disc-shaped test specimens (TS) of each commercial brand were fabricated, measuring 10 mm in circumference and 2 mm in thickness, the size corresponding to the size of the spectrophotometer window.

The TSs were placed in individual plastic boxes numbered from 1 to 10 and labeled with their corresponding commercial brand.

The discs were fabricated first by producing black Teflon round templates, with an internal fissure of 12 mm in diameter by 3 mm in thickness, to compensate for firing contraction, thus producing final samples of 10 mm in diameter by 2 mm in thickness. The black Teflon templates were divided into two parts so that the compensated porcelain could be removed without cracking. Metal rings were produced around the Teflon templates to hold

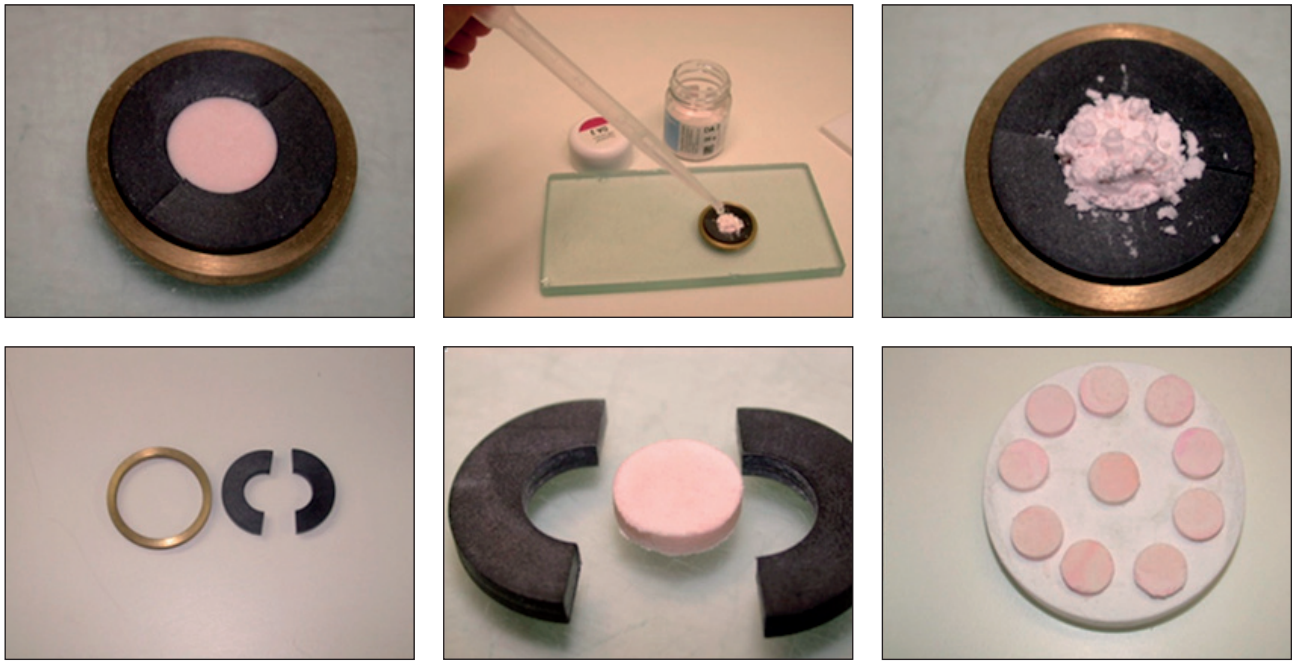

Figure 1 | Fabrication of 3 mm discs of porcelain to be fired.

them together during porcelain condensation.

Porcelain powders were condensed inside the templates and 3 drops of distilled water were added to each sample to facilitate condensation and removal of the porcelain from the inside of the templates without cracking (Figure 1). The samples were assembled on a glass plate and, after template removal, they were moved to a glass fiber holder and then taken to the porcelain oven to be fired according to the manufacturer's instructions.

After fabricating the porcelain discs, they were placed on the refractory holder and taken to the oven for the first dentin firing, following the recommendations of each manufacturer.

After the first firing, the thickness of the discs was measured at their center with a micrometer (Otto, São Paulo, SP, Brazil) and any samples less than 2 mm thick were eliminated. The samples were then cut by a buffing machine with circular sand paper at a rotation of 80 rpm under abundant flowing water. Measurements were constantly made during cutting using digital calipers (Mitutoyo, Suzano, SP, Brazil) until reaching 2 mm in thickness. The samples were then cleaned in an ultrasonic bowl with distilled water for 15 minutes in order to remove impurities (Figure 2).

The samples were placed individually into numbered plastic boxes from V1 to V10 for the VITA samples, N1 to N10 for the Noritake samples, and A1 to A10 for the AllCeram samples (Figure 2).

Color analysis of each TS was performed using a Shimadzu UV-2401PC spectrophotometer (Shimadzu Corp., Kyoto, Japan) with which the reflection curve for an average daylight (D65) illumination and an observer at 2° was obtained. The x, y and z coordinates of chromaticity recommended by the Comission Internationale d'Eclairage (CIE-1976) were taken from the reflection spectrophotometric curve, thus obtaining the LAB color-space. The "L*," "a*" and "b*" values were obtained according to the norms.[4]

For the color intervals, L* indicates luminosity and a* and b* indicate color direction, where +a* is the red direction and –a* is the green direction, +b*

Figure 2 | Procedures to obtain a 2 mm sample free of dust.

indicates the yellow direction and –b* indicates the blue direction. The center has no color.

In this study, color intervals were recorded after the 1st firing, after the 3rd firing, after the 5th firing and after the 10th firing.

The following formulas recommended by the CIE LAB method were used to measure the color differences observed after repeated firings:

$$\Delta E = [(\Delta L)^2 + (\Delta a)^2 + (\Delta b)^2]\ ½$$

$$\Delta L = L1 - Lo \text{ (final – initial record)}$$

$$\Delta a = a1 - ao \text{ (final – initial record)}$$

$$\Delta b = b1 - bo \text{ (final – initial record)}$$

Only visible light (400 to 700 nm) is of interest, and human eyes are more sensitive to a wave length of about 550 nm.[5]

After the TSs were manufactured and cleaned, they were taken to the spectrophotometer for the first recording in the 400 to 700 nm light zone, and the spectrophotometric curves at intervals of 0.5 nm were obtained and recorded.

The samples were grouped again in the holder for firing in the oven, following the 1 to 10 sequence, and two more firings were performed, following the instructions of each manufacturer for the 2nd dentin firing. A new spectrophotometric recording was taken of each sample. The samples were grouped again in the holder for firing in the oven, following the 1 to 10 sequence and 2 more firings were performed, following the instructions of each manufacturer for the 3rd dentin firing. A new spectrophotometric recording was taken of each sample; the CIE LAB values were obtained and recorded.

The samples were grouped again in the holder for firing in the oven, following the 1 to 10 sequence and 5 more firings were performed, following the instructions of each manufacturer for the 4th dentin firing. A new spectrophotometric recording was taken of each sample; the CIE LAB values were obtained and recorded.

The color difference among the samples was calculated using the CIELAB method, and named ΔE. The ΔE value is obtained by calculating the square root of the sum of the squares of the values of ΔL, Δa and Δb. The ΔE value for each sample was calculated between the first and the third firings, ΔE1; between the third and the fifth firings, ΔE2; and between the fifth and the tenth firings, ΔE3.

RESULTS

The data obtained from the spectrophotometric recordings (Figure 3) were submitted to one-way ANOVA at a level of significance of 0.05. When the p value < 0.05, the null hypothesis is rejected and the mean values are statistically different, which means at least one of the mean values is different from the others. Bonferroni and Tukey tests were applied.

There were no statistically significant differences among the ΔE1 values of the Noritake Cerabien CZR, VitaVM7 and AllCeram all-ceramic systems.

However, the ΔE2 mean value of the AllCeram porcelain was significantly higher than that of Noritake Cerabien CZR and VitaVM7 (p = 9.97533).

There was no statistically significant difference between the ΔE3 mean values of the three commercial brands.

At a significance level of 0.05, there was no statistically significant difference between the ΔE2 means of the Noritake Cerabien CZR and VitaVM7 all-ceramic systems.

The color differences of Noritake Cerabien CZR and AllCeram were calculated after the 3rd firing because both should show the same color, i.e. A2. The mean ΔE value between the two brands was 3.8.

DISCUSSION

A ΔE value below 1 is hardly visible. A ΔE value between 1 and 2 may be clinically visible by some observers, and a ΔE value above 2 can be identified 100% of the time. A ΔE value above 3.3 is not clinically acceptable.[2,6]

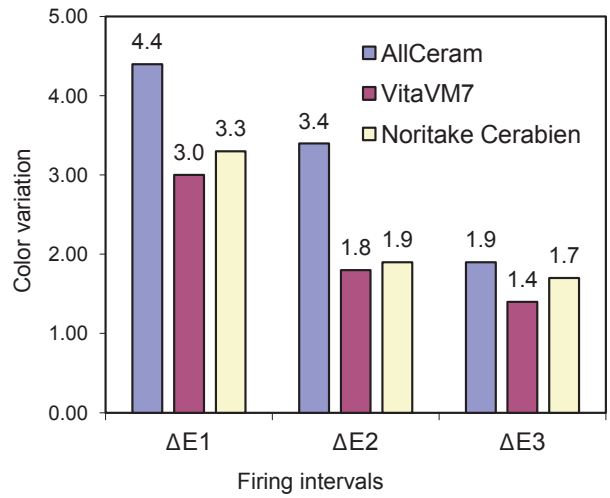

Figure 3 | Color variation of the three porcelain brands.

Observing Figure 3, we can see that the ΔE1 values of the VitaVM7 and Noritake Cerabien CZR samples were noticeable, but clinically acceptable, while the ΔE1 of AllCeram was noticeable and not clinically acceptable. The mean ΔE2 values of the Vita VM7 and Noritake Cerabien CZR samples were not noticeable by the ordinary observer and were clinically acceptable, whereas the mean ΔE2 value of the AllCeram samples were noticeable and not clinically acceptable. The ΔE3 values of the three commercial brands ranged between 1 and 2, which is not noticeable by the ordinary observer and is clinically acceptable.

Possible color change after repeated firings is due to the elimination of air pores from the inside of the porcelain during the firings.[7]

There is a microscopic decrease and change in the shape of the pores on the surface of the aluminized porcelains when there is an increase in firing time or temperature.[8] The results obtained in this study confirm this, because a change in the color of the dental porcelains studied occurred together with the increase in firing time.

Translucency and color intensity of dental porcelain depend on the percentage of vitreous phase

present in the structure. Both become more intense with the increase of the vitreous phase. The sintering phase, vitreous phase and crystalline phase influence not only translucency, but color intensity of the porcelain as well.[1]

Dependence on the porcelain firing conditions is clearly shown by the percentage of vitreous and sintering phases present in the micro structure of the porcelain.

By increasing the maintenance and temperature time, as well as the warming up time, a decrease in the sintering phase and an increase in the vitreous phase are observed. With an increase in the vitreous phase there is an increase in translucency and color intensity.

Our study has shown that, if firing time is increased, there is a color change in the dental porcelains tested.

Color changes happened more intensely especially between the 1st and 3rd firings because, after the first firing, the samples were finished with only a buffing machine, and after the 3rd firing the test specimens appeared self glazed, showing a greater glow due to an increase in the vitreous phase and migration of glass particles to the surface. This greater surface glow and color intensity alter the quantity of reflected light and, consequently, the LAB values. It is important to observe the color change in this phase, because dental porcelains are normally tried out and adjusted before the glaze firing.

According to the instructions of the three manufactures, three firings are recommended:

- 1st dentin firing,
- 2nd dentin firing and
- 3rd firing for glaze.

The number of firings varies according to the laboratory and patient;[9] however, the color change that occurs from the 3rd firing on is of special interest, because it is from this point on that the correction firings take place. According to Figure 3, between the 3rd and 5th firings the ΔE value was 3.4 for AllCeram, 1.8 for Vita VM7 and 1.9 for Noritake Cerabien CZR. The mean ΔE2 value of the AllCeram samples was statistically higher than that of the Vita VM7 and Noritake Cerabien CZR samples. Considering the recommendations of the AllCeram manufacturer, corrections from the 3rd firing on should be made with a corrective paste, whose firing temperature is much lower than that of the 2nd dentin firing.

The smallest color change occurred in the interval between the 5th and the 10th firings for the three commercial brands, with a ΔE3 value of 1.4 for Vita VM7, 1.7 for Noritake Cerabien CZR and 1.9 for AllCeram .

Analyzing the color stability of the three commercial brands tested in this study, we can see that the ΔE1 value was higher than the ΔE2 value, which was higher than the ΔE3 value, which means the color change decreased along with the repeated firings, indicating that porosity and color intensity changed more markedly during the first firings.

ΔE values vary according to the commercial brand tested.[10] Each commercial brand in this study had its own ΔE value in the firing intervals tested. However, statistically, the AllCeram porcelain had a greater color change than the Noritake and Vita VM7 porcelains in the interval between the 3rd and 5th firings.

A spectrophotometric analysis of the color differences among the dental porcelain systems showed that equivalent shades of different commercial brands have visible color differences.[11] We agree with the authors, for the reason that, when comparing the color of the AllCeram and Noritake Cerabien CZR A2 dentin porcelains, after the standard number of three firings, we observed a ΔE color difference of 3.8, which is a visible value for the ordinary observer and not clinically acceptable.

After testing the color stability of the three com-

mercial brands after repeated firings, by means of spectrophotometry, we have come to the conclusion that there is a clinically acceptable color variation and that this variation depends on the number of firings performed and on the commercial brand used.

REFERENCES

1. Claus H. The structure and microstructure of dental porcelain in relationship to the firing conditions. Int J Prosthodont. 1989 Jul-Aug;2(4):376-84.
2. Paul SJ, Peter A, Rodoni L, Pietrobon N. Conventional visual vs spectrophotometric shade taking for porcelain-fused-to-metal crowns: a clinical comparison. Int J Periodontics Restorative Dent. 2004 Jun;24(3):222-31. doi: 10.1016/j.prosdent.2004.07.004.
3. Rinke S, Huls A, Kettler MJ. Colorimetric analysis as a means of quality control for dental ceramic materials. Eur J Prosthodont Restor Dent. 1996 Sep;4(3):105-10.
4. McLaren K. M. The development of the CIE 1976 (L*a*b*)uniform colour-space and colour-difference formula. J Soc Dyers Colour. 1976 Sep;92(9):338-41. doi: 10.1111/j.1478-4408.1976.tb03301.x.
5. Southan DE. Factors affecting the translucency of dental porcelain. Quintessence Int. 1987 Mar;18(3):197-202.
6. Ruyter IE, Nilner K, Moller B. Color stability of dental composite resin materials for crown and bridge veneers. Dent Mater. 1987 Oct;3(5):246-51. doi: 10.1016/S0109-5641(87)80081-7.
7. Barghi N, Goldberg. Porcelain shade stability after repeated firing. J Prosthet Dent. 1977 Feb;37(2):173-5. doi: http://dx.doi.org/10.1016/0022-3913(77)90239-6.
8. Cheung KC, Darvell BW. Sintering of dental porcelain: effect of time and temperature on appearance and porosity. Dent Mater. 2002 Mar;18(2):163-73. doi: doi:10.1016/s0109-5641(01)00038-0.
9. Seghi RR, Johnston WM, O'Brien WJ. Spectrophotometric analysis of color differences between porcelain systems. J Prosthet Dent. 1986 Jul;56(1):35-40. doi: 10.1016/0022-3913(86)90279-9.
10. O'Brien WJ, Kay KS, Boenke KM, Groh CL. Sources of color variation on firing porcelain. Dent Mater. 1991 Jul;7(3):170-3. doi: 10.1016/0109-5641(91)90038-Z.
11. Seghi RR, Hewlett ER, Kim J. Visual and instrumental colorimetric assessments of small color differences on translucent dental porcelain. J Dent Res. 1989 Dec;68(2):1760-4. 10.1177/00220345890680120801.

Quantitative analysis of dental enamel removal during a microabrasion technique

• **Karen Müller Ramalho** Biodentistry MSc Program, School of Dentistry, Ibirapuera University (UNIB), São Paulo, SP, Brazil • **Ana Cecília Correa Aranha** Special Laboratory of Lasers in Dentistry (LELO), Department of Restorative Dentistry, School of Dentistry, University of São Paulo, São Paulo, SP, Brazil • **Carlos de Paula Eduardo** Special Laboratory of Lasers in Dentistry (LELO), Department of Restorative Dentistry, School of Dentistry, University of São Paulo, São Paulo, SP, Brazil • **Rodney Garcia Rocha** Discipline of Integrated Clinical Dentistry, Department of Stomatology, School of Dentistry, University of São Paulo, São Paulo, SP, Brazil • **Marina Stella Bello-Silva** Department of Restorative Dentistry, School of Dentistry, Nove de Julho University (UNINOVE), São Paulo, SP, Brazil • **Friedrich Lampert** Department of Operative Dentistry, Periodontology and Preventive Dentistry, Medical Faculty, RWTH Aachen University, Aachen, Germany • **Marcella Esteves-Oliveira** Department of Operative Dentistry, Periodontology and Preventive Dentistry, Medical Faculty, RWTH Aachen University, Aachen, Germany

ABSTRACT | *Objective:* To quantify, by means of profilometry, the removal of dental enamel during the use of a microabrasion technique involving the use of hydrochloric acid and manual abrasion with a plastic spatula. *Method:* Thirty six specimens obtained from human third molars were polished to obtain flat surfaces and divided into 3 groups (n = 12) according to the different treatments received: A placebo treatment with deionized water as a negative control (CG); microabrasion with 6.6% hydrochloric acid, Opalustre™ (G1); and microabrasion with 6% hydrochloric acid, Whiteness RM™ (G2). The microabrasion was performed in a standardized manner by submitting the specimens to 4 cycles of 10 seconds each and manual abrasion using a plastic spatula (200 g load). The loss of enamel surface was measured after each cycle of treatment by contact profilometry. *Results:* Enamel loss was already observed after the first 10 seconds of abrasion with hydrochloric acid in both treated groups (G1 and G2). After 4 abrasions of 10 seconds each, the average final enamel losses in the treated groups were 46.04 µm (G1) and 54.65 µm (G2). In the G1 and G2 groups, a significant increase in enamel wear was detected in each cycle in comparison to the control group ($p \leq 0.05$). A significant difference in enamel loss between G1 and G2 was found after 30 and 40 seconds of microabrasion. *Relevance:* The results of this study provide objective data for safely performing the microabrasion technique on dental enamel using hydrochloric acid and manual abrasion using a plastic spatula.

DESCRIPTORS | Dental Enamel; Hydrochloric Acid; Enamel Microabrasion.

RESUMO | **Análise quantitativa da remoção de esmalte dental durante a técnica de microabrasão** • *Objetivo:* Quantificar, por meio de perfilometria, a profundidade de esmalte dental removido durante o emprego de uma técnica de microabrasão utilizando-se ácido clorídrico e abrasão manual com espátula plástica. *Método:* Trinta e seis espécimes obtidos de terceiros molares humanos foram polidos, para obtenção de superfícies planas, e divididos em 3 grupos (n = 12) de acordo com os diferentes tratamentos recebidos: tratamento placebo com água deionizada, como controle negativo (CG); microabrasão com ácido clorídrico a 6.6%, Opalustre™ (G1); e ácido clorídrico a 6%, Whiteness RM™ (G2). A microabrasão foi realizada, de forma padronizada, submetendo os espécimes a 4 ciclos de 10 segundos cada e abrasão manual utilizando-se uma espátula plástica com carga de 200 g. A perda da superfície de esmalte foi medida após cada um dos ciclos de tratamento por meio de perfilômetro de contato. *Resultados:* Após os primeiros 10 segundos de abrasão, já foi encontrada perda de esmalte em ambos os grupos tratados (G1 e G2). Nos grupos G1 e G2, a cada ciclo de 10 segundos, foi observado um aumento significativo na perda de esmalte ($p \leq 0.05$). Após 4 abrasões de 10 segundos cada, as médias de perda de esmalte nos grupos tratados foram 46.04 µm (G1) e 54.65 µm (G2). Foi encontrada uma diferença significativa entre G1 e G2 com relação à perda de esmalte após 30 e 40 segundos de microabrasão. *Relevância:* Os resultados deste estudo fornecem referências para a realização do procedimento de microabrasão em esmalte dental com segurança, utilizando-se ácido clorídrico e abrasão manual com espátula plástica.

DESCRITORES | Esmalte Dentário; Ácido Clorídrico; Microabrasão do Esmalte.

CORRESPONDING AUTHOR | • **Karen Müller Ramalho** Biodentistry MSc Program, School of Dentistry, Ibirapuera University • **Av. Interlagos, 1329** São Paulo, SP, Brazil • **04661100** E-mail: karenramalho@hotmail.com

• **Received** Dec 17, 13 • **Accepted** May 7, 14
• **DOI** http://dx.doi.org/10.11606/issn.2357-8041.clrd.2014.69159

INTRODUCTION

Enamel microabrasion is a conservative technique that uses strong acids in association with abrasive agents to remove an outer layer of enamel.[1-3] It is indicated to correct surface irregularities and for the removal of superficial stains on the dental enamel due to imperfect amelogenesis, fluorosis, hyperplasia, or other conditions.[4-8] The use of acids to remove stains on enamel was first described in 1916.[9] A correct diagnosis is the first step to a successful approach, since different levels of compromised dental structure require different decisions to avoid sub- or over-treatment.[10] Initially, the enamel microabrasion technique used a finishing and polishing bur at high speed on the altered surface with a highly concentrated acid solution (18% hydrochloric acid).[11] Later on, weaker acids were used with smaller abrasive particles, which were soluble in water and easy to apply, without the use of a finishing bur.[5, 12]

Today, microabrasion techniques typically use hydrochloric acid at concentrations in the order of 6%, mixed with an abrasive agent containing small particles of silicon carbide. According to Chandra and Chawla (1975), the use of an abrasive substance increases the speed of stain removal by mechanical action.[13]

Although microabrasion is a conservative procedure, knowledge of the technique is fundamental to perform it correctly. Since there is a structural loss of enamel, prolonged enamel microabrasion may lead to marked enamel structure wear and cause excessive tooth color alteration.[14] When a tooth surface is microabraded, the thickness of enamel is reduced and the color of the dentin becomes more pronounced.[14] Some authors have reported a darker or yellowish color on teeth subjected to enamel microabrasion.[14] According to Lynch and McConnell (2003),[2] based on laboratory studies,[15] enamel removal varying from 45.5 μm to more than 100 μm is not clinically significant. On the other hand, according to Shillingburg *et al.* (1973), the removal of more than 0.13 mm (130 μm) may be clinically significant, especially in repeated treatments.[16] So, based on the information above, we may assume that enamel removal below 100 μm is not clinically significant,[2] and, above 130 μm, it may be clinically significant.[16]

Data can be found in the literature on the amount of enamel removal after microabrasion with hydrochloric acid (6%–18%) in association with application of a low speed handpiece and rubber cups at several rotations per minute.[3,10,11,17-19] The microabrasion technique can also be performed with manual abrasion, using a plastic spatula, with satisfactory results.[20] Among some of the positive points supporting the application of manual abrasion using a plastic spatula during microabrasion are the ability to control the scattering of HCl over the enamel surface, to manage the exact stained enamel areas to be abraded, and to control the intensity of the procedure by the operator. There is little information in the literature about the amount of enamel loss after microabrasion when hydrochloric acid (6%) is used and abrasion is performed manually with a plastic spatula. Additionally, to the best of our knowledge, the profilometry method has not yet been used to precisely measure hard tissue loss and to identify the limits to a micro invasive clinical application. Since manual abrasion is a possible alternative in the microabrasion technique, and since the amount of enamel wear when the technique is performed combining 6% HCl with manual abrasion is not known, the aim of the present study was to investigate through profilometry the amount of enamel surface loss after a microabrasive treatment using two commercially available gels and manual abrasion using a plastic spatula.

The hypothesis of the study was that enamel microabrasion using 6%–6.6% HCl, at a 200 g load,

manually rubbed using a plastic spatula, during 4 cycles of 10 seconds each, would remove an amount of enamel that is clinically acceptable.

MATERIAL AND METHODS

Sample Preparation

After receiving the approval of the ethics committee of the School of Dentistry, University of São Paulo, Brazil (#08044212.8.0000.0075), eighteen extracted human third molar crowns were selected for this study. Each crown was cut in the buccolingual direction into two halves (Isomet, Buehler, IL, USA). The samples were glued onto a plastic plate measuring 50 × 100 × 2 mm (Exakt GmbH, Norderstedt, Germany) using transparent adhesive (Technovit 7230VLC, HeraeusKulzer GmbH, Wehrheim, Germany) keeping the enamel facing up. The specimens were then serially polished using silicon carbide paper (grit 800, 1200 and 4000; Buehler, IL, USA) under water refrigeration and, subsequently, using a 1 µm diamond paste (Buehler, IL, USA) and felt disk (Buehler, IL, USA). Between each series of polishing, samples were washed in deionized water for 3 minutes. The blocks were cleaned properly and observed through a stereomicroscope to ensure the absence of structural defects and then stored in deionized water. A disk of adhesive tape (Scotch Rubber Tape 2242, 3M, St Paul, MN, USA) with a diameter of 2.5 mm was attached to the center of the enamel surface, and the rest of the block was covered with an acid-resistant varnish (Figures 1 A, B and C). After drying, the tape was removed and the surface was cleaned with cotton, soaked with deionized water to remove any remaining adhesive. Samples were stored in deionized water at 4°C and randomly allocated into the study groups, according to Table 1.

Table 1 | Group distribution and treatment applied.

Group	Composition of microabrasion products applied according to manufacturer
Control (CG; n = 12)	-
Experiment 1 (G1; n = 12)	6.6% hydrochloric acid and microparticles of water-soluble silicon carbide paste (granulation: 20–160 µm), pH < 1. Opalustre™, Ultradent, South Jordan, UT, USA
Experiment 2 (G2; n = 12)	6% hydrochloric acid and silicon carbide (granulation: 82 µm). Propylene glycol USP, thickener and deionized water, pH < 1. Whiteness RM™, FGM, Joinville, SC, Brasil

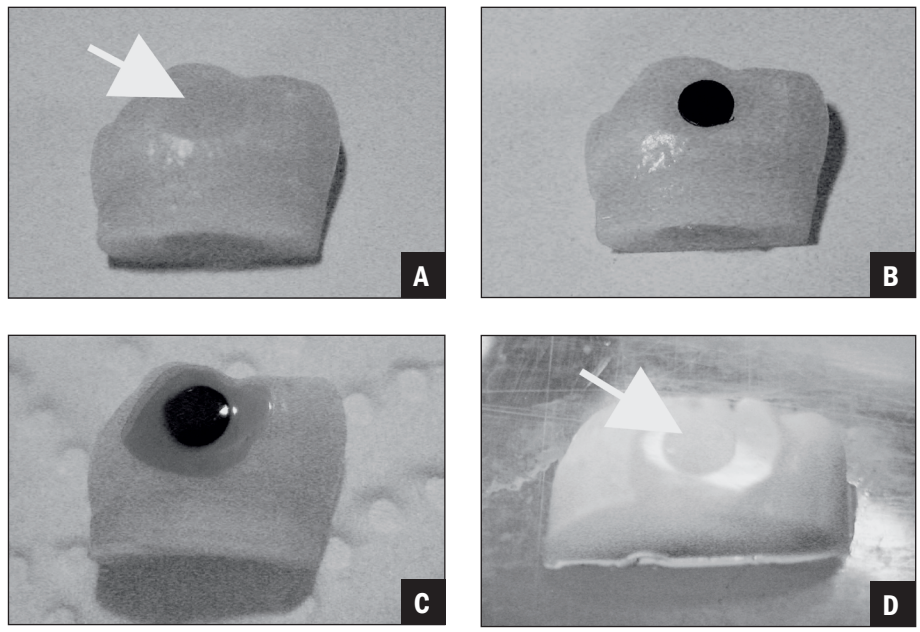

Figure 1 | Sample preparation (A-C). **A**: Polished area (arrow); **B**: Adhesive disk in position; **C**: Area covered with acid-resistant varnish. Sample after microabrasion procedure (D). **D**: After microabrasion and removal of acid-resistant varnish, enamel loss in the area submitted to microabrasion can be observed (arrow).

The steps of sample preparation and treatments are illustrated in Figure 2.

Microabrasion

The enamel surfaces were dried with absorbent paper and the exposed enamel in the experimental groups (G1 and G2) was covered with microabrasion gel. Immediately after that, the gel was rubbed onto the enamel surface for 10 seconds with a plastic spatula and under a standardized 200 g load (controlled using a 200 g metal piece attached to the spatula). The operator made only horizontal movements to promote microabrasion, moving the spatula as illustrated in Figure 2. One movement back and forth was performed per second, for a total of 10 movements each 10 seconds.

After the first application, samples were washed in deionized water and dried. The varnish was removed and the surface loss was measured through profilometry. After the first cycle, another three cy-

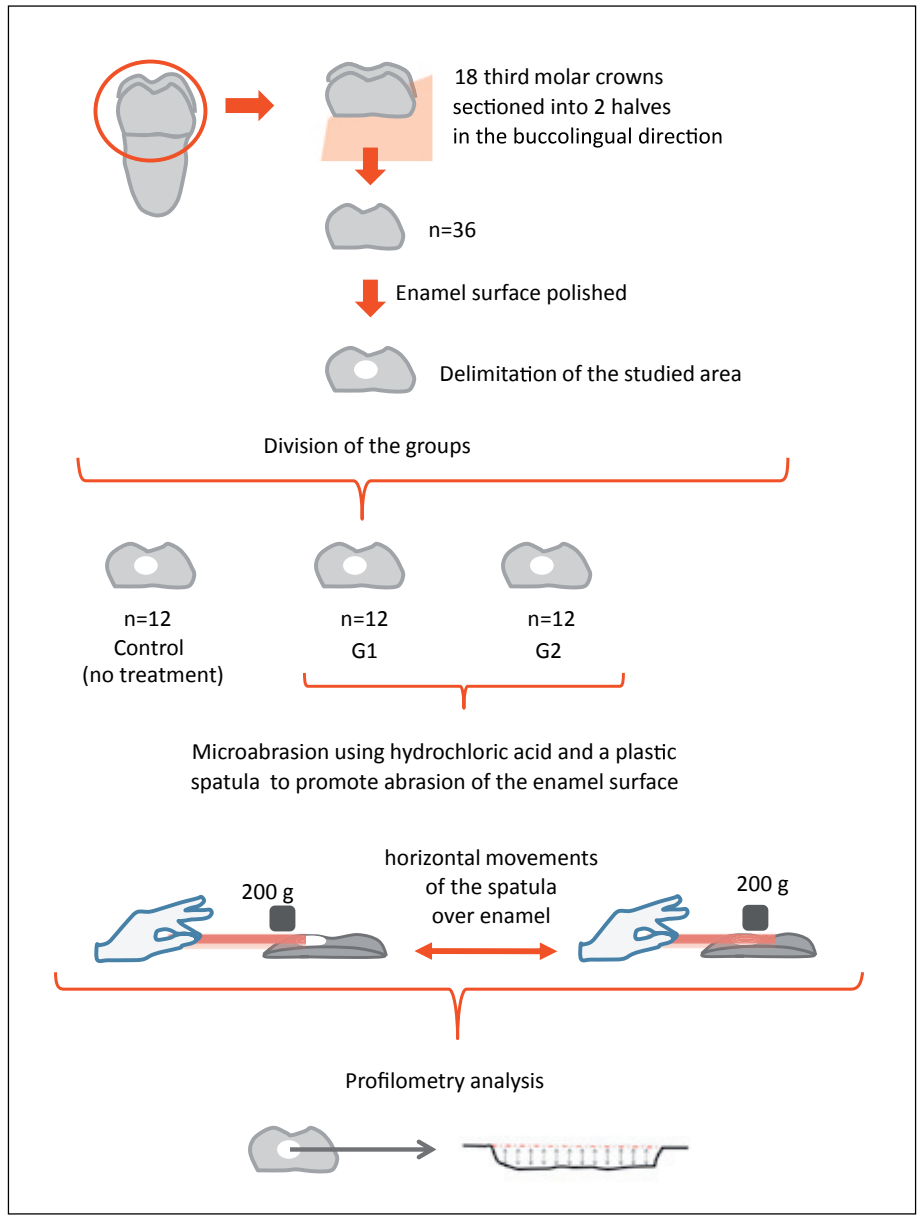

Figure 2 | Methodology applied in the study.

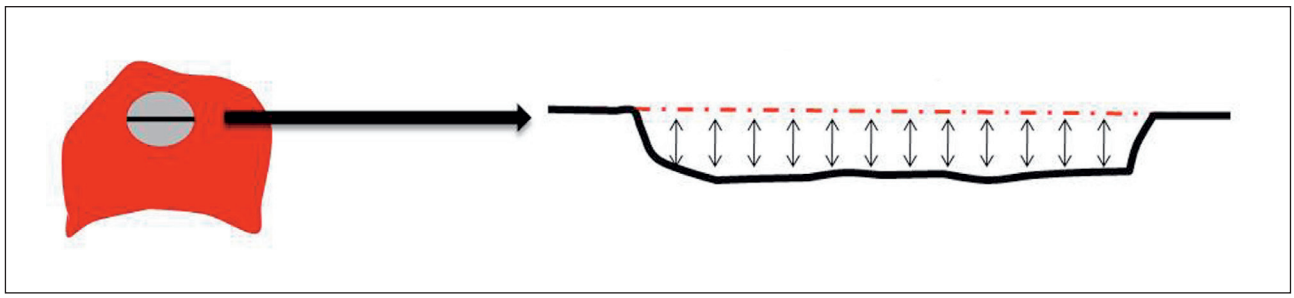

Figure 3 | Illustration of depth measurements made using profilometry of enamel after microabrasion. Twelve depth measurements were made over the extension of a perpendicular line from the surface to the bottom of the enamel lesion formed.

Table 2 | Average (μm) and standard deviation of enamel removal quantified using profilometry.

Duration	Control group	Group 1	Group 2
10 s	0.10 ± 0.05[a]	12.23 ± 2.38[b]	11.11 ± 2.73[b]
20 s	0.12 ± 0.10[a]	23.09 ± 4.00[b]	22.77 ± 4.97[b]
30 s	0.22 ± 0.12[a]	35.95 ± 3.36[b]	42.69 ± 6.31[c]
40 s	0.18 ± 0.11[a]	46.04 ± 5.29[b]	54.65 ± 9.15[c]

Statistically significant difference between treatments at each microabrasion cycle is indicated by different letters ($p \leq 0.05$).

cles of microabrasion were repeated, and, between each one, new measurements of enamel loss were made. In the control group (CG), the same procedures were performed; however, deionized water was used instead of hydrochloric acid.

Profilometry analysis

The enamel surface loss was analyzed using a contact digital profilometer (Konturenmessgerät - MarSurf XC2, Hersteller Firma Mahr GmbH, Mahr GmbH, Göttingen, Germany) with the aid of software (Konturenmessgerät - MarSurf XC2, Hersteller Firma Mahr GmbH, Mahr - GmbH, Göttingen, Germany). The surface scanning was conducted under a 0.7 mN load with a tungsten carbide tip and a 25 μm radius. The scanning line started at the reference surface on the left side of the treated area and continued through the whole treated surface, ending at the next reference enamel surface on the right side of the sample, as previously described.[21,22] Under each scanning line, twelve measurements of depth were made as illustrated in Figure 3.

Statistical analysis

The mean values obtained of the depth of enamel surface loss for each sample at each experimental time were used for the statistical analysis. Since the data of all groups showed homoscedasticity, they were statistically analyzed using ASSISTAT (version 7.7) software by means of 2-way RM ANOVA and post-hoc Tukey tests at a 5% significance level.

RESULTS

The removal of enamel was already detected after the first 10 seconds of hydrochloric acid contact with the enamel in association with manual abrasion in the G1 and G2 groups (Table 2, Figure 4). In all treated groups, after every 10 seconds of treatment, a significant increase in removal of enamel was observed ($p \leq 0.05$; Table 2). After the third and fourth cycle of microabrasion, enamel surface loss was also observed for both treated groups (G1 and G2, $p \leq 0.05$; Figure 4). The G2 group showed greater enamel loss in comparison to the G1 group ($p \leq 0.05$). After 4 cycles of abrasion, the high-

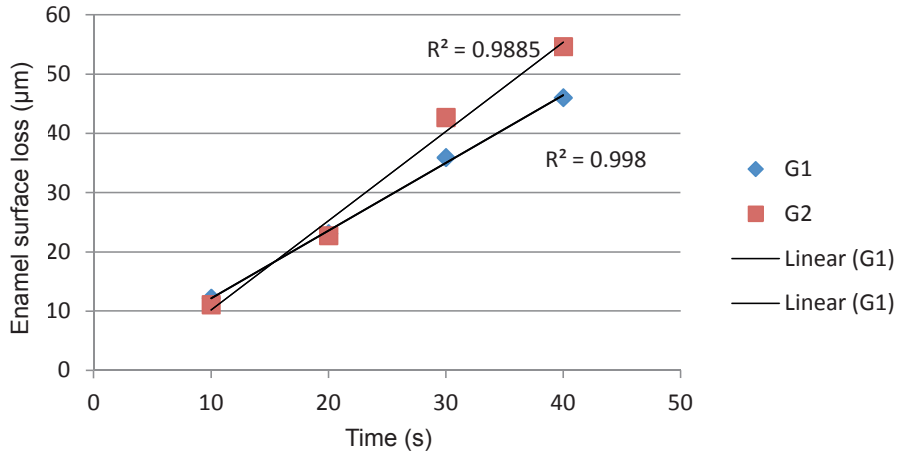

Figure 4 | Graph showing enamel surface loss (µm) over time (s). The increase in surface loss appeared to have a linear trend for both groups (R^2 = 0.998 and 0.9885 respectively for G1 and G2).

est average loss of enamel was found to be 46.04 (± 0.29) µm in the G1 group and 54.65 (± 9.15) µm in the G2 group (Table 2).

DISCUSSION

Microabrasion is a well-defined technique to remove superficial enamel stains caused by several etiologies, such as fluorosis, amelogenesis imperfecta and decalcification defects.[2,6,20,23-25] The literature presents some clinical assessment,[2,6,8,20,24,26] microscopic surface evaluations,[5,27] and hardness measurements of the enamel surface,[27] as well as enamel wear after microabrasion techniques,[3,10,11,17,18] which provide references for technique development. However, although microabrasion should be considered a micro-invasive method, clinical application should be used with caution to avoid excessive substance removal.[3] Excessive enamel removal can lead to esthetic damage and increase dentin sensitivity.[7, 18]

Many factors are reported that can interfere with enamel surface wear after microabrasion, such as manual or mechanical techniques, amount of application, interval between applications, mechanical speed and pressure.[10] Different enamel loss values have been reported in the literature following microabrasion with different hydrochloric acid concentrations, using manual abrasion or a low-speed torpedo-shaped silicone rubber cup for abrasion.[3,10,11,17,18,20,28] However, results seem difficult to compare, since different methodologies, acid concentrations and acid types were tested. Additionally, most studies that have quantified structural loss after microabrasion used hydrochloric acid at a higher concentration than that currently recommended.[11,18,19,28] Currently, the hydrochloric acid concentration applied for enamel microabrasion is approximately 6%. Additionally, most of the studies that evaluated enamel removal after microabrasion with 6% hydrochloric acid used low-speed rubber cup abrasion.[3,10,17] Manual abrasion with a plastic spatula, for example, seems to be a good alternative in microabrasion technique.[20] Since enamel thickness varies in different regions of the crown, removal of the same amount of enamel in different regions of the crown could lead to different treatment outcomes.[18] In gingival regions, deeper removal of enamel may cause a problem of dentinal sensitivity.[18] A clinical study by Kilpatrick and Welbury (1993) reported that, after 2.7 years, 10% of patients submitted to enamel microabrasion reported sensitivity to cold.[29] Additionally, stains on the enamel surface, due to fluorosis, amelogenesis imperfecta, hyperplasia, or other conditions, can appear in localized areas of the enamel. Therefore, dentists should perform microabrasion

only in compromised regions of the enamel. The precision of the abrasion is an important factor to be considered when performing the enamel microabrasion technique. In some clinical conditions, manual abrasion could be an alternative method in performing microabrasion.

Regarding enamel removal using microabrasion with high concentrations of hydrochloric acid (18%) in association with abrasion performed using a low-speed handpiece and a silicone rubber cup, values of 7–22 μm, 160 μm, 36–62 μm, 156 μm and 360 μm of enamel removal were obtained after abrasion during 5, 10, 25, 50 and 100 seconds, respectively.[11,18,30] When manual abrasion was applied by Dalzell *et al.* (1995)[28] with 18% HCl after 100 seconds, a 250 μm enamel loss was obtained. So, despite the differences in methodology applied, the use of manual abrasion seemed to remove less enamel structure after 100 seconds[28] than abrasion using a low-speed handpiece and a silicone rubber cup[18] when performing enamel microabrasion.

Concerning enamel loss during microabrasion with around 6% hydrochloric acid and slight manual abrasion using a plastic spatula, a clinical report by Ramalho *et al.* (2010)[20] observed 40 μm of enamel loss after 50 seconds of abrasion. The final result was considered esthetically successful.[2] The images of the initial and final enamel profiles showed no alteration in the original anatomy of the tooth.[20] In laboratory studies, Paic *et al.* (2008)[3] performed microabrasion for 40 seconds under standardized conditions (300 rpm) using 6.6% hydrochloric acid and an application force of 100 g. Enamel loss was calculated to be 53.1 μm.[3] In a study by Schmidlin *et al.* (2003),[17] surface loss was 134.8 μm after 20 seconds of microabrasion with 6.6% HCl, performed using a 1,000 rpm low-speed contra-angle hand piece and an application force of 200 g.[17] A study by Schmidlin *et al.* (2003)[17] applied another important variable by using previously demineralized enamel, not applied by other studies,[10,19,28,31] nor by the present study. A comparison of the published data[3,17] and the results of the present study suggests that some of the technical variables, such as application force, type of abrasion (mechanical or manual) and duration of procedure, can directly affect the amount of tissue removed.

A significant difference in enamel loss between groups G1 and G2 was found after 30 and 40 seconds of microabrasion. According to manufacturers' instructions, both products tested have similar hydrochloric acid concentrations; however, the G1 group uses hydrochloric acid at a concentration of 6.6% and the G2 group, 6%. Nevertheless, despite the minor hydrochloric acid concentration difference, group G2 had significantly higher enamel loss. It should be pointed out that this difference may not be clinically significant, since the mean difference between both groups was only 8.61 μm at the end of the microabrasion cycles. It can be speculated that this difference occurred due to different granulation sizes of the silicon carbide microparticles of the two products tested. The manufacturer of the gel used in the G1 group indicates a greater variation of silicon carbide granulation (20–160 μm) than indicated for the product used in the G2 group (82 μm). The variation in silicon carbide granulation and the presence of larger particles in the G1 group may have been responsible for the difference in enamel removal found. Despite this, the results found in both treated groups seemed to be appropriate with regard to maximum enamel removal.[16] The average enamel loss in both treated groups after 40 seconds of microabrasion can be considered safe and clinically acceptable.[2,3]

Enamel microabrasion is a procedure that has precise indications and several advantages, but it requires caution and special care by both the professional and patient. According to Shillingburg *et al.* (1973), given that enamel thickness is approximately 1 mm, removal of 0.13 mm may be clinically

significant, especially in repeated treatments.[16] Therefore, clinicians must be aware of the remaining enamel thickness when treating discolored areas.[3] The removal of excessive enamel can lead to color alteration, esthetic damage and high tooth sensitivity. The results of this study showed that during microabrasion treatment approximately 12 to 14 μm were lost during each 10 second rubbing cycle when gels containing approximately 6% of hydrochloric acid were used, and the increase of enamel surface loss appears to have a linear trend ($r^2 = 0.9$, Figure 4).

It should be pointed out that in the cases where microabrasion is indicated (fluorosis staining, hyperplasia, hypomineralized defects in enamel), the mineralized structure of the enamel is compromised and hypomineralization is found. In these specific cases of hypomineralized enamel, a different effect of microabrasion in comparison to sound enamel could be expected. Most studies in the literature used sound enamel to assess enamel wear during microabrasion.[3,10,11,19] The study by Schmidlin *et al.* (2003)[17] performed enamel microabrasion of previously demineralized enamel with 6.6% hydrochloric acid for 20 seconds and under a 200 g load, resulting in 134.8 μm of enamel wear. Nevertheless, the authors used mechanical abrasion at 1,000 rpm and, therefore, results seem difficult to compare to those of the present study, that used sound enamel. This difference would seem to be an important factor to be considered by future studies.

Within the limitations of this study and based on its results, it may be concluded that, *in vitro,* the number of rubbing cycles performed during the microabrasion treatment increases surface loss, and that, for gels containing 6% to 6.6% hydrochloric acid, significantly higher surface loss can be expected for those containing silicon carbide particles of 82 μm (G2) than for those with the same particles but with a larger variation in granulation (20–160 μm; G1). The hypothesis of the study was confirmed since *in vitro* enamel microabrasion using 6%–6.6% hydrochloric acid and a 200 g load, rubbed manually using a plastic spatula, during 4 cycles of 10 seconds each removed an amount of enamel that is clinically acceptable.

ACKNOWLEDGMENTS

The authors would like to express their gratitude to FGD (Forschungsgemeinschaft Dental, #360303, Germany) for the financial support, to the START Program of the Medical Faculty of the RWTH Aachen University (#AZ43/09, Germany), and to CNPq (#305574/2008-6, Brazil). We are also thankful to Mrs. Patricia Butler-Bücher and Mr. Thomas Fischer (Institute of Metrology and Quality Management of RWTH Aachen University) for the laboratorial support.

REFERENCES

1. Croll TP. Enamel microabrasion: the technique. Quintessence Int. 1989 Jun;20(6):395-400.
2. Lynch CD, McConnell RJ. The use of microabrasion to remove discolored enamel: a clinical report. J Prosthet Dent. 2003 Nov;90(5):417-9.
3. Paic M, Sener B, Schug J, Schmidlin PR. Effects of microabrasion on substance loss, surface roughness, and colorimetric changes on enamel in vitro. Quintessence Int. 2008 Jun;39(6):517-22.
4. Killian CM, Croll TP. Enamel microabrasion to improve enamel surface texture. J Esthet Dent. 1990 Sep-Oct;2(5):125-8.
5. Allen K, Agosta C, Estafan D. Using microabrasive material to remove fluorosis stains. J Am Dent Assoc. 2004 Mar;135(3):319-23.
6. de Macedo AF, Tomazela-Herndl S, Corrêa MS, Duarte DA, Santos MT. Enamel microabrasion in an individual with Cohen syndrome. Spec Care Dentist. 2008 May-Jun;28(3):116-9.

7. Balan B, Madanda Uthaiah C, Narayanan S, Mookalamada Monnappa P. Microabrasion: an effective method for improvement of esthetics in dentistry. Case Rep Dent. 2013;2013:951589.
8. Celik EU, Yildiz G, Yazkan B. Comparison of enamel microabrasion with a combined approach to the esthetic management of fluorosed teeth. Oper Dent. 2013 Sep-Oct;38(5):E134-43.
9. McCloskey RJ. A technique for removal of fluorosis stains. J Am Dent Assoc. 1984 Jul;109(1):63-4.
10. Rodrigues MC, Mondelli RF, Oliveira GU, Franco EB, Baseggio W, Wang L. Minimal alterations on the enamel surface by micro-abrasion: in vitro roughness and wear assessments. J Appl Oral Sci. 2013 Mar-Apr;21(2):112-7.
11. Tong LS, Pang MK, Mok NY, King NM, Wei SH. The effects of etching, micro-abrasion, and bleaching on surface enamel. J Dent Res. 1993 Jan;72(1):67-71.
12. Levy SM. An update on fluorides and fluorosis. J Can Dent Assoc. 2003 May;69(5):286-91.
13. Chandra S, Chawla TN. Clinical evaluation of the sandpaper disk method for removing fluorosis stains from teeth. J Am Dent Assoc. 1975 Jun;90(6):1273-6.
14. Sundfeld RH, Croll TP, Briso AL, de Alexandre RS, Sundfeld Neto D. Considerations about enamel microabrasion after 18 years. Am J Dent. 2007 Apr;20(2):67-72.
15. Welbury RR, Shaw L. A simple technique for removal of mottling, opacities and pigmentation from enamel. Dent Update. 1990 May;17(4):161-3.
16. Shillingburg HT Jr, Grace CS. Thickness of enamel and dentin. J South Calif Dent Assoc. 1973 Jan;41(1):33-6 passim.
17. Schmidlin PR, Göhring TN, Schug J, Lutz F. Histological, morphological, profilometric and optical changes of human tooth enamel after microabrasion. Am J Dent. 2003 Sep;16 Spec No:4A-8A.
18. Kendell RL. Hydrochloric acid removal of brown fluorosis stains: clinical and scanning electron micrographic observations. Quintessence Int. 1989 Nov;20(11):837-9.
19. Waggoner WF, Johnston WM, Schumann S, Schikowski E. Microabrasion of human enamel in vitro using hydrochloric acid and pumice. Pediatr Dent. 1989 Dec;11(4):319-23.
20. Ramalho KM, Eduardo Cde P, Rocha RG, Aranha AC. A minimally invasive procedure for esthetic achievement: enamel microabrasion of fluorosis stains. Gen Dent. 2010 Nov-Dec;2010; 58(6):e225-9.
21. Esteves-Oliveira M, Pasaporti C, Heussen N, Eduardo CP, Lampert F, Apel C. Prevention of toothbrushing abrasion of acid-softened enamel by CO(2) laser irradiation. J Dent. Sep;39(9):604-11.
22. Ramalho KM, Eduardo Cde P, Heussen N, Rocha RG, Lampert F, Apel C, et al. Protective effect of CO2 laser (10.6 mum) and fluoride on enamel erosion in vitro. Lasers Med Sci. Jan;28(1):71-8.
23. Bertassoni LE, Martin JM, Torno V, Vieira S, Rached RN, Mazur RF. In-office dental bleaching and enamel microabrasion for fluorosis treatment. J Clin Pediatr Dent. 2008 Spring;32(3):185-7.
24. Higashi C, Dall'Agnol AL, Hirata R, Loguercio AD, Reis A. Association of enamel microabrasion and bleaching: a case report. Gen Dent. 2008 May;56(3):244-9.
25. Setien VJ, Roshan S, Nelson PW. Clinical management of discolored teeth. Gen Dent. 2008 May;56(3):294-300; quiz 1-4.
26. Croll TP, Killian CM, Miller AS. Effect of enamel microabrasion compound on human gingiva: report of a case. Quintessence Int. 1990 Dec;21(12):959-63.
27. Fragoso LS, Lima DA, de Alexandre RS, Bertoldo CE, Aguiar FH, Lovadino JR. Evaluation of physical properties of enamel after microabrasion, polishing, and storage in artificial saliva. Biomed Mater. 2011 Jun;6(3):035001.
28. Dalzell DP, Howes RI, Hubler PM. Microabrasion: effect of time, number of applications, and pressure on enamel loss. Pediatr Dent. 1995 May-Jun;17(3):207-11.
29. Kilpatrick NM, Welbury RR. Hydrochloric acid/pumice microabrasion technique for the removal of enamel pigmentation. Dent Update. 1993 Apr;20(3):105-7.
30. Mendes RF, Modelli J, Freitas CA. Avaliação da quantidade de desgaste do esmalte dentário submetido a microabrasão. Rev Fac Odontol Bauru. 1999 Jan-Jun;7(1/2):35-40.
31. Price RBT, Loney RW, Doyle G, Moulding B. An evaluation of a technique to remove stains fron teeth using microabraion. J Am Dent Assoc. 2003 Aug;134(8):1066-71.

AUTORES

ASSUNTOS

SUBJECTS

Clinical and Laboratorial Research in Dentistry

Volume 20 • Número 3
Julho / Setembro • 2014

ORIGINAL RESEARCH

USP

Faculdade de Odontologia • Universidade de São Paulo •

FFO Fundecto